

Cite this: *Chem. Sci.*, 2023, 14, 6493Received 18th March 2023
Accepted 5th May 2023

DOI: 10.1039/d3sc01435e

rsc.li/chemical-science

Progress in the chemistry of molecular actinide-nitride compounds

Megan Keener,^a Leonor Maria^b and Marinella Mazzanti^{*a}

The chemistry of actinide-nitrides has witnessed significant advances in the last ten years with a large focus on uranium and a few breakthroughs with thorium. Following the early discovery of the first terminal and bridging nitride complexes, various synthetic routes to uranium nitrides have since been identified, although the range of ligands capable of stabilizing uranium nitrides still remains scarce. In particular, both terminal- and bridging-nitrides possess attractive advantages for potential reactivity, especially in light of the recent development of uranium complexes for dinitrogen reduction and functionalization. The first molecular thorium bridged-nitride complexes have also been recently identified, anticipating the possibility of expanding nitride chemistry not only to low-valent thorium, but also to the transuranic elements.

1. Introduction

Metal nitrides are important intermediates in the biological and industrial conversion of dinitrogen (N₂) to ammonia (NH₃), as

well as in stoichiometric and catalytic N-transfer reactions. As a result, the synthesis, characterization, and reactivity of molecular nitride compounds of transition metals have been, and continue to be, extensively studied.^{1–7} In contrast, the

^aGroup of Coordination Chemistry, Institute of Chemical Sciences and Engineering – ISIC, Ecole Polytechnique Fédérale de Lausanne (EPFL), 1015 Lausanne, Switzerland. E-mail: marinella.mazzanti@epfl.ch

^bCentro de Química Estrutural, Institute of Molecular Sciences, Instituto Superior Técnico, Universidade de Lisboa, 2695-066 Bobadela, Portugal



Megan Keener obtained her B.Sc. degree in Chemistry in 2015 at California State University, Chico, where she did undergraduate research with Professor David Ball. In 2020, she received her Ph.D. in Chemistry from the University of California, Santa Barbara, under the supervision of Professor Gabriel Ménard. Her Ph.D. research was focused on synthetic inorganic chemistry, in which her thesis was entitled,

“From Transition Metals to Actinides: A Homogenous Approach for Clean Alternative Energy and Storage Applications”. She is a current postdoctoral researcher in the group of coordination chemistry of Professor Marinella Mazzanti at École Polytechnique Fédérale of Lausanne (EPFL). Her current research interests are focused on developing highly reactive *f* element complexes for the transformation of widely available feedstocks into higher-added value compounds.



Leonor Maria was born in Caparica (Portugal). She graduated in chemical engineering at Faculdade de Ciências e Tecnologia - Universidade Nova de Lisboa in 1996 and obtained a PhD degree in Chemistry in 2003 from Instituto Superior Técnico – Universidade Técnica de Lisboa (IST). After post-doctoral fellowships at Instituto Tecnológico Nuclear (ITN, Bobadela) and Centro de Química Estrutural – Instituto Superior Técnico (CQE-IST), she was awarded an Assistant Researcher contract under FCT program Ciência-2008, and in 2009, she joined the *f*-Element Chemistry Group at ITN (later Centro de Ciências e Tecnologias Nucleares of IST). Since January 2020, she is a member of the Inorganic and Organometallic Architectures, Reactivity and Catalysis (IOARC) Group of CQE-IST. Her main research interests are in the synthesis, structure, reactivity and bonding of lanthanide and actinide complexes, with focus on multi-electron transfer reactions and metal-ligand multiple bond formation.

“From Transition Metals to Actinides: A Homogenous Approach for Clean Alternative Energy and Storage Applications”. She is a current postdoctoral researcher in the group of coordination chemistry of Professor Marinella Mazzanti at École Polytechnique Fédérale of Lausanne (EPFL). Her current research interests are focused on developing highly reactive *f* element complexes for the transformation of widely available feedstocks into higher-added value compounds.





Scheme 1 Molecular nitrides of uranium in the +4 and +5 oxidation states reported before 2014.

chemistry of molecular actinide-nitrides is significantly less developed than their *d*-block counterparts, however, inorganic actinide-nitride materials (uranium, thorium, neptunium, and plutonium) have attracted large attention as advanced nuclear fuels.^{8–14} Notably, uranium nitride (UN) materials were some of the first compounds reported as active catalysts in the industrial Haber–Bosch process for the production of NH_3 from N_2 and H_2 .^{15,16}

Three solid uranium nitrides are known (UN , UN_2 , and U_2N_3).¹¹ The synthesis of phase pure ThN ,^{17–19} PuN ,²⁰ and NpN ²¹ are also well established, however, these are less studied than uranium nitrides, with the most common synthetic route for actinide mono-nitrides involving carbothermic reduction of dioxides.²²

Molecular actinide-nitrides were first isolated in noble gas matrices at cryogenic temperatures, and characterized by infrared spectroscopy for uranium (UN , $\text{N}=\text{UF}_3$, $\text{N}=\text{U}=\text{N}$, $\text{N}=\text{U}=\text{N}-\text{H}$, $\text{NUN}(\text{NN})_x$, $(\text{UN})(\text{NN})_x$),^{23–28} plutonium (PuN ,

PuN_2),²⁹ and thorium (ThN , NThN , NThO),^{30–32} but are only stable at cryogenic temperatures. Since, molecular actinide-nitrides have garnered significant attention due to their key role in understanding actinide bonding interactions, covalency, and electronic structure properties, as well as their ability to mediate important small molecule transformations.^{33–41} Early attempts to prepare molecular uranium-nitride complexes were already covered in a review published in 2014,⁴² therefore those systems will not be described in detail here.

However, we would like to summarize the main milestones in nitride chemistry that occurred before 2014 (Scheme 1).^{33,34} Seminal attempts from the Cummins group to prepare uranium nitride complexes by N_2 cleavage,³⁵ or N-transfer reactions³⁶ with the Hdbabh (2,3,5-dibenzo-7-azabicyclo[2.2.1]hepta-2,5-diene), led to stable molybdenum/uranium (Mo/U) dinitrogen and uranium hexakis-imido complexes. Remarkably, the first example of a U(IV)/U(V) uranium-nitride was obtained in 2002 by reduction of a U(III) tetrapyrrole complex, $[\text{K}(\text{DME})][(\text{Et}_5\text{-calix}[4]\text{tetrapyrrole})\text{U}^{\text{III}}(\text{DME})]$ ($\text{DME} = 1,2\text{-dimethoxyethane}$), with $[\text{K}(\text{naphthalenide})]$ under N_2 , and presented a diamond core UN_2 motif (A, Scheme 1).³⁷ Shortly after, two uranium azide (N_3^-)/nitride (N^{3-}) clusters of very different structure (one presenting a $\text{U}=\text{N}=\text{U}$ motif, and the other with an interstitial $\mu\text{-N}_3$), were obtained from the reaction of U(III) complexes with alkali azides (complexes B and C).^{38,39}

Utilizing bulkier ligand environments, and the methodology involving the reduction of inorganic azides with U(III) complexes, the groups of Hayton and Cummins were able to effect the controlled synthesis of dinuclear bridged-nitride complexes in varying oxidation states (complexes 16 (Section 3.1.1) and D).^{40,41} Finally, the group of Liddle demonstrated that utilization of the bulky triamidoamine ($\text{TREN}^{\text{TIPS}}$) ligand, and the analogous U(III) azide reduction route, allowed the preparation and isolation of the first uranium(V) terminal nitride (50-M), which was then subsequently oxidized to yield the U(VI) terminal-nitride analogue (Section 4.2).^{43,44} It should be noted, prior to the isolation of the relatively stable U(V) and U(VI) terminal nitrides by the Liddle group, Kiplinger and co-workers demonstrated that a putative terminal-nitride could be generated by a different synthetic route, involving photolysis of a U(IV) azide precursor.⁴⁵ The high reactivity of the putative nitride towards C–H activation of one of the methyl groups of the ligand resulted in the isolation



Marinella Mazzanti is a Professor at the Ecole Polytechnique Fédérale de Lausanne (EPFL) in Switzerland since 2014. She was born in Vinci (Italy). She obtained a master degree in Inorganic Chemistry from the University of Pisa and a PhD in Chemistry from the University of Lausanne with Carlo Floriani. She was post-doc in UC-Berkeley and at UC-Davis working with Alan Balch. From 1996 to 2014

she held a position as research scientist at a National Laboratory in France (CEA-Grenoble) working in *f*-elements chemistry. She is an associate editor of *Chemical Communications*. She was awarded the ACS F. Albert Cotton Award in Synthetic Inorganic Chemistry in 2021 and the Le Coq de Boisbaudran award in 2023 for her work on uranium and lanthanide chemistry. Her research interests are centered on synthetic inorganic chemistry and in the development of new molecules with unusual properties and original reactivity with focus on small molecule activation.



of a U(IV) amido derivative (**E**; Scheme 1).⁴⁵ These early studies demonstrated that different synthetic routes could be used to access bridging- and terminal-nitrides, such as azide reduction, photolysis, or N₂ reduction, but choice of the supporting ligands was crucial in controlling both the nuclearity and reactivity of the nitride products. Since then, careful tuning of the reaction conditions has significantly expanded the chemistry of molecular uranium nitrides, leading to the isolation of nitrides in a broad range of oxidation states (+3 to +6), which have shown high reactivity towards small molecules such as CO, CO₂, H₂, and N₂.^{46–53} Notably, the use of the monodentate amide ligand, –N(SiMe₃)₂, in the groups of Hayton and Mazzanti, and the siloxide ligand, –OSi(O^tBu)₃, in the group of Mazzanti, have led to the expansion of nitride-bridged complexes of uranium and thorium in the last 20 years. The use of the polydentate tripodal amido ligands (Tren^R: N(CH₂CH₂NR)^{3–}) in the Liddle group has led to important advancements in terminal nitride chemistry and An–N bonding analysis. This chemistry, and all other actinide-nitrides reported since 2014, will be reviewed herein according to the supporting ligand environment, synthetic method, and actinide ion utilized.

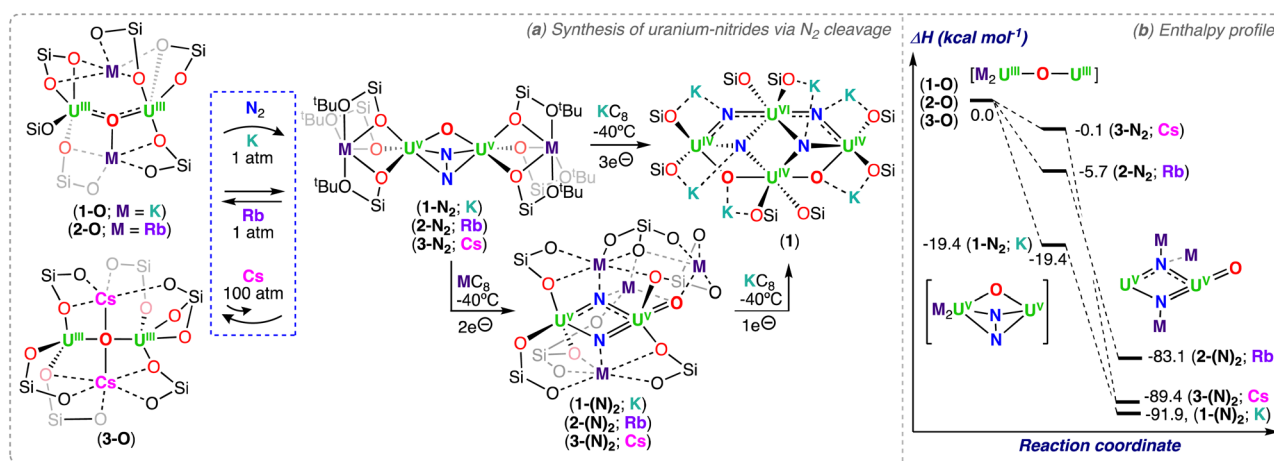
2. Actinide nitride complexes derived from N₂ cleavage

Metal complexes capable of effectively splitting N₂ to nitrides remain rare, and are mostly limited to complexes of *d*-block metals.^{1,2} The N₂ chemistry of actinides is significantly less developed, and typically involves labile N₂ binding, the 2e[–] reduction of N₂, or more recent examples demonstrating the 4e[–] reduction by two U(III) complexes or dinuclear U(III)/U(III) species.^{35,48,54–61} Based on the structure of the final nitride complex, multimetallic cooperation of transition metals and Lewis acids, potassium (K) in particular, was invoked to be crucial in the 6e[–] cleavage of N₂ to nitride involving alkali ions as reducing agents.^{62,63} Notably, the first actinide-nitride complex isolated in any significant quantity was synthesized

in 2002 by Gambarotta and co-workers *via* full reductive cleavage of N₂, promoted by the reaction of the trivalent uranium complex, [K(DME)][(Et₈-calix[4]tetrapyrrole)U^{III}(DME)], with [K(naphthalenide)] under N₂ (**A**, Scheme 1).³⁷ It is interesting to note that the U(III) precursor was not reported to react with N₂ in the absence of reducing agent, or at least in the polar solvent, DME. However, it is likely that reversible binding may occur, based on recent results from the Mazzanti group, where the mechanism of N₂ cleavage to nitride involves reduction of the U(III)-bound N₂ by excess alkali metal, yielding a U(V)/U(V) bis-nitride.⁶⁴ However, an alternative mechanism involving the binding and reduction of N₂ by a putative “U(II)” species cannot be ruled out without further studies.

Falcone, Mazzanti and co-workers first demonstrated that a well-defined, multimetallic oxide-bridged diuranium(III) complex, [K₂(U^{III}(OSi(O^tBu)₃)₂(μ-O))] (**1-O**), supported by siloxide ligands (–OSi(O^tBu)₃), is capable of effecting the 4e[–] reduction of N₂, forming the bridging hydrazido (N₂^{4–}) complex [K₂(U^V(OSi(O^tBu)₃)₂(μ-O)(μ-η²:η²-N₂))] (**1-N₂**).⁵⁹ In a later study by Jori, Mazzanti and co-workers, full reduction of the N₂^{4–} moiety to nitride was accomplished by addition of K₂S₈, with formation of the U(VI)/U(IV)₃ tetranitride cluster, [K₆((OSi(O^tBu)₃)₂U^{IV})₃((OSi(O^tBu)₃)₂U^{VI})(μ₄-N)₃(μ₃-N)(μ₃-O)₂] (**1**) (Scheme 2).⁶⁴ Computational studies showed that the reduction of the N₂ complex **1-N₂** proceeds *via* successive 1e[–] transfer from the alkali ion first to the uranium center, and then to the coordinated hydrazido (N₂^{4–}) moiety, generating a putative diuranium(V) bis-nitride terminal oxo complex, [K₃-(U^V(OSi(O^tBu)₃)₃(μ-N)₂(U^V(OSi(O^tBu)₃)₂(κ-O))][KOSi(O^tBu)₃] (**1-(N)₂**), that could not be isolated.⁶⁴ Cooperative K binding to the uranium–N₂^{4–} ligand facilitates the N–N bond cleavage during electron transfer. Further reduction of the putative **1-(N)₂** resulted in the multimetallic U(VI)/U(IV) tetranitride **1**. This combined experimental and computational study of the step-wise reduction of N₂ clearly shows that N₂ splitting proceeds *via* a N₂^{4–} intermediate (Scheme 2).

The molecular structure of the complex **1** shows three U(IV), one U(VI), and six K cations bridged by four nitride and two oxo



Scheme 2 (a) Synthesis of uranium nitrides supported by siloxide (–OSi(O^tBu)₃) ligands *via* N₂ cleavage. –O^tBu substituents were omitted for clarity. (b) Computed enthalpy profile in kcal mol^{–1} at room temperature for the formation of 1-(N)₂, 2-(N)₂, and 3-(N)₂ from the reduction of N₂ by 1-O, 2-O, and 3-O, respectively.



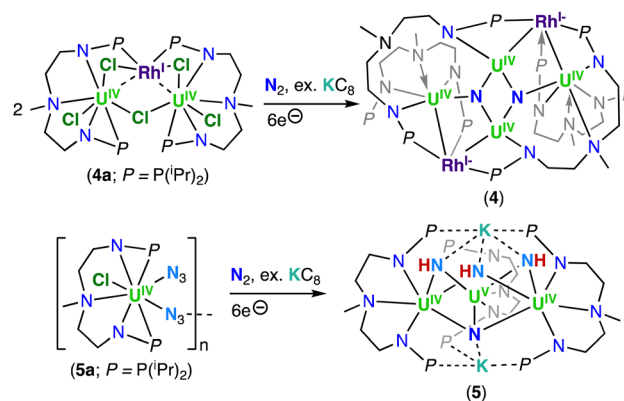
ligands. Remarkably, the $U_4N_4O_2K_6$ cluster contains a U(vi) coordinated by four bridging-nitride ligands, with two nitride groups bound in a trans mode with an almost linear N–U–N angle ($178.7(3)^\circ$), providing the second example of a *trans*-(N=U^{VI}=N) moiety analogue of UO_2^{2+} .^{65,66} The two *trans* U–N_{nitride} bond lengths (1.963(8) and 1.902(8) Å) are shorter than the *cis*-coordinated nitrides (2.256(6) and 2.265(7) Å) in **1**; however, they are longer than the *trans* U^{VI}–N_{nitride} bonds (1.799(8)–1.870(9) Å) reported by Rudel, Kraus and co-workers for $[(NH_3)_8U(\mu-N)(NH_3)_3(X)_2U(\mu-N)U(NH_3)_8]Y_n \cdot ZNH_3$ (where X = NH₃, Br[−], or Cl[−]; n = 6–8; Y = Cl[−] or Br[−]; Z = 26, 21, or 6) (Section 3.2; Scheme 11).⁶⁵ The elongated U^{VI}–N distances in **1** are most likely due to the presence of a more electron-rich uranium center bound by four additional anionic siloxide ligands compared to the neutral NH₃ ligands in the complexes reported by Rudel, Kraus and co-workers. The U^{IV}–N_{nitride} bond distances in **1** range from 2.183(7) to 2.319(78) Å and are comparable with those found in other reported nitride-bridged U(IV) clusters and consistent with U–N single bonds.^{39,67} In a more recent study, Jori, Mazzanti and co-workers reported the reactivity of the analogous rubidium (Rb) and cesium (Cs) complexes, $[M_2(U^{III}(OSi(O^tBu)_3)_3)_2(\mu-O)]$ (M = Rb (**2-O**), Cs (**3-O**)) with N₂ (Scheme 2a).⁶¹ The three alkali cations (K, Rb, Cs) display differences in the ability to bind N₂, which are not correlated to differences found in the redox potentials of the three complexes,⁶¹ but instead, a decrease with increasing size and decreasing Lewis acidity of the alkali ion binding to the U^{III}–O–U^{III} complex. Complex **1-O** irreversibly reduces N₂ at ambient conditions, while N₂ is reversibly reduced by the Rb₂–U^{III}–O–U^{III} complex **2-O** in the same conditions. In contrast, the reaction of the Cs₂U^{III}–O–U^{III} complex (**3-O**) with N₂, could only be detected by ¹H NMR spectroscopy at high pressures (12 to 100 atm) and low temperatures. DFT analysis showed that N₂ binding to **3-O** is hindered by steric effects, but, the calculated uranium(v)–N₂^{4−} species presented a similar degree of activation of the bound N₂ for the three uranium-alkali ion M₂U^V–(N₂)–U^V complexes (M = K, Rb, Cs; Scheme 2b).⁶¹ In the case of Rb, it was possible to isolate the intermediate hydrazido (N₂^{4−}) complex $[Rb_2(U^V(OSi(O^tBu)_3)_3)_2(\mu-O)(\mu-\eta^2:\eta^2-N_2)]$ (**2-N₂**). Analysis by ¹H NMR spectroscopy indicated that addition of 2.0 equiv. of RbC₈ to **2-N₂** (or **2-O**) under N₂ generates a putative bis-nitride (**2-(N)**₂), that could not be isolated. Even though the formation of the Cs–N₂^{4−} intermediate complex, “[Cs₂–U^V(OSi(O^tBu)₃)₃)₂(μ-O)(μ-η²:η²-N₂)” (**3-N₂**), was not observed by ¹H NMR spectroscopy under 1 atm of N₂, the reaction of **3-O** with 2.0 equiv. of CsC₈ at low temperature under N₂ led to full N₂ cleavage and isolation of the U(v)/U(v) bis-nitride complex, $[Cs_3(U^V(OSi(O^tBu)_3)_3)(\mu-N)_2(U^V(OSi(O^tBu)_3)_3)(\kappa-O)]$ $[CsOSi(O^tBu)_3]$ (**3-(N)**₂) (Scheme 2a).⁶¹ The molecular structure of **3-(N)**₂ shows two Cs–nitrides linking two U(v) ions in a U₂N₂ diamond-shaped core with asymmetric U–N bond lengths ranging from 1.85(1) to 2.34(1) Å. The shorter and longer U–N_{nitride} bond distances are those of the bridging nitride which is *trans* to the oxo group (U–O 1.856(4) Å, O–U–N 172.6(4)°), suggesting that the nitride ligand binds the oxo-bound U(v) ion with a multiple bond and the other U(v) ion with a single bond. Complex **3-(N)**₂ represents a rare example of

a U(v) molecular compound featuring a O=U=N moiety analogue of uranyl(v). The only other known example of a uranium complex with such a moiety was reported by Fortier, Hayton and co-workers for a *trans* oxo-nitride U(vi) complex.⁴⁰

In 2020, Xin, Zhu and co-workers reported the multimetallic (U(IV))₄(Rh(−I))₂ bis-nitride complex, $[(U^{IV}(NNP_2)_2)(Rh^{-I})(\mu-N)]_2$ (**4**), that was isolated from the reduction of the U₂–Rh complex, $[(U^{IV}(NNP_2)_2Cl_2)_2(\mu-Cl)(\mu-Rh^I)]$ (**4a**) (NNP₂ = (N(CH₃)(CH₂CH₂–NP^tPr₂)₂)^{2−}), under N₂ with excess KC₈ (top, Scheme 3).⁶⁸ To confirm the nitride ligands in **4** originated from N₂ cleavage, the isotopically enriched complex ¹⁵N-**4** was prepared under 1 atm of ¹⁵N₂. Acidification of complexes **4** and ¹⁵N-**4** resulted in ¹⁴NH₄⁺ and ¹⁵NH₄⁺, respectively.⁶⁸ The bis-nitride complex **4** was also obtained from reduction with 4.0 equiv. of KC₈ under N₂ of the U(IV)/Rh(−I) complex, $[(U^{IV}(NNP_2)_2Cl_2)(\mu-Cl)(\mu-Rh^{-I})]$, obtained from the reduction of **4a** under Argon. Computational studies suggested that the N₂ cleavage proceeds through N₂ binding by two $[(U^{IV}(NNP_2)_2Cl_2)(\mu-Cl)(\mu-Rh^{-I})]$ complexes following addition of 2.0 equiv. of KC₈, and is promoted by the cooperative multimetallic binding of N₂ by four uranium centers and two Rh ions. However, the intermediates involved in the N₂ splitting could not be isolated and the oxidation state of the uranium ions involved in N₂ binding remains ambiguous.

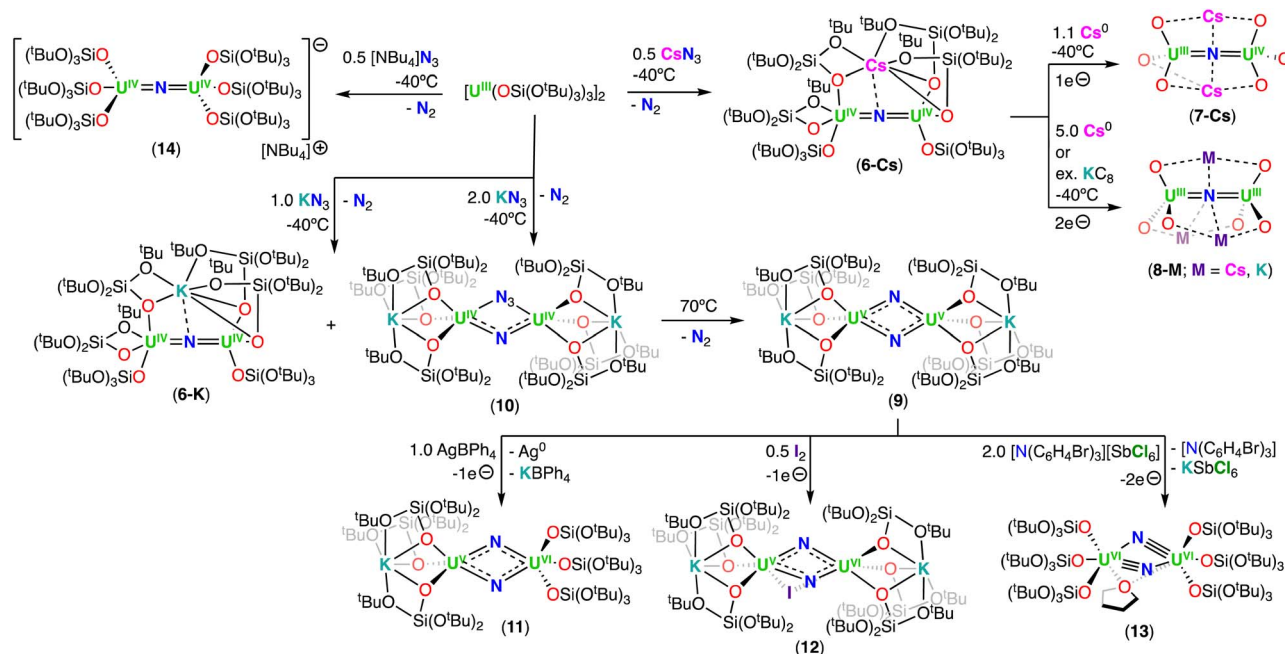
The importance of cooperativity between the U(III) and inner sphere alkali ions had already been identified in the reduction of N₂ by well-defined multimetallic uranium complexes.^{48,59,64} The solid-state structure of **4** revealed a centrosymmetric structure with two bridging nitride ligands in a U₄Rh₂N₂ core, with U and Rh in oxidation states +4 and −1, respectively. The oxidation state of uranium was confirmed by magnetic studies. Each nitride binds three U(IV) ions, with one U–N_{nitride} bond (2.302(6) Å) being significantly longer than the other two, which are similar (2.158(7) and 2.154(7) Å). The three U–N_{nitride} bond lengths are comparable to those found in a hydrazide-bridged uranium complex (2.163(13)–2.311(13) Å)⁴⁸ and are consistent with U–N single bonds.

More recently, Xin, Zhu and co-workers also reported that the reduction of a U(IV) azide complex, supported by the (NNP₂)^{2−} ligand (**5a**), with excess KC₈ under N₂ generates the



Scheme 3 Synthesis of uranium nitrides supported by the diamidoamine (NNP₂) ligand via N₂ cleavage.





Scheme 4 Synthesis of uranium nitrides supported by the siloxide ($-\text{OSi}(\text{O}^t\text{Bu})_3$) ligand. The ligands on complexes 7-Cs and 8-M were omitted for clarity.

trinuclear imido–nitride complex, $[\text{K}_2((\text{U}(\text{NNP})_2)_2(\mu\text{-NH})_3(\mu\text{-N}))]$ (5) (bottom, Scheme 3).⁶⁹ The molecular structure of 5 consists of three uranium centers that are bridged by three imido (NH) ligands, and one nitride (N^{3-}) ligand with U–N_{nitride} bond lengths which range from 2.204 to 2.218 Å. These distances are comparable to those reported for the U(IV)/U(VI) tetranitride cluster 1, and slightly longer than those found in the nitride bridged cluster, $[(\text{U}^{\text{IV}}\text{Cp}^*(\mu\text{-I})_2)_3(\mu\text{-N})]$, reported by Evans and co-workers (2.138(3)–2.157(3) Å).⁶⁷ The U–NH bond lengths range from 2.188 to 2.31 Å and are comparable to other bridged U–N_{imido} distances reported previously (2.10–2.55 Å).^{59,60,70}

Variable temperature magnetic data, UV-visible-NIR absorption, and X-ray photoelectron spectroscopy (XPS) were consistent with the presence of two U(IV) ions and one U(V) ion in the cluster complex 5, which was corroborated by computational studies. The authors proposed that the nitride ligand in 5 arises from N_2 reduction, while the imido ligands arise from reduction of the azide ligand which yields a nitride that is subsequently protonated. The origins of the protons remain ambiguous. To support that the nitride originated from N_2 reduction, an experiment was conducted in the presence of ^{15}N -labelled N_2 . Acidification of the isotopically enriched complex ^{15}N -5 resulted in $^{15}\text{NH}_4\text{Cl} : ^{14}\text{NH}_4\text{Cl}$ in a ratio of 0.5 : 3, demonstrating that the nitride moiety was a result of N_2 cleavage, and not from azide reduction. The lower-than-expected ratio (expected ratio was 1 : 3) was proposed by the authors to result from the $^{14}\text{N}_2$ generated *in situ* by the reduction of three $\text{U}-^{14}\text{N}_3$ moieties. DFT calculations demonstrated that the K cations are involved in the activation of N_2 , therefore, once again demonstrating that N_2 cleavage is the result of a multimetallic synergistic processes.

3. Mono- and bis-nitride bridged actinide complexes

3.1. Chemical reduction of azide precursors

As discussed in a previous review of the subject,⁴² the rational synthesis of actinide nitride complexes remained elusive, despite the isolation in 2002 of the bis-nitride complex from N_2 reduction by Gambarotta.³⁷ The most explored synthetic routes to actinide nitrides involves: (i) reduction of alkali metal-azides with U(III) complexes and (ii) the reaction of an actinide-azide complex with a reducing agent. Azides can act both as a $2e^-$ oxidant and a source of nitride (*i.e.*, $(\text{N}_3)^- + 2e^- \rightarrow \text{N}^{3-} + \text{N}_2$). These synthetic strategies led first to the isolation of multimetallic uranium nitride/azide clusters,^{38,39,67} and later the isolation of the first dinuclear nitride bridged complexes presenting either a bent $\text{U}=\text{N}-\text{U}^{40}$ or a linear $\text{U}=\text{N}=\text{U}$ core in three different oxidation states,⁴¹ which were discussed in detail in the previous review by Liddle.⁴² The only reactivity of bridging nitride complexes reported up to 2014 was the reaction of the linear $\text{U}^{\text{V}}=\text{N}=\text{U}^{\text{V}}$ with cyanide (CN^-), where the complex behaved as an electrophilic nitride to yield the bimetallic U(IV)/U(IV) bridging cyanoimide complex, $[\text{U}^{\text{IV}}(\text{N}^t\text{Bu})(3,5\text{-Me}_2\text{C}_6\text{H}_3)_2(\mu\text{-NCN})]$.⁴¹

This work incited other researchers to pursue the synthesis of uranium bridged-nitride complexes utilizing other supporting ligand frameworks. However, the isolation of actinide bridged-nitride complexes remains not trivial, and requires careful tuning of the supporting ligands steric and electronic properties, as well as the reaction conditions. Successful production of uranium bridged-nitride complexes in different oxidation states is reviewed in the following sections.



3.1.1. Complexes with OSi(O^tBu)₃ and N(SiMe₃)₂ ligands.

In 2013, Camp, Mazzanti and co-workers reported the reactivity of the dimeric U(III) complex supported by siloxide (–OSi(O^tBu)₃) ligands, [U^{III}(OSi(O^tBu)₃)₂(μ–OSi(O^tBu)₃)₂], with 1.0 equiv. of CsN₃ at low temperature, forming the U(IV)/U(IV) bridging nitride complex [Cs(U^{IV}(OSi(O^tBu)₃)₂(μ–N))] (**6-Cs**) (Scheme 4).⁷¹ The analogous potassium complex, [K(U^{IV}(OSi(O^tBu)₃)₂(μ–N))] (**6-K**), was obtained in a later study from the reaction with KN₃.⁵²

The X-ray crystallographic structures of **6-Cs** and **6-K** are analogous and consist of a heterometallic configuration, U₂M (M = K, Cs), in which the two U(IV) cations are bridged by an azide (N^{3–}) ligand in an almost linear fashion (U–N–U: 170.2(3)° **6-Cs**; 170.1(5)° **6-K**), with short U–N bond distances (2.058(5)–2.089(9) Å), consistent with U–N multiple bond character. The linear U^{IV}=N=U^{IV} core shows metrical parameters similar to those found in the dinuclear U(IV) nitride complex, Na[U^{IV}(N^tBu)(3,5–Me₂C₆H₃)₂(μ–N)], reported by Cummins and co-workers.⁴¹ The main difference is the presence of the inner sphere alkali cation in the neutral complexes, **6-K** and **6-Cs**. In these, either five or six oxygen atoms of the –OSi(O^tBu)₃ ligands tightly bind the alkali cation, which also binds the nitride ligand at the exact apical position, with M–N distances of 3.393(4) Å and 3.245(8) Å for **6-Cs** and **6-K**, respectively. Bond valence sum calculations and magnetization data are consistent with the U(IV) oxidation state for both uranium ions.

The reduction of the CsU^{IV}=N=U^{IV} nitride complex (**6-Cs**) with 1.0 equiv. or excess of metallic cesium at low temperature, resulted in the formation of the U(III)/U(IV) and U(III)/U(III) bridging-nitride complexes, [Cs₂(U^{III/IV}(OSi(O^tBu)₃)₂(μ–N))] (**7-Cs**) and [Cs₃(U^{III}(OSi(O^tBu)₃)₂(μ–N))] (**8-Cs**), respectively, which were the first isolated uranium nitride complexes incorporating U(III) ions (Scheme 4).⁷² As observed for **6-Cs**, the uranium nitrides, **7-Cs** and **8-Cs**, are also stabilized by two and three Cs cations, respectively, which are bound in the pocket formed by the –OSi(O^tBu)₃ ligands, and have a bonding interaction with the bridging nitride moiety. In complex **7-Cs**, the two OSi(O^tBu)₃-ligated Cs cations lie at the apical position of the U^{III}–N–U^{IV} core, while in **8-Cs**, the three OSi(O^tBu)₃-ligated Cs cations bind the nitride ligand and form a distorted triangular array that is perpendicular to the U^{III}–N–U^{III} fragment. The U–N–U moiety is almost linear in both compounds and the U–N_{nitride} bond lengths (2.081(1)–2.150(1) Å) are consistent with a non-delocalized U=N=U bonding mode. The U–N_{nitride} bond distances increase by about 0.08 Å from CsU^{IV}=N=U^{IV} to the fully reduced Cs₃U^{III}=N=U^{III} species, which can be related to the differences in ionic radii of U(III) and U(IV). Complexes **7-Cs** and **8-Cs** are very reactive and can only be handled in solution at low temperatures. The cyclic voltammogram of **6-Cs**, measured in THF with [NBu₄][BAR₄^F] as the supporting electrolyte, showed two irreversible redox events at –2.34 and –0.92 V (vs. [Cp₂Fe]^{0/+}). The irreversibility of these redox events was attributed to the rearrangement of the coordination sphere during the redox processes, but supports access to the low-valent U(III) species **7-Cs** and **8-Cs**.

The diuranium(III) potassium analogue of **8-Cs**, [K₃–(U^{III}(OSi(O^tBu)₃)₂(μ–N))] (**8-K**), was prepared by reduction of the

CsU^{IV}=N=U^{IV} complex **6-Cs** with excess of KC₈ in THF.⁴⁸ The presence of the inner sphere K cations in **8-K** resulted in a higher stability when compared to the Cs₃U^{III}=N=U^{III} complex (**8-Cs**), both in solid- and solution-state, making **8-K** more suitable for reactivity studies with small molecules (Section 6.2.3). It should be noted that the alkali ion is so strongly bound in **8-K**, that addition of 2.2.2-cryptand does not allow its removal.

With the aim of generating terminal-nitrides, rather than bridging moieties, Camp, Mazzanti and co-workers found that the anionic U(III) tetrakis complex, [K(18C6)][U^{III}(OSi(O^tBu)₃)₄], which is sterically saturated by the coordination of four –OSi(O^tBu)₃ ligands, reacts with 1.0 equiv. of CsN₃ at low temperature. However, in this case, a mixture of compounds was obtained, most likely resulting from the decomposition of a putative terminal nitride intermediate. Among the products, the second example of a diuranium(V) bis-nitride complex was identified, [K₂(U^V(OSi(O^tBu)₃)₂(μ–N)₂)] (**9**), comprising of a diamond-shaped U₂N₂ core.⁷¹

In 2019, the same group reported an improved and reproducible route for complex **9**. The reaction of [U^{III}(OSi(O^tBu)₃)₂(μ–OSi(O^tBu)₃)₂] with 2.0 equiv. of KN₃ at low temperature afforded the U(IV)/U(IV) bridged nitride-azide complex, [K(U^{IV}(OSi(O^tBu)₃)₂(μ–N)(μ–N₃))] (**10**), which is unstable at room temperature and can be fully converted at 70 °C into the diuranium(V) bridged bis-nitride complex **9** (Scheme 4).⁵² Complex **9** has a crystallographically imposed symmetry center in between the two uranium cations with a U⋯U distance of 3.2960(6) Å, and two distinct short U–N bond lengths of 2.101(6) and 2.023(5) Å,⁷¹ which are similar to those reported by Gambarotta for the bis-nitride complex, [K(DME)₄][(K(DME))(calix[4]tetrapyrrole)U₂(μ–NK)₂].³⁷ Bond valence sum calculations agree with a U(V) oxidation state, in which no EPR signal was observed for **9**,⁵² indicative of a 3/2 magnetic ground state.⁷³ The magnetic data measured for the U^V–(μ–N)₂–U^V complex showed an unusually strong antiferromagnetic coupling between the two f¹ ions with a T_N (Néel temperature) of approximately 77 K,⁵² slightly higher than that found in the U^V–(μ–O)₂–U^V complex [(U^V((^{nP},^{Me}ArO)₃tacn))₂(μ–O)₂] (tacn = triazacyclononane, nP = neopentyl) (~70 K).⁷⁴

More recently, Barluzzi, Mazzanti and co-workers reported that oxidation of complex **9** afforded the first bis-nitride uranium complexes containing U(VI) ions.⁷⁵ Addition of AgBPh₄ or I₂ afforded the mixed-valent, U(V)/U(VI) bis-nitride complexes, [K(U^{V/VI}(OSi(O^tBu)₃)₂(μ–N)₂)] (**11**) and [K₂(U^{V/VI}(OSi(O^tBu)₃)₂(μ–N)₂(μ–I))] (**12**), respectively, whereas addition of the strong oxidant, [N(C₆H₄Br)₃][SbCl₅] (“magic blue”), afforded the U(VI)/U(VI) bis-nitride complex, [(U^{VI}(OSi(O^tBu)₃)₂(μ–N)₂(μ–THF))] (**13**) (Scheme 4).⁷⁵ All the U–N bond distances in **11** (avg. 2.06(3) Å) and in **12** (avg. 2.13(5) Å) are nearly equivalent for the two uranium centers, suggesting the presence of a charge delocalized species. In the U(VI)/U(VI) complex **13**, short U–N bond distances (1.966(16) and 1.850(12) Å) are observed with much longer distances (2.292(13) and 2.252(16) Å), indicating one nitride ligand binds the U(VI) ion with a triple bond, whereas the other nitride with a single dative bond. An equivalent asymmetric bonding was calculated for the



matrix isolated U(vi) bis-nitride, $[\text{UN}(\mu\text{-N})_2]$, ($\text{U-N}_{\text{bridging}}$: 1.859 and 2.281 Å).³⁰ Computational studies were consistent with a delocalized bond across the U–N–U bonding for the U(v)/U(v) bis-nitride **9** and for the mixed valent U(v)/U(vi) bis-nitride **11**, but an asymmetric bonding mode was established for the U(vi)/U(vi) bis-nitride complex, **13**, which showed a U–N σ orbital well localized over the $\text{U}\equiv\text{N}$, and π orbitals which are partially delocalized to form a U–N single bond with the other U(vi) ion.⁷⁵

Using a similar strategy previously applied by Cummins,⁴¹ in 2019, Palumbo, Mazzanti and co-workers verified that by using the non-metallic azide, $[\text{NBu}_4][\text{N}_3]$, in the oxidation of $[\text{U}^{\text{III}}(\text{OSi}(\text{O}^t\text{Bu})_3)_2(\mu\text{-OSi}(\text{O}^t\text{Bu})_3)_2]$, the U(iv)/U(iv) bridged nitride complex, $[\text{NBu}_4][[\text{U}^{\text{IV}}(\text{OSi}(\text{O}^t\text{Bu})_3)_2(\mu\text{-N})]]$ (**14**) (Scheme 4) could be obtained.⁷⁶ In the molecular structure of **14**, the $-\text{OSi}(\text{O}^t\text{Bu})_3$ ligands coordinate to the uranium centers in a monodentate mode, $\kappa^1\text{-OSi}(\text{O}^t\text{Bu})_3$, in a staggered orientation with respect to those of the adjacent $[\text{U}^{\text{IV}}(\text{OSi}(\text{O}^t\text{Bu})_3)_3]^+$. Complex **14** shows average U–N_{nitride} bond lengths of 2.05(2) Å, comparable to those observed for the Cs-capped nitride, $\text{CsU}^{\text{IV}}=\text{N}=\text{U}^{\text{IV}}$ (**6-Cs**) (avg. 2.09(1) Å),⁷¹ while the U–N–U angle is slightly more linear (avg. 174(3)°).

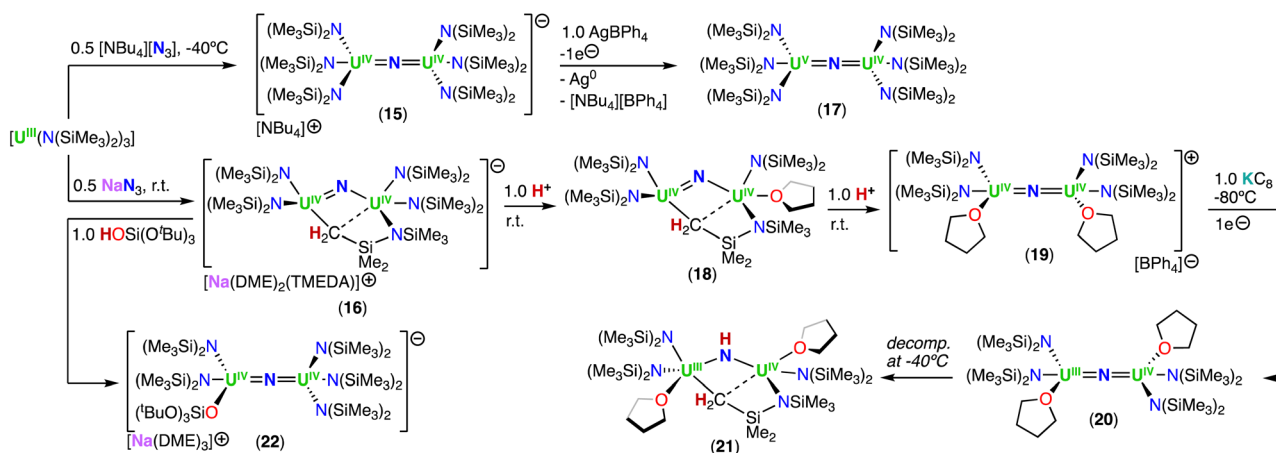
Using the same approach, the authors demonstrated that reduction of the azide precursor, $[\text{NBu}_4][\text{N}_3]$, could be carried out with the analogous monometallic U(III) amide ($-\text{N}(\text{SiMe}_3)_2$) complex, $[\text{U}^{\text{III}}(\text{N}(\text{SiMe}_3)_2)_3]$, at low temperature (-40°C) (Scheme 5),⁷⁶ affording the U(iv)/U(iv) nitride complex, $[\text{NBu}_4][[\text{U}^{\text{IV}}(\text{N}(\text{SiMe}_3)_2)_2(\mu\text{-N})]]$ (**15**). Performing the reaction at low temperature prevented cyclometallation, which had been previously described by Fortier, Hayton and co-workers for the U(iv)/U(iv) bridging nitride complex, $[\text{Na}(\text{DME})_2(\text{TMEDA})][[\text{N}(\text{SiMe}_3)_2)_2\text{U}^{\text{IV}}(\mu\text{-N})(\mu\text{-}\kappa^2\text{:C,N-CH}_2\text{SiMe}_2\text{NSiMe}_3)(-\text{U}^{\text{IV}}(\text{N}(\text{SiMe}_3)_2)]$ (**16**).⁴⁰ The molecular structure of complex **15** shows two staggered $[\text{U}^{\text{IV}}\text{N}(\text{SiMe}_3)_2]^+$ units bridged by a nitride ligand. The U–N–U bond angle is close to linearity (avg. 179.3°), and the U–N_{nitride} bond lengths are equivalent, consistent with a delocalized $\text{U}=\text{N}=\text{U}$ bonding mode, similar to that observed for the U(iv)/U(iv) amido complex, $[\text{NBu}_4][[\text{U}^{\text{IV}}(\text{N}^t\text{Bu})(3,5\text{-Me}_2\text{C}_6\text{H}_3)_3)_2(\mu\text{-N})]$, reported by the Cummins group.⁴¹ The $1e^-$ oxidation of **15** with AgBPh_4 , afforded the neutral nitride-

bridged U(iv)/U(v) complex, $[[\text{U}^{\text{IV/V}}(\text{N}(\text{SiMe}_3)_2)_2(\mu\text{-N})]]$ (**17**) (Scheme 5).⁷⁶ The molecular structure shows two different U–N_{nitride} bond lengths (2.080(5) and 2.150(5) Å), consistent with the presence of a localized valence.

In a later study, the authors found that reacting complex **16** (ref. 40) with 1.0 and 2.0 equiv. of $\text{HNet}_3\text{BPh}_3$, resulted in the neutral $[[\text{N}(\text{SiMe}_3)_2)_2\text{U}^{\text{IV}}(\mu\text{-N})(\mu\text{-}\kappa^2\text{:C,N-CH}_2\text{SiMe}_2\text{NSiMe}_3)\text{U}(\text{N}(\text{SiMe}_3)_2)(\text{THF})]]$ (**18**) and cationic $[[\text{U}^{\text{IV}}(\text{N}(\text{SiMe}_3)_2)_2(-\text{THF})_2(\mu\text{-N})][\text{BPh}_4]]$ (**19**), U(iv)/U(iv) nitride complexes by successive protonolysis of one $-\text{N}(\text{SiMe}_3)_2$ ligand and of the uranium–CH₂ bond, respectively (Scheme 5).⁷⁰ Notably, the authors found that reducing complex **19** with 1.0 equiv. KC_8 at -80°C led to the formation of a rare U(III)/U(iv) bridging-nitride complex, $[[\text{U}^{\text{III/IV}}(\text{N}(\text{SiMe}_3)_2)_2(\text{THF})_2(\mu\text{-N})]]$ (**20**).⁷⁰ The solid-state molecular structure of the U(III)/U(iv) bridged nitride **20** is similar to the parent U(iv)/U(iv) complex **19**, but with U–N(SiMe_3)₂ and U–THF bond distances consistent with a reduction to U(III). The U–N_{nitride} bond lengths are comparable (**19**: 2.0634(3) Å; **20**: 2.055(3) and 2.064(3) Å), however, the U–N–U bond angle is completely linear in complex **19**. The U(III)/U(iv) complex **20** is highly reactive and above -40°C , undergoes 1,2-addition of the C–H bond of a $\text{N}(\text{SiMe}_3)_2$ ligand across the $\text{U}^{\text{III}}=\text{N}=\text{U}^{\text{IV}}$ moiety, generating a U(III)/U(iv) imido-cyclometalate complex, $[[\text{N}(\text{SiMe}_3)_2)_2(\text{THF})\text{U}^{\text{III}}(\mu\text{-NH})(\mu\text{-}\kappa^2\text{:C,N-CH}_2\text{SiMe}_2\text{NSiMe}_3)\text{U}^{\text{IV}}(\text{N}(\text{SiMe}_3)_2)(\text{THF})]]$ (**21**).

These results demonstrated that a U(III)/U(iv) nitride could be isolated with strong sigma donor supporting ligands ($-\text{N}(\text{SiMe}_3)_2$) upon careful choice of the reaction conditions. However, further reduction of the U(iv) ion to yield a U(III)/U(III) was not accessible in this $\text{N}(\text{SiMe}_3)_2$ -nitride complex. This incited the same group to pursue heteroleptic complexes to maximize the electron-rich character without hampering access to a U(III)/U(III) nitride (*vide infra*).

Treatment of complex **16** (ref. 40) with 1.0 equiv. of $\text{HOSi}(\text{O}^t\text{Bu})_3$ generated the heteroleptic U(iv)/U(iv) nitride complex $[\text{Na}(\text{DME})_3][[\text{N}(\text{SiMe}_3)_2)_3\text{U}^{\text{IV}}(\mu\text{-N})\text{U}^{\text{IV}}(\text{N}(\text{SiMe}_3)_2)_2(-\text{OSi}(\text{O}^t\text{Bu})_3)]$ (**22**) (Scheme 5).⁷⁶ The presence of one $-\text{OSi}(\text{O}^t\text{Bu})_3$ ligand resulted in a significant deviation of the U–N–U bond angle from linearity (168.4(3)°).



Scheme 5 Synthesis of uranium nitrides supported by the amide ($-\text{N}(\text{SiMe}_3)_2$) ligand.

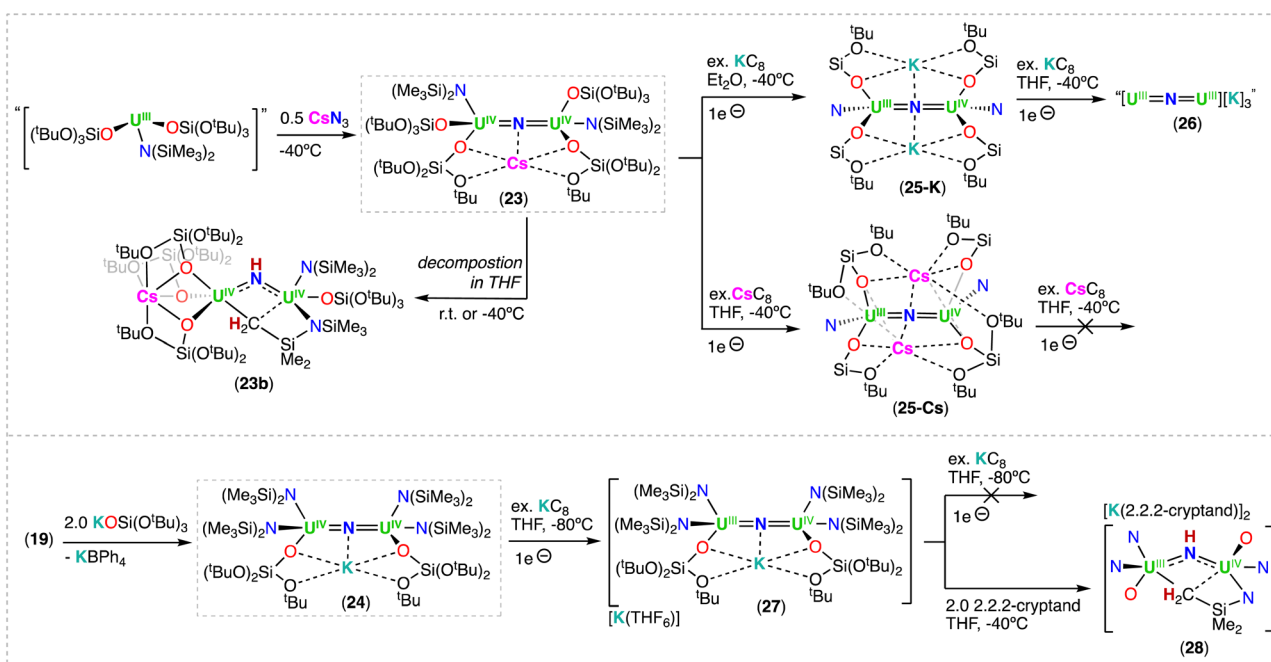


The magnetic behavior of complexes **14**, **15**, and **22** were studied. The χ versus T plots for the all- $\text{N}(\text{SiMe}_3)_2$ and heteroleptic complexes, **15** and **22**, respectively, are consistent with an antiferromagnetic coupling of the $\text{U}(\text{IV})/\text{U}(\text{IV})$ centers, with maximums at 90 and 55 K, respectively.⁷⁶ The highest χ maximum (at 110 K) ever measured for an actinide complex was reported by Vlaisavljevich, Cummins and co-workers for a dimeric arene-bridged $\text{U}(\text{III})/\text{U}(\text{III})$.⁷⁷ Additionally, Liddle and co-workers reported a strong antiferromagnetic coupling (~ 60 K maximum) for a triamidoamine ($\text{Tren}^{\text{TIPS}}$) bridged nitride complex with a linear $\text{U}^{\text{IV}}=\text{N}=\text{U}^{\text{IV}}$ core.⁷⁸

Shorter $\text{U}\cdots\text{U}$ bond distances were found for the all- $\text{OSi}(\text{O}^t\text{Bu})_3$ nitride complexes, $[\text{Cs}(\text{U}^{\text{IV}}\text{OSi}(\text{O}^t\text{Bu})_3)_2(\mu\text{-N})]$ (**6-Cs**) and $[\text{NBu}_4][[\text{U}^{\text{IV}}(\text{OSi}(\text{O}^t\text{Bu})_3)_2(\mu\text{-N})]$ (**14**) (4.121(1) and 4.107(2) Å, respectively), compared to the all- $\text{N}(\text{SiMe}_3)_2$ complex, $[\text{NBu}_4][[\text{U}^{\text{IV}}(\text{N}(\text{SiMe}_3)_2)_2(\mu\text{-N})]$ (**15**) (4.15 Å), but magnetic coupling was only detected in **15**. The heteroleptic complex **22** exhibits antiferromagnetic coupled $\text{U}(\text{IV})/\text{U}(\text{IV})$ centers, but the structure displays a $\text{U}\cdots\text{U}$ bond distance of 4.101(1) Å, and the $\text{U}-\text{N}-\text{U}$ bond angle is similar to the all- $\text{OSi}(\text{O}^t\text{Bu})_3$ complex **6-Cs**, suggesting there is no correlation between the geometric parameters and magnetic properties in these complexes.⁷⁶ Computational studies showed that the all- $\text{N}(\text{SiMe}_3)_2$ complex **15** has a singlet antiferromagnetic ground-state, while the quintet state is the most stable for the all- $\text{OSi}(\text{O}^t\text{Bu})_3$ complex **14**. The difference in magnetic properties were rationalized in terms of the different nature and strength of the $\text{U}-\text{L}$ bonding interaction for the $-\text{N}(\text{SiMe}_3)_2$ and $-\text{OSi}(\text{O}^t\text{Bu})_3$ ligands.

The synthetic strategy used in the preparation of $[\text{Cs}(\text{U}^{\text{IV}}\text{OSi}(\text{O}^t\text{Bu})_3)_2(\mu\text{-N})]$ (**6-Cs**)⁷¹ was also successfully applied by Keener, Mazzanti and co-workers for the isolation of other heteroleptic $\text{U}(\text{IV})/\text{U}(\text{IV})$ bridged nitrides.⁷⁹ First, the

heteroleptic complex, $[\text{Cs}\{\text{U}^{\text{IV}}\text{OSi}(\text{O}^t\text{Bu})_3\}_2(\text{N}(\text{SiMe}_3)_2)_2(\mu\text{-N})]$ (**23**), containing a combination of $-\text{OSi}(\text{O}^t\text{Bu})_3$ and $-\text{N}(\text{SiMe}_3)_2$ ligands (4 : 2 ratio), was obtained from the reaction of CsN_3 with the *in situ* generated heteroleptic $\text{U}(\text{III})$ precursor, $[\text{U}^{\text{III}}\text{OSi}(\text{O}^t\text{Bu})_3\}_2(\text{N}(\text{SiMe}_3)_2)]$ (Scheme 6).⁷⁹ Complex **23** is quite stable at low temperatures in toluene, but slowly decomposes at -40 °C in THF, and undergoes full decomposition at room temperature forming the $\text{U}(\text{IV})/\text{U}(\text{IV})$ bridged imido-cyclometallate complex, $[\text{Cs}\{\text{OSi}(\text{O}^t\text{Bu})_3\}_3\text{U}^{\text{IV}}(\mu\text{-NH})(\mu\text{-}\eta^2\text{-C,N-CH}_2\text{SiMe}_2\text{NSiMe}_3\text{U}^{\text{IV}}(\text{N}(\text{SiMe}_3)_2)(\text{OSi}(\text{O}^t\text{Bu})_3)]$ (**23b**), involving a 1,2-addition of a C–H bond of $\text{N}(\text{SiMe}_3)_2$ across the uranium-nitride bond, similar to what was observed for the $\text{U}(\text{III})/\text{U}(\text{IV})$ nitride complex **20**. From the same study, a second heteroleptic $\text{U}(\text{IV})/\text{U}(\text{IV})$ nitride complex, $[\text{K}(\text{U}^{\text{IV}}\text{OSi}(\text{O}^t\text{Bu})_3)(\text{N}(\text{SiMe}_3)_2)_2(\mu\text{-N})]$ (**24**), containing a different combination of $-\text{OSi}(\text{O}^t\text{Bu})_3$ and $-\text{N}(\text{SiMe}_3)_2$ ligands (2 : 4 ratio), was prepared by the addition of 2.0 equiv. $\text{KOSi}(\text{O}^t\text{Bu})_3$ to the cationic nitride complex **19** (ref. 70) (Scheme 6), and was found to be stable in various solvents.⁷⁹ The increased stability of **24** towards C–H bond activation of a $\text{N}(\text{SiMe}_3)_2$ ligand, in comparison to complex **23**, was attributed to the number of $-\text{OSi}(\text{O}^t\text{Bu})_3$ ligands (two vs. four). The authors found that a higher number of $-\text{OSi}(\text{O}^t\text{Bu})_3$ ligands resulted in an increased nucleophilicity of the nitride in **23**, leading to 1,2-addition of a C–H bond of a $\text{N}(\text{SiMe}_3)_2$ ligand. This is consistent with the lower nucleophilicity of bridging nitrides in $\text{U}(\text{IV})$ complexes supported by amide compared to those supported by siloxides (see reactivity studies). The X-ray diffraction analysis of the bridging nitride complexes, **23** and **24**, revealed similar $\text{U}-\text{N}_{\text{nitride}}$ bond distances to those of **6-Cs**⁷¹ and **6-K**.⁵² As expected, the $\text{U}-\text{N}_{\text{imido}}$ bond distances in **23b** (2.167(8) and 2.198(8) Å) are longer than those in the parent $\text{U}(\text{IV})/\text{U}(\text{IV})$ nitride precursor, **23**.



Scheme 6 Synthesis of heteroleptic uranium nitrides supported by varying combinations of siloxide ($-\text{OSi}(\text{O}^t\text{Bu})_3$) and amide ($-\text{N}(\text{SiMe}_3)_2$) ligands.



The heteroleptic $\text{CsU}^{\text{IV}}=\text{N}=\text{U}^{\text{IV}}$ complex **23**, which contains more $-\text{OSi}(\text{O}^t\text{Bu})_3$ ligands, could be reduced at $-40\text{ }^\circ\text{C}$ with excess KC_8 (Et_2O) or CsC_8 (THF), generating the $\text{U}(\text{III})/\text{U}(\text{IV})$ analogues, $[\text{K}_2(\text{U}^{\text{III/IV}}(\text{OSi}(\text{O}^t\text{Bu})_3)_2(\text{N}(\text{SiMe}_3)_2)_2(\mu\text{-N}))]$ (**25-K**) and $[\text{Cs}_2(\text{U}^{\text{III/IV}}(\text{OSi}(\text{O}^t\text{Bu})_3)_2(\text{N}(\text{SiMe}_3)_2)_2(\mu\text{-N}))]$ (**25-Cs**), respectively. However, by changing the solvent from Et_2O to THF in the reduction of $\text{CsU}^{\text{IV}}=\text{N}=\text{U}^{\text{IV}}$ complex **23** with KC_8 , afforded a putative heteroleptic $\text{U}(\text{III})/\text{U}(\text{III})$ bridging nitride, $[\text{K}_3(\text{U}^{\text{III}}(\text{OSi}(\text{O}^t\text{Bu})_3)_2(\text{N}(\text{SiMe}_3)_2)_2(\mu\text{-N}))]$ (**26**). Alternatively, reduction of the heteroleptic $\text{KU}^{\text{IV}}=\text{N}=\text{U}^{\text{IV}}$ complex **24**, containing more $-\text{N}(\text{SiMe}_3)_2$ ligands, with excess KC_8 at $-80\text{ }^\circ\text{C}$ yielded the $\text{U}(\text{III})/\text{U}(\text{IV})$ nitride complex, $[\text{K}(\text{THF})_6][\text{K}(\text{U}^{\text{III/IV}}(\text{OSi}(\text{O}^t\text{Bu})_3)(-\text{N}(\text{SiMe}_3)_2)_2(\mu\text{-N}))]$ (**27**) (Scheme 6).⁷⁹ Interestingly, the two additional $-\text{OSi}(\text{O}^t\text{Bu})_3$ ligands in the $\text{U}(\text{III})/\text{U}(\text{IV})$ complex **27**, compared to the cationic $\text{U}(\text{III})/\text{U}(\text{IV})$ complex **20**, results in an increased stability towards the 1,2-addition of the C–H bond of a $-\text{N}(\text{SiMe}_3)_2$ ligand across the uranium–nitride, most likely due to the $\text{OSi}(\text{O}^t\text{Bu})_3$ -bound K cation capping the nitride. Removal of the K cation by addition of 2.2.2-cryptand, increases nitride reactivity towards C–H activation, affording the imido cyclo-metallated complex, $[(\text{Me}_3\text{Si})_2\text{N}_2\text{U}^{\text{IV}}(\text{OSi}(\text{O}^t\text{Bu})_3)(\mu\text{-NH})(\mu\text{-}\kappa^2\text{:C,N-CH}_2\text{SiMe}_2\text{NSiMe}_3\text{U}^{\text{III}}(\text{N}(\text{SiMe}_3)_2)(\text{OSi}(\text{O}^t\text{Bu})_3)[\text{K}(\text{2.2.2-cryptand})])_2]$ **28**. Reduction of the complexes, $\text{Cs}_2\text{U}^{\text{III}}=\text{N}=\text{U}^{\text{IV}}$ (**25-Cs**) and $[\text{K}(\text{THF})_6][\text{KU}^{\text{III}}=\text{N}=\text{U}^{\text{IV}}]$ (**27**), with excess CsC_8 and KC_8 , respectively, to afford their $\text{M}_3\text{U}^{\text{III}}=\text{N}=\text{U}^{\text{III}}$ ($\text{M} = \text{K, Cs}$) analogues revealed impossible due to the very electron-rich character of uranium by influence of the different ancillary ligands or alkali-metal (*Cs versus K*) (Scheme 6). This contrasts with what was observed for the all- $\text{OSi}(\text{O}^t\text{Bu})_3$ complex, **6-Cs**, which could be reduced to the analogous $\text{M}_3\text{U}^{\text{III}}=\text{N}=\text{U}^{\text{III}}$ ($\text{M} = \text{K}$ (**8-K**), Cs (**8-Cs**)) complexes.

3.1.2. Complexes with triamidoamine ligands

The triamidoamine ligand ($\text{Tren}^{\text{R}}: \text{N}(\text{CH}_2\text{CH}_2\text{NR})^3$) was introduced in actinide coordination chemistry by Scott and co-workers in 1994.⁸⁰ Since 2012,⁴³ the Liddle group has used this tripodal-framework to promote the formation of terminal uranium nitrides and to investigate their chemistry.⁴³ In 2019, Du, Liddle and co-workers reported the use of $\text{Tren}^{\text{DMBS}}$ ($\text{DMBS} = \text{N}(\text{CH}_2\text{CH}_2\text{NSiMe}_2\text{Bu})^3$) in the synthesis of mono nitride-bridged uranium complexes.⁷⁸ The chemical reduction of the uranium(IV) azide complex, $[(\text{U}^{\text{IV}}(\text{Tren}^{\text{DMBS}})(\mu\text{-N}_3))_4]$ (**29**), with KC_8 afforded the bridged nitride complexes, $[\text{K}(\text{THF})_6][(\text{U}^{\text{IV}}(\text{Tren}^{\text{DMBS}}))_2(\mu\text{-N})]$ (**30**) and $[(\text{U}^{\text{V/IV}}(\text{Tren}^{\text{DMBS}}))_2(\mu\text{-N})]$ (**31**),⁷⁸ while photolysis of the $\text{U}(\text{IV})$ azide precursor, **29**, led only to formation of the mixed-valent $\text{U}(\text{IV})/\text{U}(\text{V})$ complex **31** (Scheme 7). It should be noted that this work provided the first example of nitride complexes isolated from the reduction or photolysis of a $\text{U}(\text{IV})$ -azide precursor, rather than reaction of a $\text{U}(\text{III})$ complex with a metal azide. Seminal attempts to form nitrides using these routes had failed to result in N_2 elimination (as for the reduction of $[\text{U}(\text{N}(\text{SiMe}_3)_2)_3(\text{N}_3)_2]$ reported by Fortier, Hayton and co-workers)⁸¹ or generated highly reactive nitride intermediates that underwent insertion into the ligand framework.⁴⁵

In the solid-state molecular structure of **30**, the anion lies on a crystallographic 3-fold rotation axis and therefore the $\text{U}^{\text{IV}}\text{-N-}$

U^{IV} angle is 180° , and the $\text{U-N}_{\text{nitride}}$ bonds are equivalent ($2.0648(2)\text{ \AA}$). In the mixed-valent $\text{U}(\text{IV})/\text{U}(\text{V})$ complex, **31**, the $\text{U-N}_{\text{nitride}}$ bond lengths are inequivalent ($2.081(5)$ and $2.136(5)\text{ \AA}$) and the $\text{U}^{\text{V}}\text{-N-U}^{\text{IV}}$ bond angle is bent ($161.2(2)^\circ$). The magnetic data of complexes **30** and **31** are consistent with the $\text{U}(\text{IV})/\text{U}(\text{IV})$ and $\text{U}(\text{IV})/\text{U}(\text{V})$ combinations, respectively. The presence of $\text{U}(\text{V})$ in complex **31** was unambiguously confirmed by S- and X-band EPR spectroscopies.

Moreover, antiferromagnetic $\text{U}(\text{IV})/\text{U}(\text{IV})$ coupling was suggested by a maximum at 60 K in the χ vs. T plot for complex **30**.

The uranium bridged nitrides **30** and **31** are chemically robust, and are reversibly interconverted by oxidation and reduction, respectively, with no evidence of C–H bond activation, which is instead observed with the analogous $\text{Th}(\text{IV})$ system (Section 3.1.3) indicating a lower reactivity of the uranium nitride.⁷⁸

More recently, the sterically bulkier $\text{Tren}^{\text{TIPS}}$ ($\text{N}(\text{CH}_2\text{CH}_2\text{-NSi}^i\text{Pr}_3)^3$) ligand, was utilized to stabilize the bridged $\text{U}(\text{IV})/\text{U}(\text{IV})$ bis-nitride complex, $[\text{Li}_4(\text{U}^{\text{IV}}(\text{Tren}^{\text{TIPS}}))_2(\mu\text{-N})_2]$ (**32**),⁸² which was obtained by reduction of the $\text{U}(\text{IV})$ azide precursor, $[\text{U}^{\text{IV}}(\text{Tren}^{\text{TIPS}})(\text{N}_3)]$ (**32a**) (Scheme 7), with excess metallic lithium (Li), and concomitant formation of the $\text{U}(\text{III})$ complex, $[\text{U}^{\text{III}}(\text{Tren}^{\text{TIPS}})]$. The solid-state structure of complex **32** comprises of a U_2N_2 diamond-shaped core, with a $\text{U}\cdots\text{U}$ distance of $3.404(1)\text{ \AA}$. Each nitride (N^{3-}) ligand is bridging two $\text{U}(\text{IV})$ centers, and both nitrides are bound to two Li cations, which seemingly facilitate formation of the $\text{U}^{\text{IV}}\text{-(}\mu\text{-N)}_2\text{-U}^{\text{IV}}$ bonds. Attempts to prepare high-valent species by addition of benzo-9-crown-3 ether (B9C3) or AgBPh_4 , resulted in exchange of the Li cation for a proton (H^+), converting complex **32** to the $\text{U}(\text{IV})/\text{U}(\text{IV})$ nitride-imido complex, $[\text{Li}_3(\text{U}^{\text{IV}}(\text{Tren}^{\text{TIPS}}))_2(\mu\text{-NH})(\mu\text{-N})]$ (**33**).⁸² The $\text{U-N}_{\text{nitride}}$ bond lengths of **32** ($2.153(2)\text{ \AA}$) and **33** ($2.171(4)\text{ \AA}$) are longer than in the $\text{U}(\text{IV})/\text{U}(\text{IV})$ bridging mono-nitride complexes ($1.95(1)\text{--}2.12(1)\text{ \AA}$), but are more consistent with the $\text{U}(\text{V})/\text{U}(\text{V})$ bis-nitride complex, $[\text{K}_2([\text{U}^{\text{V}}(\text{OSi}(\text{O}^t\text{Bu})_3)_2]_2(\mu\text{-N})_2)]$ (**9**) ($2.101(6)\text{--}2.022(5)\text{ \AA}$).⁷¹

Variable-temperature magnetic data for the $\text{U}(\text{IV})/\text{U}(\text{IV})$ bridging nitride complexes, **32** and **33**, revealed high, low-temperature magnetic moments, consistent with doubly degenerate ground states, where the effective symmetry of the strong crystal field of the nitride dominates over the spin-orbit coupled nature of the ground state multiplet of $\text{U}(\text{IV})$. Spin Hamiltonian modelling of the magnetic data for complexes, **32** and **33**, suggest $\text{U}\cdots\text{U}$ anti-ferromagnetic coupling of -4.1 and -3.4 cm^{-1} , respectively. Computational studies show a borderline case where the prospect of direct U-U bonding was raised, but high-level *ab initio* calculations revealed that if any U-U bonding is present, it is weak, and instead the bridging nitride ligands facilitate the $\text{U}\cdots\text{U}$ electronic communication.⁸² This is consistent with the strong antiferromagnetic coupling measured for the $\text{U}(\text{V})/\text{U}(\text{V})$ bis-nitride complex, $[\text{K}_2([\text{U}^{\text{V}}(\text{OSi}(\text{O}^t\text{Bu})_3)_2]_2(\mu\text{-N})_2)]$ (**9**).⁵²

Recently, Zhu and co-workers investigated the reactivity of $\text{U}(\text{IV})$ azide complexes supported by a phosphorus-substituted Tren ligand, ($\text{N}(\text{CH}_2\text{CH}_2\text{NP}^i\text{Pr}_3)^3$) = Tren^{NP} , containing three rigid N–P units.⁸³ Reaction of the $\text{U}(\text{IV})$ complex, $[\text{U}^{\text{IV}}(\text{Tren}^{\text{NP}})\text{Cl}]$, with NaN_3 led to the $\text{U}(\text{IV})/\text{U}(\text{IV})$ azide complex, $[(\text{U}^{\text{IV}}(\text{Tren}^{\text{NP}}))_2(\mu\text{-N}_3)_2]$ (**34a**). Subsequent addition of metallic Li





Scheme 7 Synthesis of uranium-nitrides supported by the triamidoamine ($\text{TREN}^{\text{DMBS}}$ and $\text{TREN}^{\text{TIPS}}$) or phosphorus-TREN (TREN^{NP}) ligands.

or sodium (Na) afforded the $\text{U}(\text{IV})/\text{U}(\text{IV})$ bridging nitride complexes, $[\text{Li}(\text{U}^{\text{IV}}(\text{Tren}^{\text{NP}}))_2(\mu\text{-N})]$ (**34-Li**) and $[\text{Na}(\text{THF})(\text{U}^{\text{IV}}(\text{Tren}^{\text{NP}}))_2(\mu\text{-N})]$ (**34-Na**), respectively (Scheme 7).⁸⁴ In contrast, the reduction with metallic K generated the $\text{U}(\text{IV})/\text{U}(\text{IV})$ complex, $[\text{K}_2(\text{U}^{\text{IV}}(\text{Tren}^{\text{NP}}))(\mu\text{-NH})_2]$, with two bridging imido ($\mu\text{-NH}^{2-}$) ligands linking the two uranium centers, while coordinated to the K cations. The X-ray diffraction structures of **34-Li** and **34-Na** are similar and both complexes exhibit an alkali metal-capped uranium nitride unit, $\text{MU}^{\text{IV}}\text{-N-U}^{\text{IV}}$ ($\text{M} = \text{Li}, \text{Na}$).⁸⁴ The U-N-U bond angle in complex **34-Na** ($127.8(2)^\circ$) is bent when compared to **34-Li** ($146.6(3)^\circ$), which could arise from the bound THF molecule coordinated to the Na cation in **34-Na**. Photolysis and thermolysis of $[(\text{U}^{\text{IV}}(\text{Tren}^{\text{NP}}))_2(\mu\text{-N}_3)_2]$ (**34a**), led to a $\text{U}(\text{IV})/\text{U}(\text{IV})$ ligand-insertion product, $[\text{U}^{\text{IV}}(\text{N}(\text{CH}_2\text{CH}_2\text{NP}^i\text{Pr}_2)_2(\text{CH}_2\text{CH}_2\text{NP}^i\text{Pr}_2\text{N}))_2]$ (**35**) (Scheme 7), in which a uranium-nitride intermediate was proposed by the authors for its formation.

3.1.3. Thorium nitrides from azide reduction

Thorium nitrides are less common than uranium nitrides, and until 2019, examples of thorium nitrides had only been isolated under cryogenic matrix conditions, such as ThN , NThN and NThO molecular species.^{30–32} Du, Liddle and co-workers reported the reduction of $\text{Th}(\text{IV})/\text{Th}(\text{IV})$ azide precursors supported by two different triamidoamine ligands, $[(\text{Th}^{\text{IV}}(\text{Tren}^{\text{DMBS}})(\mu\text{-N}_3)_3)]$ (**36a**) and $[\text{Th}^{\text{IV}}(\text{Tren}^{\text{TIPS}})(\text{N}_3)]$ (**37a**) ($\text{Tren}^{\text{DMBS}}$: $\text{N}(\text{CH}_2\text{-CH}_2\text{NSiMe}_2^t\text{Bu})_3^{3-}$; $\text{Tren}^{\text{TIPS}}$: $\text{N}(\text{CH}_2\text{CH}_2\text{NSi}^i\text{Pr}_3)_3^{3-}$), which generate highly nucleophilic and transient thorium-nitrides. These complexes were found to activate C-H bonds from various solvents, yielding parent $\text{Th}(\text{IV})/\text{Th}(\text{IV})$ bridging imido complexes, $[(\text{Th}^{\text{IV}}(\text{Tren}^{\text{DMBS}}))_2(\mu\text{-NH})]$ (**36**) and $[\text{M}_2\text{-}(\text{Th}^{\text{IV}}(\text{Tren}^{\text{TIPS}})(\mu\text{-NH}))_2]$ ($\text{M} = \text{Li}, \text{Na}, \text{K}, \text{Rb}, \text{Cs}$; **37-M**), respectively (Scheme 8a).^{78,85} These results provided the first evidence of transient $\text{Th}^{\text{IV}}=\text{N}=\text{Th}^{\text{IV}}$ species that could be generated by

chemical reduction of thorium azides; however, the transient thorium-nitride complex can easily activate C-H bonds of the solvent, or of the supporting $\text{Tren}^{\text{DMBS}}$ ligand, demonstrating that thorium-nitride bonds are highly reactive, and are more so than their uranium analogues. Indeed, DFT calculations suggested that the thorium complex contains more polar and ionic nuclear orbitals that comprise the ThNTh bonding interactions are destabilised by ~ 1.1 (σ) and ~ 0.4 (π) eV compared to the corresponding UNU orbitals. Instead, the first example of a dinuclear thorium nitride isolated in any significant quantity was prepared by Staun, Hayton and co-workers, *via* a synthetic approach that comprises of the reaction with a Th-NH_2 precursor (Section 3.2).⁸⁶

In 2022, Hsueh, Mazzanti and co-workers demonstrated that stable multimetallic thorium nitride complexes supported by $-\text{OSi}(\text{O}^t\text{Bu})_3$ ligands could be generated from the reduction of actinide azide precursors.⁸⁷ In fact, the reaction of the $\text{Th}(\text{IV})$ bridging azide complexes, $[\text{K}(\text{OSi}(\text{O}^t\text{Bu})_3)_3\text{Th}^{\text{IV}}(\mu\text{-N}_3)_3\text{-Th}^{\text{IV}}(\text{OSi}(\text{O}^t\text{Bu})_3)_3(\text{THF})]$ (**38a**) and $[\text{Cs}(\text{OSi}(\text{O}^t\text{Bu})_3)_3\text{Th}^{\text{IV}}(\text{N}_3)(\mu\text{-N}_3)_2\text{Cs}]_\infty$ (**39a**), with excess KC_8 or CsC_8 , respectively, at low temperatures generated the respective $\text{Th}(\text{IV})/\text{Th}(\text{IV})$ bridged-nitride complexes, $[\text{K}_3(\text{Th}^{\text{IV}}(\text{OSi}(\text{O}^t\text{Bu})_3)_3)_2(\mu\text{-N})(\mu\text{-N}_3)_2]$ (**38**) and $[\text{Cs}_3(\text{Th}^{\text{IV}}(\text{OSi}(\text{O}^t\text{Bu})_3)_3)_2(\mu\text{-N})(\mu\text{-N}_3)_2]$ (**39**) (Scheme 8b). A $\text{Th}(\text{IV})$ bridging-imido complex, $[\text{K}(\text{Th}^{\text{IV}}(\text{OSi}(\text{O}^t\text{Bu})_3)_3)_2(\mu\text{-NH})(\mu\text{-N}_3)]$ (**38b**), was also formed during the synthesis of **38**, showing that the nature of the alkali ion plays an important role in generating the nitride complex. The presence of three alkali ions bound to the nucleophilic nitride moiety provides high stability for the azide/nitride clusters, **38** and **39**, but the nature of the cation led to vast structural differences. The molecular structure of **38** exhibits a bent Th-N-Th angle ($114.4(3)^\circ$) with a short $\text{K-N}_{\text{nitride}}$ distance ($2.760(3)$ Å), while in complex **39**, the $\text{Th}^{\text{IV}}=\text{N}=\text{Th}^{\text{IV}}$ fragment adopts a linear geometry ($178.1(15)^\circ$) with a $\text{Cs-N}_{\text{nitride}}$ distance of (avg. $3.49(6)$ Å). The $\text{Th-N}_{\text{nitride}}$





Scheme 8 Synthesis of thorium (a) imidos and (b) nitrides supported by triamidoamine ($TREN^{DMBS}$ and $TREN^{TIP5}$) and siloxide ($-OSi(O^tBu)_3$) ligands, respectively.

bond lengths (**38**: 2.185(4) Å; **39**: avg. 2.13(5) Å) are shorter than those found in reported thorium bridging imido complexes,⁷⁸ but consistent with those found in the linear $Th^{IV}=N=Th^{IV}$ complex reported by Staun, Hayton and co-workers.⁸⁶

Computational studies of $Th^{(IV)}/Th^{(IV)}$ bridged nitrides demonstrated that the An–N–An bonding involves three-center-two-electron interactions of σ and π -type, with two Th–N σ bonds strongly polarized toward N (90%). However, some differences were also revealed from the theoretical calculations: in the bent nitride structure **38**, the π orbitals are lower in energy than the σ orbital, whereas in the linear nitride structure **39** the σ is the lowest one. The $\sigma > \pi$ phenomenon is known for terminal uranium nitrides^{43,44} and uranyl,^{88,89} and was recently reported for Th–nitrogen multiple bonds complexes and assigned to the “pushing from below effect”.⁸⁵

3.1.4. Other ligands

In 2015, Maria and co-workers reported the solid-state structure of a $U^{(IV)}/U^{(IV)}$ nitride-bridged complex supported by a bis-aryloxy cyclam ligand, $((^{tBu_2}ArO)_2Me_2-cyclam)^{2-}$.⁹⁰ Few crystals suitable for XRD analysis of the complex, $[(U^{IV}(\kappa^4-(^{tBu_2}ArO)_2Me_2-cyclam)(N_3))(\mu-N)](U^{IV}(\kappa^5-(^{tBu_2}ArO)_2Me_2-cyclam))]$ (**40**), were obtained from a NMR scale reaction of the $U^{(III)}$ precursor $[U^{III}(\kappa^6-(^{tBu_2}ArO)_2Me_2-cyclam)]I$ (**40a**) with CsN_3 in pyridine at room temperature (Scheme 9).⁹⁰ The asymmetric $U^{(IV)}/U^{(IV)}$ nitride complex **40** exhibits a U–N–U bond angle of 173.2(2)°, and U–N_{nitrido} bond distances of 2.086(3) and 2.035(3) Å, that are within the values reported for other mono-nitride bridged $U^{(IV)}/U^{(IV)}$ complexes (1.95(1)–2.09(1) Å).

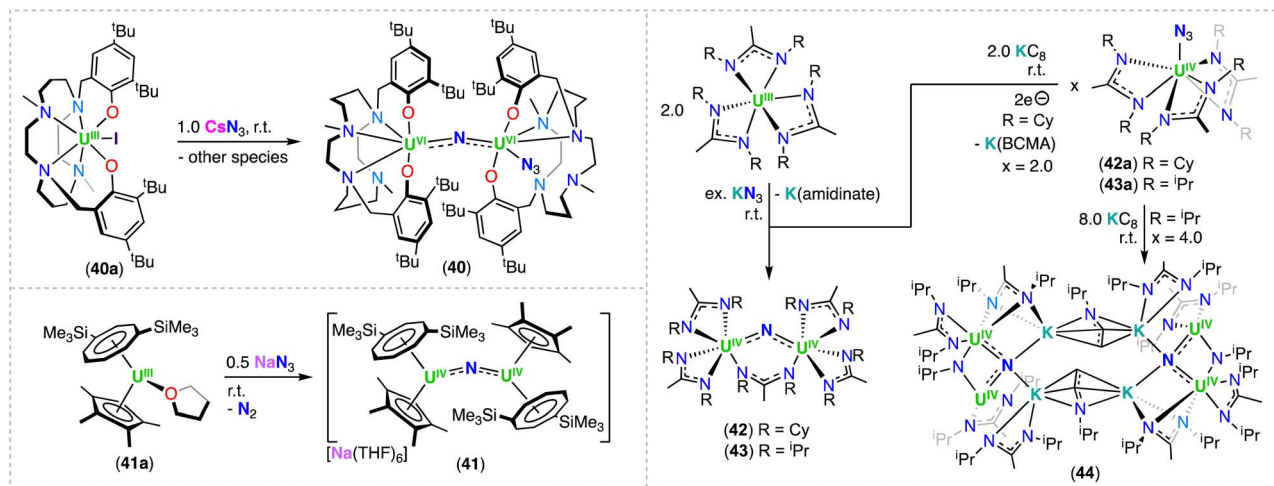
In 2016, Tsoureas, Cloke and co-workers reported an organometallic $U^{(IV)}/U^{(IV)}$ bridging nitride complex, $[Na(THF)_6][U^{IV}(\eta^8-C_8H_6(1,4-SiMe_3)_2(Cp^*))_2(\mu-N)]$ (**41**), by reacting the monometallic heteroleptic $U^{(III)}$ complex, $[U^{III}(\eta^8-C_8H_6(1,4-SiMe_3)_2)(Cp^*)]$ (**41a**), with NaN_3 at room temperature, leading to a delocalized $U^{IV}=N=U^{IV}$ bonding interaction (Scheme 9).⁹¹ Alternatively, with use of bulkier substituents, the same group was able to isolate a capped terminal nitride, $[Na(U^V(\eta^8-C_8H_6(1,4-Si^iPr_3)_2)(\eta^5-Cp^*))(\mu-N)]$ **66** (see Section 4.2; Scheme 13).

More recently, Straub, John Arnold and co-workers explored the ability of amidinate ligands to stabilize uranium nitride complexes. The homoleptic $U^{(III)}$ amidinate complexes, $[U^{III}(BCMA)_3]$ (BCMA = *N,N*-bis(Cy)methylamidinate) and $[U^{III}(BIMA)_3]$ (BIMA = *N,N*-bis(*t*Pr)methylamidinate), reduce KN_3 to give the diuranium complexes, $[(U^{IV}(BCMA)_2)_2(\mu-N)(\mu-\kappa^1:\kappa^1-BCMA)]$ (**42**) and $[(U^{IV}(BIMA)_2)_2(\mu-N)(\mu-\kappa^1:\kappa^1-BIMA)]$ (**43**), respectively (Scheme 9).⁹² The molecular structures of complexes **42** and **43** are similar, with the two $U^{(IV)}$ centers bridged by a nitride and a $\mu-\kappa^1:\kappa^1$ bound amidinato ligand, where the U–N_{nitrido} bond distances range from 2.023(3) to 2.057(3) Å. Complex **42** can also be obtained by reduction of the $U^{(IV)}$ azide complex, $[U^{IV}(BCMA)_3(N_3)]$ (**42a**), with 2.0 equiv. KC_8 . Alternatively, addition of excess KC_8 to $[U^{IV}(BCMA)_3(N_3)]$ (**43a**) led to the formation of a tetra- $U^{(IV)}$ cluster incorporating two $U^{IV}-N-U^{IV}$ fragments, $[K(U^{IV}(BIMA)_2(\mu-N^iPr))_2(\mu-N)(\mu-\eta^3:\eta^3-CH_2CHN^iPr)]_2$ (**44**). Interestingly, the solid-state structure of **44** also revealed the presence of imido ($(N^iPr)^{2-}$) and vinylamido ($(CH_2CHN^iPr)^-$) ligands formed by amidinate cleavage. In the structure of **44** all four uranium atoms are N-bound to ligands having formal mono-, di-, and tri-anionic character. Overall, **44** is stabilized by additional interactions of K cations with the nitride and amidinato ligands.⁹² Preparation of the isotopically enriched complexes, ^{15}N -**42** and ^{15}N -**43**, and acidification with acid (H^+) to $^{15}NH_4^+$, and IR spectroscopic analysis, allowed confirmation of the presence the bridging nitride ligand.⁹² This study provides a rare example in which uranium nitride complexes could be isolated by reduction of a $U^{(IV)}$ precursor with alkali ions, where this methodology was previously unsuccessful in generating uranium nitride complexes.

3.2. Reactions involving NH_3 and derivatives

In 2019, Staun, Hayton and co-workers reported the first molecular thorium nitride isolated outside low temperature matrices.⁸⁶ The $Th^{(IV)}/Th^{(IV)}$ bridged nitride complex, $[Na(18C6)(Et_2O)][Th^{IV}(N(SiMe_3)_2)_2(\mu-N)]$ (**45-Na**), was obtained from addition of 1.0 equiv. $NaNH_2$ to the metallacycle, $[Th^{IV}(N(SiMe_3)(SiMe_2CH_2))(N(SiMe_3)_2)_2]$ (**46**),⁹³ in the presence





Scheme 9 Synthesis of uranium-nitrides supported by other ligand systems.

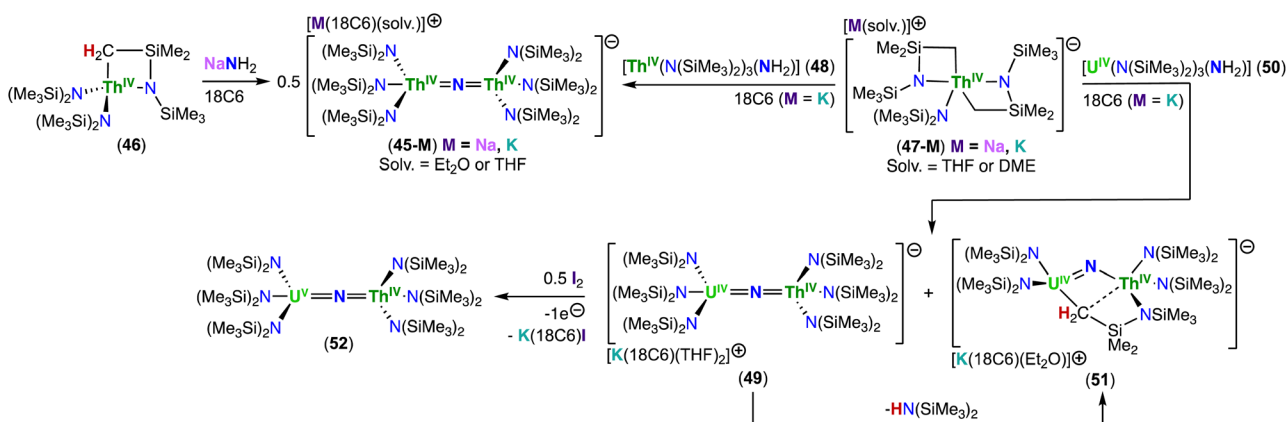
of 18-crown-6 (18C6) (Scheme 10).⁸⁶ Based on mechanistic studies, the authors suggested that the first step is the deprotonation of **46** with NaNH_2 , which results in the thorium bis-metallacycle complex, $[\text{Na}(\text{THF})_x][\text{Th}(\text{N}(\text{SiMe}_3)(\text{SiMe}_2\text{CH}_2))_2(\text{N}(\text{SiMe}_3)_2)]$ (**47-Na**), and NH_3 . Then, NH_3 reacts with another molecule of **46** to create the $\text{Th}(\text{IV})\text{-NH}_2$ complex, $[\text{Th}^{\text{IV}}(\text{N}(\text{SiMe}_3)_2)_3(\text{NH}_2)]$ (**48**), which protonates complex **47-Na** to produce the thorium nitride complex **45-Na** (mechanistic scheme not shown here). This hypothesis was supported by the reaction of **48** with the bis-metallacycle complex **47-K**⁹⁴ in the presence of 18-crown-6, which led to the formation of $[\text{K}(18\text{c}6)(\text{THF})_2][(\text{Th}(\text{N}(\text{SiMe}_3)_2)_3)_2(\mu\text{-N})]$ (**45-K**).⁸⁶

The solid-state structure of complex **45-M** ($\text{M} = \text{Na}, \text{K}$) exhibits a linear Th-N-Th bond angle ($179(1)^\circ$), and the $\text{Th-N}_{\text{nitride}}$ bond lengths (2.14(2) and 2.11(2) Å) are much shorter than the $\text{Th-N}_{\text{silylamido}}$ bond lengths (avg. 2.41 Å), consistent with Th-N multiple bond character. NBO/NLMO analysis revealed two orthogonal π bonds and two predominant σ bonds in Th-N-Th bonding, with σ -bonding having three-center character, consistent with $\text{Th}=\text{N}$ double bonds. Covalency in the $\text{Th-N}_{\text{nitride}}$ bonds in **45-M** was found to be larger than that

reported for the $\text{Th-N}_{\text{imido}}$ in $[\text{Th}^{\text{IV}}(\text{NAr}^{\text{iPr}2})(\text{N}(\text{SiMe}_3)_2)_3]^-$ ($\text{Ar}^{\text{iPr}2} = 2,6\text{-iPr}_2\text{C}_6\text{H}_3$)⁹⁴ and for the Th-O_{oxo} in $[\text{Th}(\text{O})(\text{N}(\text{SiMe}_3)_2)_3]^-$,⁹⁵ with a greater participation of the 5f orbital in bonding and higher Wiberg bond index.

¹⁵N NMR spectroscopy was also used for the first time to evaluate $\text{Th-N}_{\text{nitride}}$ bond covalency. To achieve that, the isotopically enriched analogues of complexes **48** and **45-K** were prepared. The thorium nitride ¹⁵N-**45-K** was obtained in low yield by addition of ¹⁵NH₄Cl to complex **47-K**. Whereas, $[\text{Th}^{\text{IV}}(\text{N}(\text{SiMe}_3)_2)_3(^{15}\text{NH}_2)]$ (¹⁵N-**48**) was isolated from the reaction of **46** with 1.0 equiv. of ¹⁵NH₃ gas. The solution-state ¹⁵N NMR spectroscopy chemical shifts of the bridging nitride in ¹⁵N-**45-K** appeared at 298.8 ppm (referenced to CH_3NO_2), whereas the ¹⁵N resonance of the ($-\text{NH}_2^-$) in ¹⁵N-**48** appeared at -198.4 ppm. The magnitude of the downfield shift correlates with the degree of 5f character in the An-N bond, which is lower in **48**.⁸⁶ Similar conclusions about covalency were achieved when the ¹⁵N NMR solid-state spectra of ¹⁵N-**48** and ¹⁵N-**45-K** were measured.⁹⁶

Using a similar synthetic approach to the one used for the synthesis of **45-K**, Staun, Hayton and co-workers also prepared

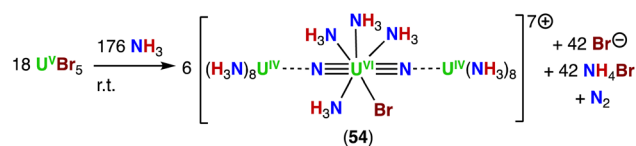
Scheme 10 Synthesis of thorium- and uranium-thorium nitrides supported by the amide ($-\text{N}(\text{SiMe}_3)_2$) ligands via amine derivatives.

the first mixed-actinide nitrides.⁹⁷ The Th(IV)/U(IV) complex, $[\text{K}(\text{18C6})(\text{THF})_2][\text{N}(\text{SiMe}_3)_2]_3\text{U}^{\text{IV}}(\mu\text{-N})\text{Th}^{\text{IV}}(\text{N}(\text{SiMe}_3)_2)_3]$ (**49**), was isolated in moderate yield from the reaction of complex **47-K**⁹⁴ with the U(IV)-NH₂ complex, $[\text{U}^{\text{IV}}(\text{N}(\text{SiMe}_3)_2)_3(\text{NH}_2)]$ (**50**), previously prepared by reaction of the uranium metallacycle $[\text{UN}(\text{SiMe}_3\{\text{SiMe}_2\text{CH}_2\})\{\text{N}(\text{SiMe}_3)_2\}_2]$ with NH₃, in the presence of 18-crown-6. The cyclometallate mixed-actinide nitride complex, $[\text{K}(\text{18c6})][\text{K}(\text{18c6})(\text{Et}_2\text{O})_2][\text{N}(\text{SiMe}_3)_2]_2\text{U}^{\text{IV}}(\mu\text{-N})(\mu\text{-}\kappa^2\text{-C,N-CH}_2\text{SiMe}_2\text{NSiMe}_3)\text{Th}^{\text{IV}}(\text{N}(\text{SiMe}_3)_2)_2]$ (**51**), was also isolated from the reaction mixture, and was thought to proceed through a similar pathway as the analogous cyclometallate U(IV)/U(IV) nitride complex **16**.⁴⁰ Oxidation of **49** with 0.5 equiv. of iodine afforded the U(v)/Th(IV) bridged nitride $[\text{N}(\text{SiMe}_3)_2]_3\text{U}^{\text{V}}(\mu\text{-N})\text{Th}^{\text{IV}}(\text{N}(\text{SiMe}_3)_2)_3]$ (**52**) (Scheme 10).⁹⁷

The solid-state molecular structure of the mixed-actinide Th(IV)/U(IV) bridging nitride complex **49** showed that the uranium and thorium atoms are mutually disordered over both actinide sites in a 50 : 50 ratio. The An-N-An moiety is linear, while the An-N_{nitride} bond length is 2.1037(9) Å.⁹⁷ The Th(IV)/U(IV) cyclometallate complex **51** displays a bent U-N-Th angle (122.2(2)°), a U-N_{nitride} bond length of 2.002(4) Å, and a Th-N_{nitride} bond length of 2.160(5) Å.⁹⁷ Comparable crystallographic data were observed for the isostructural U(IV)/U(IV) analogue, complex **16**,⁴⁰ which is indicative of a localized Th-N=U bonding motif. In the solid-state structure of **52**, the uranium and thorium atoms were refined over both metal sites in a 50 : 50 ratio, resulting in An-N_{nitride} bond lengths of 2.10(1) Å and 2.17(1) Å, and a U-N-Th bond angle of (177.9(6)°), which can be compared with those observed for the U(IV)/U(V) nitride complex, $[(\text{U}^{\text{IV/V}}(\text{N}(\text{SiMe}_3)_2)_3)_2(\mu\text{-N})]$ (**17**), with bond metrics of 2.080(5), 2.150(5) Å and 179.4(3)°, respectively.⁷⁶

The disorder found in the structure of **49** did not definitively confirm the presence of Th and U in the molecule, however, preparation of the Th(IV)/U(V) bridged nitride **52** from complex **49**, coupled with spectroscopic analysis, reinforced the hetero-bimetallic formulation of **52**. A comparative study with the U(V) Li-capped nitride complex, $[\text{Li}(\text{12C4})(\text{U}^{\text{V}}(\text{Tren}^{\text{TIPS}})(\mu\text{-N}))]$ (**64-Li**),⁹⁸ based on EPR spectroscopy, SQUID magnetometry, NIR-visible spectroscopy, and crystal field analysis supported the presence of a U(V) ion in **52**. Moreover, the study demonstrated that the energies of the 5f orbitals of the U(V)/Th(IV) bridged nitride complex **52** are essentially determined by the strong ligand field of the nitride ligand.

In 2020, Rudel, Kraus and co-workers described the first crystallographically authenticated complexes incorporating the linear N=U=N moiety, isoelectronic to the uranyl cation, prepared outside matrix conditions.⁶⁵ Three closely related molecular uranium nitrides were prepared by reaction of uranium pentahalides UCl₅ or UBr₅ with anhydrous liquid NH₃ (Scheme 11), instead of an azide (N₃⁻) precursor, which is the most commonly utilized pathway to produce actinide nitrides. In the structures of the trinuclear complexes, $[\text{U}_3(\mu\text{-N})_2(\text{NH}_3)_{21}]^{8+}$ (**53**), $[\text{U}_3\text{Br}(\mu\text{-N})_2(\text{NH}_3)_{20}]^{7+}$ (**54**), and $[\text{U}_3\text{Cl}_2(\mu\text{-N})_2(\text{NH}_3)_{19}]^{6+}$ (**55**), the N-U_{center}-N angle is nearly linear and the U(VI)_{center} is coordinated by five additional ligands (NH₃, Cl⁻ or Br⁻) in a pentagonal bipyramidal geometry, which is regularly found in complexes of uranyl (UO₂²⁺). Additionally, each nitride



Scheme 11 Synthesis of uranium-nitrides *via* ammonia (NH₃) addition.

ligand binds a $[\text{U}(\text{NH}_3)_8]^{4+}$ fragment, forming almost linear trinuclear complex cations.

The U_{center}-N_{nitrido} bond distances in the three compounds are similar, with an average value of 1.84(4) Å that is longer than those calculated at the CASPT2 level for $[\text{N}\equiv\text{U}\equiv\text{N}]$ (1.73 Å),²⁴ but close to the terminal U^{VI}≡N triple bond of the uranium complex with the Tren^{TIPS} supporting ligand reported by Liddle and co-workers (Section 4.2).⁴⁴ The U^{IV}-N_{nitrido} bond distances in complexes **53–55** (2.235(5) to 2.392(8) Å) are longer than those found in the single-bonded U(IV) nitride complex, $[(\text{U}^{\text{IV}}\text{Cp}^*(\mu\text{-I})_2)_3(\mu\text{-N})]$ (2.138(3) to 2.157(3) Å),⁶⁷ consistent with less donation of the nitride ligand to the terminal U(IV) ions. Quantum chemical calculations, as well as Raman and infrared spectroscopy studies of the ¹⁴N/¹⁵N-complexes of $[\text{U}_3\text{Br}(\mu\text{-N})_2(\text{NH}_3)_{20}]^{7+}$ (**54**), support the presence of two U-N triple bonds in the *trans*-(N≡U^{VI}≡N) core.

The formation of the three U(VI) bis-nitride complexes was proposed to proceed *via* disproportionation of the U(V) precursor in NH₃ to U(IV) and U(VI) species. The authors suggest that some NH₃ is oxidized by such a U(VI) species to N₂, while formation of the trinuclear U complexes **53–55** proceeds *via* deprotonation of ammine ligands. The resulting nitrido ligands stabilize the central U(VI) species, while the nitrido complexes are stabilized by the coordination of $[\text{U}(\text{NH}_3)_8]^{4+}$ complexes.

3.3. Other methods

Li, Chen and co-workers reported the first actinide-nitride fullerene cluster, U₂N@I_h(7)-C₈₀ (**56**),⁹⁹ which was produced by a modified Krätschmer-Huffman DC arc-discharge method.¹⁰⁰ Graphite rods, packed with U₃O₈ and graphite powders, were vaporized in the arcing chamber under helium atmosphere with 1 torr NH₃, and after work-up, the cluster was isolated and fully characterized by single X-ray crystallography and multiple other spectroscopic methods. The stabilization of this uranium-nitride cluster demonstrated that the combination of the unique properties of actinides and the special chemical environment inside the fullerene cage allows stabilization of a bimetallic uranium nitride moiety.

The U=N=U encaged moiety exhibits an angle of 150.0(2)°, which is significantly bent when compared with other diuranium bridged mono-nitride compounds supported by chelating ligands, in which the U-N-U units adopt close to linear configurations. The bent angle was rationalized to have resulted from the steric effect of encapsulation in the C₈₀ cage. The two U-N bond distances are inequivalent (2.058(3) Å and 1.943(3) Å), creating an unsymmetrical bonding. The shortest U-cage distances range from 2.448(4) to 2.543(5) Å. Although the U-N_{nitride} bond distances are shorter, the U=N=U bonding



resemble that of the U(IV)/U(V) nitride complex **17**, reported by the Mazzanti group, where the two different U–N_{nitride} bond lengths are the result of localized valences.⁷⁶ Computational studies combined with X-ray absorption spectroscopy suggest two uranium ions with different oxidation states of U(IV) and U(V). Quantum-chemical investigation further revealed that f¹/f² population dominantly induces a distortion of the U=N=U moiety, which leads to the unsymmetrical structure. A comparative study of U₂X@C₈₀ (X = C, N and O) revealed that the U–X interaction in the U=X=U clusters can hardly be considered as classical multiple bonds, but is more like an anionic central ion Xⁿ⁻ with biased overlaps with the two metal ions, which decrease as the electronegativity of the ligand X increases.⁹⁹

4. Terminal and Lewis acid-capped nitride actinide complexes

4.1. Seminal studies and putative terminal nitrides

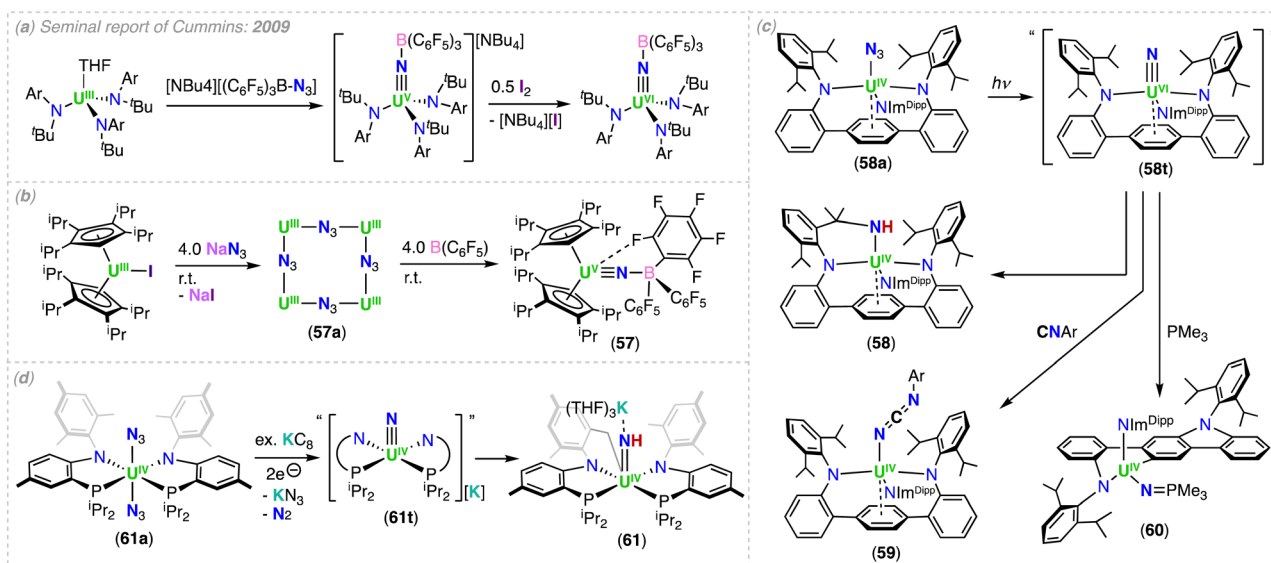
The synthesis of terminal nitrides has been a long sought-after target in actinide chemistry because of the potential reactivity and fundamental relevance in the study of An–N multiple bonds. The most typical route to generate terminal nitride species involves the reaction of azide (N₃⁻) anions with reducing metal complexes containing bulky ligands, in order to prevent the formation of bridging nitrides (Section 3), however, an alternative route involves the photolysis of terminally bound azides ligands.

Seminal studies (2009) from the Cummins group led to the isolation of the first uranium nitridoborate complexes, [NBu₄][U^V((μ-N)B(C₆F₅)₃)(N^tBu)](3,5-Me₂C₆H₃)₃] and the U(VI) analogue, that could also be viewed as borane-capped uranium nitrides.¹⁰¹ Related to this work, in 2020, Boren, John Arnold and co-workers reported the reaction of [U^{III}(Cp^{Pr})₂I] with NaN₃, yielding an unusual U(III) azide-bridged tetrameric

complex, [(Cp^{Pr})₂U^{III}(μ-η¹:η¹-N₃)₄] (57a), but the subsequent addition of a strong Lewis acid, B(C₆F₅)₃, results in loss of N₂ and trapping of a nitride fragment, forming the U(V) nitridoborate complex, [U^V(Cp^{Pr})₂(μ-N)B(C₆F₅)₃] (57) (Scheme 12).¹⁰² The metrical parameters of **57** are comparable to the borane-capped complex, [NBu₄][U^V((μ-N)B(C₆F₅)₃)(N^tBu)](3,5-Me₂C₆H₃)₃], reported by Cummins. This result highlights that not all U(III) complexes necessarily reduce the coordinated azide ligand, but reduction of the azide can be promoted by the presence of a strong Lewis acid.

The isolation of uncapped terminal nitrides became more attainable with the first report by Kiplinger and co-workers, in which they proposed a transient terminal nitride generated by photolysis of a U(IV) azide complex.⁴⁵ This study demonstrated that nitrides are photochemically accessible, but suggested an inherent instability and highlighted the very high reactivity of terminal nitrides towards C–H activation of supporting ligands. This work inspired more recent studies, in which the aim has been to utilize more robust, bulky ligand frameworks, and properly tune reaction conditions. However, this task remains far from trivial, in which isolated terminal nitrides are still limited to primarily three ligand systems (Section 4.2).

Recently, Yadav, Fortier and co-workers reported the photolytic production of a putative terminal nitride that can access both intra- and intermolecular chemistry.⁴⁷ Photolysis of the U(IV) azide complex, [U^{IV}(L^{Ar})(NIm^{Dipp})(N₃)] (58a) ((L^{Ar})²⁻ = 2,2'-bis(2,6-diisopropylanilide)-*p*-terphenyl and (NIm^{Dipp})⁻ = 1,3-bis(Dipp) imidazolin-2-iminato), generated the U(IV) amido complex, [U^{IV}(N–L^{Ar})(NIm^{Dipp})] (58). The formation of complex **58**, was rationalized in terms of the intramolecular insertion of the terminal nitride group of the transient U(VI)-nitride, “[U(L^{Ar})(N)(NIm^{Dipp})]” (58t), into a C–H bond of a pendant isopropyl group of the bis-anilide terphenyl ligand (Scheme 12). Furthermore, formation of the putative terminal nitride is supported by its intermolecular capture during the photolysis of



Scheme 12 Synthesis of putative uranium-nitrides (a)–(d).



complex **58a** in the presence of an isocyanide (CNAr) or PMe_3 , to give the U(IV)-imine products, $[\text{U}^{\text{IV}}(\text{L}^{\text{Ar}})(\text{NCN}(\text{C}_6\text{H}_3\text{-Me}_2))(\text{-NIm}^{\text{Dipp}})]$ (**59**) and $[\text{U}^{\text{IV}}(\text{N},\text{C-L}^{\text{Ar}})(\text{N}=\text{PMe}_3)(\text{NIm}^{\text{Dipp}})]$ (**60**), respectively (Scheme 12).⁴⁷ The formation of complex **60** is associated with a major structural rearrangement, which was suggested to arise from the steric congestion resulting from formation of the phosphinimide, which subsequently resulted in various unidentified chemical events that gives the complicated reaction mixture containing **60**.

An alternative mechanism for the intramolecular C–H activation *via* a transient terminal nitride was reported by Mullane, Schelter and co-workers.¹⁰³ The transient uranium terminal nitride moiety, generated from the reduction of the U(IV) bis-azide precursor, $[\text{U}^{\text{IV}}(\text{PN})_2(\text{N}_3)_2]$ (**61a**), with KC_8 led to the parent imido complex, $[\text{U}^{\text{IV}}(\text{PN})(\text{tPr}_2\text{P}(\text{C}_6\text{H}_3\text{Me})\text{N}-\text{C}_6\text{H}_2\text{Me}_2-\text{CH}_2)(\mu\text{-NH})\text{K}(\text{THF})_3]$ (**61**); $(\text{PN})^- = (\text{N}(2\text{-diisopropylphosphino})\text{-4-methylphenyl})\text{-2,4,6-trimethylanilide}$, with a very short $\text{U}=\text{NH}$ bond length (1.997(2) Å). Calculated reaction energy profiles strongly suggested that the transient terminal U(IV) nitride, “[K][$(\text{PN})_2\text{-U}^{\text{IV}}(\text{N})$]” (**61t**), engages in an unprecedented 1,2-addition of a C–H bond, instead of a reductive C–H insertion, in a distinct reaction pathway than previously observed for other uranium nitride complexes.^{44,45}

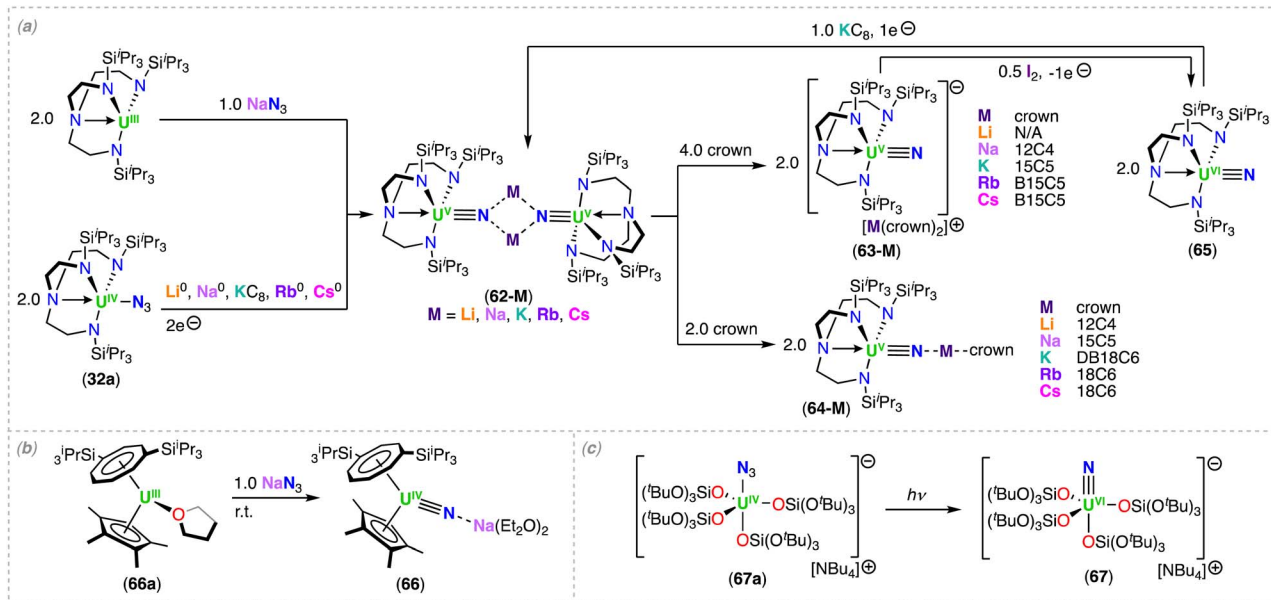
4.2. Isolated terminal nitrides

In 2012, King, Liddle and co-workers described the first isolated molecular terminal uranium nitride complex synthesized under conventional experimental techniques.⁴³ The $2e^-$ oxidation of the monometallic U(III) complex, $[\text{U}(\text{Tren}^{\text{TIPS}})]$, supported by the sterically demanding ligand $\text{Tren}^{\text{TIPS}}$, with NaN_3 allowed the

isolation of the dimeric U(V)/U(V) complex, $[\text{Na}_2(\text{U}^{\text{V}}(\text{Tren}^{\text{TIPS}})(\mu\text{-N}))_2]$ (**62-Na**), where both N^{3-} ligands are stabilized by bridging Na cation interactions (Scheme 13a). Sequestration and encapsulation of the Na cations with 4.0 equiv. of 12-crown-4 (12C4) generated the first terminal U(V) nitride complex, $[\text{Na}(12\text{C4})_2][\text{U}^{\text{V}}(\text{Tren}^{\text{TIPS}})(\text{N})]$ (**63-Na**), with a $\text{U-N}_{\text{nitride}}$ bond length of 1.825(15) Å (Scheme 13a). In contrast, treatment of **62-Na** with 15-crown ether (15C5), resulted in the U(V) nitride-capped complex, $[\text{Na}(15\text{C5})(\text{U}^{\text{V}}(\text{Tren}^{\text{TIPS}})(\mu\text{-N}))]$ (**64-Na**), where the nitride ligand is capped by the Na cation.⁴⁴ Oxidation of **63-Na** with I_2 resulted in the clean formation of the first terminal U(VI) nitride complex, $[\text{U}^{\text{VI}}(\text{Tren}^{\text{TIPS}})(\text{N})]$ (**65**) (Scheme 13a).⁴⁴ Attempts to prepare the analogous U(IV) terminal nitride afforded the uranium terminal parent imido complex, $[\text{K}(15\text{C5})_2][\text{U}^{\text{IV}}(\text{Tren}^{\text{TIPS}})(\text{NH})]$, which can also be viewed as a masked U(IV) terminal nitride. The high nucleophilic character of the nitride moiety prevented its isolation in the used reaction conditions.⁴³

In a later study, the authors prepared a library of alkali metal-capped dimeric U(V) nitride complexes, $[\text{M}_2(\text{U}(\text{Tren}^{\text{TIPS}})(\mu\text{-N}))_2]$ (**62-M**) ($\text{M} = \text{Li}, \text{K}, \text{Rb}$ and Cs), by reduction of the terminal U(VI) nitride (**65**) with KC_8 , or by reduction of the U(IV) azide (**32a**) with Li, Na, KC_8 , Rb, or Cs (Scheme 13a).^{46,98} Carefully tuning the addition of a variety of crown ethers to **62-M**, affording either the U(V) terminal- or capped-nitride complexes, $[\text{M}(\text{crown})_2][\text{U}^{\text{V}}(\text{Tren}^{\text{TIPS}})(\text{N})]$ (**63-M**) or $[\text{M}(\text{crown})(\text{U}^{\text{V}}(\text{Tren}^{\text{TIPS}})(\mu\text{-N}))]$ (**64-M**) ($\text{M} = \text{Li}, \text{Na}, \text{K}, \text{Rb}, \text{Cs}$), respectively.⁹⁸

The nitride complexes, **62-M** ($\text{M} = \text{K}, \text{Rb}, \text{Cs}$), were also reported to be generated together with a U(III)-amide complex, $[\text{M}][\text{U}^{\text{III}}(\text{Tren}^{\text{TIPS}})(\text{NH}_2)]$ ($\text{M} = \text{K}, \text{Rb}, \text{Cs}$), by disproportionation of the U(IV)-imido complex, $[(\text{U}^{\text{IV}}(\text{Tren}^{\text{TIPS}})(\mu\text{-NH})(\mu\text{-M}))_2]$, in moderate heating.¹⁰⁴ This reaction was facilitated by benzene,



Scheme 13 Synthesis of (a) alkali-capped and terminal uranium-nitrides supported by the triamidoamine ($\text{Tren}^{\text{TIPS}}$) ligands; (b) organometallic alkali-capped uranium(V)-nitride; (c) terminal uranium(VI)-nitride supported by siloxide ($-\text{OSi}(\text{O}^t\text{Bu})_3$) ligands.



but not toluene, as benzene was found to engage in further redox chemistry with the $[M][U^{III}(\text{Tren}^{\text{TIPS}})(\text{NH}_2)]$ complex ($M = \text{K, Rb, Cs}$), generating $[U^{IV}(\text{Tren}^{\text{TIPS}})(\text{NH}_2)]$, and concomitant reduced arene, $[M][C_6H_6]$ ($M = \text{K, Rb, Cs}$). This process occurred with the K, Rb, and Cs cation complexes, but not with Li or Na, reflecting the stability of the corresponding alkali metal-arene byproducts.

The U–N_{nitride} bond distances in the terminal U(v) nitride complexes, **63-M**, range from 1.801(3) to 1.825(15) Å, while the U–N_{nitride} bond length of the terminal U(vi) nitride complex **65** (1.799(7) Å) is statistically equivalent with these distances, and can be explained by the fact that a non-bonding 5f-electron is removed upon oxidation from U(v) to U(vi).

The structural assignment of the uranium nitrides **62-M** to **65** was supported by electronic absorption spectroscopy, EPR, magnetometry, electronic structure calculations, and ¹⁵N-isotopic labelling.^{43,44,46,98} The uranium(v) nitrides behave as single-molecule magnets (SMMs); the first uranium SMM was reported in 2009,¹⁰⁵ involving a U(III) complex, whereas two examples involving U(v) ions were reported in a later study^{106,107} The observed ¹⁴N/¹⁵N isotopomer shift for the U–N_{nitride} IR stretching frequencies range from 955 to 930 cm⁻¹, 936 to 900 cm⁻¹, and 914 to 883 cm⁻¹, respectively for complexes, **62-Na**, **64-Na**, and **65**, where the corresponding ¹⁵N-labelled complexes are consistent with the nitride terminal formulation.^{43,44} DFT calculations for the terminal uranium nitride complexes reveal similar composition for the U≡N bond in the two uranium oxidation states (+5 and +6). One σ and two π bonds are present in the U–N interaction, in agreement with a formal U≡N triple bond. Like in the uranyl (UO₂²⁺) case,¹⁰⁷ the σ component is higher in energy than the π, whereas uranium-imido complexes follow the normal energetic ordering of π > σ. This energetic ordering is suggested to occur due to the terminal U–N_{nitride} bond manifesting an antibonding interaction between a σ-orientated nitrogen p-orbital overlapping with the toroidal 5f and 6d lobes on uranium. QAIM analysis of the U(v) and U(vi) Tren^{TIPS} terminal-nitrides and isoalent group 6 nitrides suggested that the level of covalency in U≡N bonds are comparable with those in group 6 transition-metal nitride complexes, or even greater.⁴⁴ Moreover, the authors evaluated the covalency of the terminal U(vi)-nitride ¹⁵N-**65** by ¹⁵N nuclear magnetic resonance spectroscopy and found an exceptional nitride chemical shift (δ 968.9 ppm referenced to CH₃NO₂) and chemical shift anisotropy.¹⁰⁸ Recently, two U(vi) imido complexes were also characterized by ¹⁵N NMR spectroscopy and revealed lower downfield shifts (δ 302.4 and 256.7 ppm referenced to CH₃NO₂) as expected for U=NR bonding.¹⁰⁹ Computational benchmarking of the ¹⁵N NMR spectroscopy analysis of ¹⁵N-**65** showed that the large chemical shift results from a large contribution of the σ paramagnetic component (almost negligible contribution of the spin orbital coupling component σ^{SO}) resulted from the U≡N triple bond σ and π components. In addition, this work enabled to build a predictive M-ligand isotropic ¹⁵N chemical shift-bond order correlations to guide future studies on understanding of An–N bonding.¹⁰⁸

In 2016, Tsoureas, Cloke and co-workers reported a new example of the Na-capped U(v) terminal-nitride stabilized by (COT)²⁻ and (Cp*)¹⁻ ligands. This work confirmed the importance of steric factors in determining the formation of terminal *versus* bridging nitride complexes. The sodium-capped U(v) nitride complex, $[\text{Na}(\text{U}^{\text{V}}(\eta^8\text{-C}_8\text{H}_6(1,4\text{-Si}^i\text{Pr}_3)_2)(\eta^5\text{-Cp}^*))(\mu\text{-N})]$ (**66**), was obtained by treating the U(III) mixed sandwich complex, $[\text{U}^{\text{III}}(\eta^8\text{-C}_8\text{H}_6(1,4\text{-Si}^i\text{Pr}_3)_2)(\eta^5\text{-Cp}^*)]$ (**66a**), with NaN₃ (Scheme 13b).⁹¹ The steric protection afforded by the bulky –SiⁱPr₃ substituents on the COT ligand help in facilitating a 2e⁻ oxidation of a single U(III) center. However, when the steric hindrance around the uranium center is reduced, for example, by the use of less bulky substituents, the U(IV)/U(IV) bridged nitride complex, $[\text{Na}(\text{THF})_6][(\text{U}^{\text{IV}}(\eta^8\text{-C}_8\text{H}_6(1,4\text{-SiMe}_3)_2)(\text{Cp}^*))_2(\mu\text{-N})]$ (**41**), could be isolated instead (Scheme 9).⁹¹

Photolysis of alkali-metal azide (MN₃) complexes has been an effective route for the synthesis and isolation of terminal metal nitrides with transition metals.^{110–114} However, this strategy, until recently, had not been successful to generate stable terminal actinide nitride complexes. Photolysis of U(IV) azides with bulky amide supporting ligands such as, Tren^{TIPS} and bis(anilide) terphenyl (LAR)²⁻ (2,2'-bis(2,6-diisopropylanilide)-p-terphenyl), also failed in producing terminal uranium-nitrides, and in its place, intramolecular insertion of the nitride in the ligand framework was observed.^{44,47}

Recently, Barluzzi, Mazzanti and co-workers, by carefully tuning the reaction conditions and by using the sterically crowded monometallic U(IV) azide precursor, $[\text{NBu}_4][\text{U}^{\text{IV}}(\text{OSi}(\text{O}^i\text{Bu})_3)_4(\text{N}_3)]$ (**67a**), were able to generate the first stable U(vi) terminal-nitride by photochemical synthesis (Scheme 13c).¹¹⁵ Complex $[\text{NBu}_4][\text{U}^{\text{VI}}(\text{OSi}(\text{O}^i\text{Bu})_3)_4(\text{N})]$ (**67**) exhibits a U–N_{nitride} bond length of 1.769(2) Å, that is slightly shorter than the only other isolated U(vi) terminal-nitride complex, $[\text{U}^{\text{VI}}(\text{Tren}^{\text{TIPS}})(\text{N})]$ (**65**) (1.799(7) Å),⁴⁴ and compares with the calculated U–N distance for the matrix-isolated nitride $[\text{UNF}_3]$ (1.759 Å).²⁶

This work provided the second example of a terminal U(vi) nitride, and showed that these complexes can be prepared by photolysis, however, the steric contributions of the uranium-azide precursors, and the type of anionic azide utilized, should be carefully considered in order to maximize stability. Despite the stability of **67** under ambient conditions, the terminal nitride displays high reactivity towards electrophiles (Section 6.1).

4.3. Other methods

Charged U≡N diatomic species captured in fullerene cages, UN@Cs(6)-C82 (**68**) and UN@C2(5)-C82 (**69**), were synthesized by a modified Krätschmer–Huffman DC arc-discharge method¹⁰⁰ using a mixture of U₃O₈ and graphite powders deposited into hollow graphite rods, and reacting in a arcing chamber under He and N₂ atmosphere.¹¹⁶ X-ray crystallographic analysis of the isolated crystals showed short U–N bond lengths of 1.760(7) and 1.760(20) Å for complexes **68** and **69**, respectively, which are very close to those calculated for gas phase molecules and clusters obtained only in low temperature matrix-isolation conditions, such as U≡N, N≡UF₃ and N≡UNH.^{23,26,31} Quantum-chemical calculations were consistent



with a f^1 electronic structure for uranium and the presence of a $U^V \equiv N$ triple bond in the cluster fullerenes. This work establishes an approach to study fundamentally important actinide multiply bonded species.

5. Heterometallic actinide/transition metal nitride complexes

In 2022, Mazzanti, Agapie, and co-workers reported the first example of a heterometallic uranium-transition metal nitride complex, $[Na(U(OSi(O^tBu)_3)(\mu-N)(MoP_2))]$ (**70**) (P_2 = terphenyl diphosphine ligand), generated from partial N-transfer to the $U(III)$ precursor, $[U^{III}(OSi(O^tBu)_3)_3(THF)_2]$, from the Na-capped molybdenum(II) nitride, $[Na(N)Mo^{II}P_2]$ (**70a**) (Scheme 14a).¹¹⁷ The solid-state molecular structure of **70** displays a U–Mo heterometallic complex bridged by a N^{3-} ligand, where the U and Mo centers are in close proximity with a U–Mo distance of 3.1032(2), which was slightly shorter than the distances found in other heterometallic U–Mo complexes bridged by phosphinoamide ligands (3.1682(4), 3.159(2) Å).¹¹⁸ The short U–Mo bond distance highlights the ability of the bridging nitride and bridging arene of the P_2 ligand in **70** to promote metal–metal interactions.^{119,120} The U–N_{nitride} bond distance is very short (1.856(2) Å), indicative of a multiple $U \equiv N$ bond, and is shorter than previously reported $U(v)$ nitride complexes (range: 2.022(5)–2.2101(6) Å),^{48,52,71} and longer than $U(vi)$ nitrides (1.769(2) and 1.799(7) Å),^{44,115} however, the distances are most consistent with Na-capped $U(v)$ terminal nitrides (1.883(4) and 1.835(5) Å).^{43,91} Structural, EPR, and computational studies indicated that N-transfer is accompanied by a $2e^-$ transfer from

the uranium to molybdenum, resulting in a $U^V \equiv N$ triple bond and a Mo^0-N single bonding profile.

In the same year, Xin, Zhu and co-workers presented the isolation of two heterometallic uranium-transition metal nitrides. The transition metal-stabilized $U(vi)$ nitrides, $[U^{VI}\{N(CH_3)(CH_2CH_2NP^tPr_2)_2\}(N_3)_2\{(\mu-N)M(COD)\}_2\{M(COD)\}]$ (**71-M**; $M = Rh, Ir$), were generated by photolysis of the $U(IV)$ -azide precursors, $[U^{IV}\{N(CH_3)(CH_2CH_2NP^tPr_2)_2\}(N_3)_2\{(\mu-N_3)M(COD)\}_2\}]$ (**71a-M**; $M = Rh, Ir$). The $U(v)$ nitride intermediates, $[U^V\{N(CH_3)(CH_2CH_2NP^tPr_2)_2\}(N_3)\{(\mu-N_3)M(COD)\}_2\{(\mu-N)M(COD)\}]$ (**72-M**; $M = Rh, Ir$), could also be successfully isolated by carefully controlling the irradiation timeframe (Scheme 14b).¹²¹

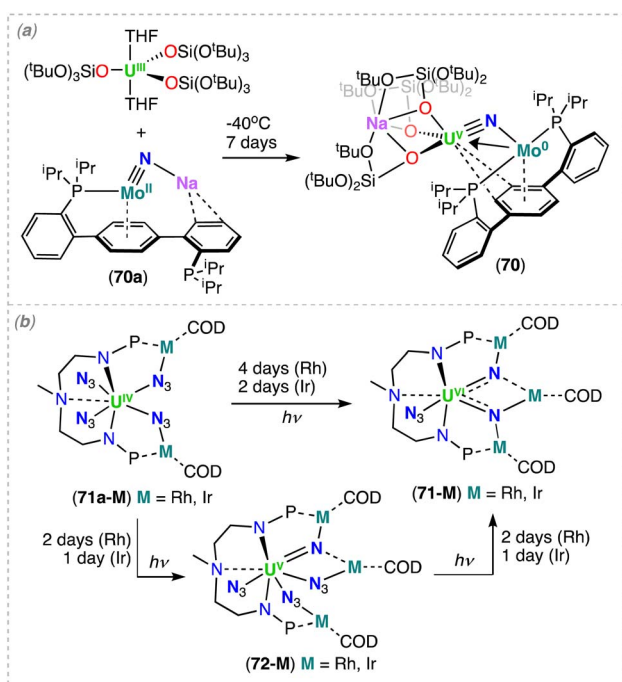
The solid-state molecular structures were determined for complexes **72-M** and **71-M**. The uranium(v) centers in **72-M** are coordinated by three azides and a nitride ligand, where the nitride moiety is bound to one U and two transition-metal atoms ($M = Rh, Ir$). The U–N_{nitride} distances are 1.963(5) Å and 2.011(4) Å in **72-Rh** and **72-Ir**, respectively, which are shorter than the bond distances of the $U(v)/U(v)$ bridged nitride complex, $[U^V(N^tBu)\{3,5-Me_2C_6H_3\}_2(\mu-N)]B(Ar^F)_4]$ (2.0470(3), 2.0511(3) Å),⁴¹ but similar to the $U(v)$ Na- or borane-capped nitride complexes, **62-Na** (1.883(4) Å) and $[NBu_4][U^V\{(\mu-N)B(C_6F_5)_3\}(N^tBu)(3,5-Me_2C_6H_3)_3\}]$ (1.916(4) Å), respectively.^{43,101} Complexes **71-M** display two bridged nitride moieties, which are capped by three Rh or Ir ions. The bond lengths of the $U(vi)$ –N_{nitride} in **71-M** (1.975(5) (Rh) and 2.005(6) Å (Ir)) are comparable with the $U(v)$ –N_{nitride} bond lengths found in **72-M**, however, they are longer than those in the $U(vi)$ –N_{imido} bond in a *trans*-imido uranium complex (1.840(4)–1.866(2) Å)¹²² or in the $U(vi)$ –N_{nitride} bond in a uranyl analog $[O=U=N]^+$ (1.818(9) Å),⁴⁰ altogether indicating $U=N$ multiple bonds. The $U(v)$ and $U(vi)$ nitride complexes showed excellent stabilities, which was attributed to the nitrides being stabilized by capped-transition metals (Rh or Ir).

6. Reactivity of actinide nitride complexes

Reactivity studies of terminal- and bridging-nitrides provide important information on the nature of the An–N bond in these complexes and in related actinide nitride materials. Moreover, promoting the reactivity of uranium nitrides towards CO, CO₂, or H₂ allows the possibility of establishing stoichiometric and catalytic N–C and N–H bond formation from U–N, with the long-term objective of using N₂ as a nitride source, thus allowing N₂ functionalization by H₂, CO, or CO₂ in ambient conditions.

6.1. Alkali- and transition-metal capped, and terminal actinide-nitride complexes

In 2012, the group of Liddle reported the first isolable $U(v)$ terminal nitride (Section 4.2), isolated by addition of 12-crown-4 (12C4) to the Na-capped $U(v)$ -nitride complex, $[Na_2(-U^V(Tren^{TIPS})(\mu-N))_2]$ (**62-Na**), and were able to demonstrate the reactive nature of these complexes, with electrophiles such as acid (H^+) and Me_3SiCl . Addition of Me_3SiCl to complexes **63-Na**⁴³ and **62-Na**,⁴⁴ yielded the $U(v)$ imide complex, $[U^V(NSiMe_3)(Tren^{TIPS})]$ (**73**). They were able to further confirm



Scheme 14 Synthesis of heterometallic uranium-nitrides with d -block metals (a) molybdenum (Mo) and (b) rhodium (Rh) and iridium (Ir).



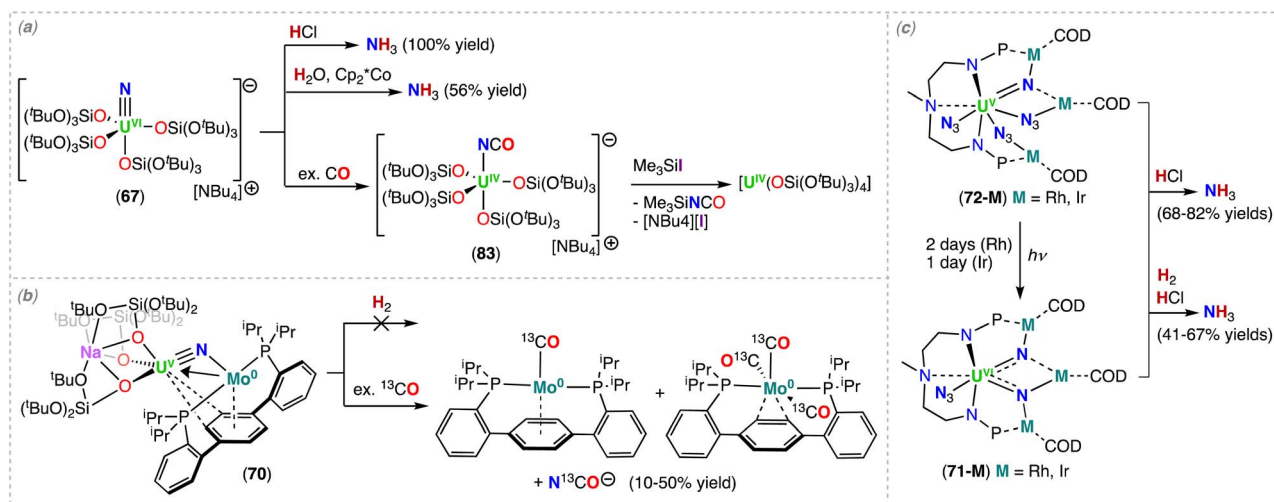
relevant towards understanding the mechanism for ammonia production through the industrial Haber–Bosch process, however, studies are limited by the paucity of metal-nitrides capable of effecting H₂ splitting in ambient conditions.

In the hydrogenolysis of **63-K**, two divergent mechanisms were found; (i) direct 1,2-dihydrogen addition of H₂ across the U(v)-nitride bond in **63-K**, coupled with H-atom migration to give a U(III)-amide complex, [K(B15C5)₂][U^{III}(Tren^{TIPPS})(NH₂)] (**80**), or (ii) a Frustrated Lewis Pair (FLP) pathway when hydrogenation is performed in the presence of trimesitylborane (BMes₃), producing a U(IV)-amide complex, [U^{IV}(Tren^{TIPPS})(NH₂)] (**81**), and a BMes₃ radical anion, [K(B15C5)₂][BMes₃]^{•-} (Scheme 15).⁵³ The isostructural U(vi)-nitride complex **65** is inert to hydrogenolysis, suggesting the 5f¹ electron of the U(v)-nitride in **63-K** is not purely non-bonding. Moreover, the authors found that the nature of the Lewis acid plays an important role in the hydrogenolysis mediated by a FLP. Notably, addition of BPh₃ to complex **63-K**, results in the formation of the uranium(v)-imido-borate complex, [K(B15C5)₂][U^V(Tren^{TIPPS})(NBPh₃)] (**82**), which does not react with H₂. In contrast, **63-K** does not form an adduct with BMes₃, however, BMes₃ promotes the reactivity of **63-K** with H₂. The computed mechanism indicated that when **63-K** is reacted with H₂ in the presence of BMes₃, the [U^V(Tren^{TIPPS})(N)]⁻ and BMes₃ components constitute the FLP complex, which reacts with H₂ and facilitates its cleavage. In the absence of BMes₃, the formation of **81** is slower and proceeds *via* the direct hydrogenation pathway previously reported for the hydrogenation of the U(IV)/U(IV) bridging nitride, [Cs(U^{IV}(OSi(O^tBu)₃)₃)₂(μ-N)] (**6-Cs**).⁴⁹ Thus, this work establishes a unique example of actinide and FLP chemistries combined. Furthermore, a synthetic cycle for ammonia (NH₃) synthesis was demonstrated, where treatment of the U(IV) complex, [U^{IV}(Tren^{TIPPS})Cl], with NaN₃, KC₈, and 2.0 equiv. of B15C5 produces the terminal U(v)-nitride **63-K**, which in turn reacts with H₂ and BMes₃ to give **81**. Treatment of **81** with Me₃SiCl, followed by work-up and acidification steps, produces ammonia.⁵³

In the same year, Barluzzi, Mazzanti and co-workers reported the synthesis of the first stable terminal U(vi)-nitride complex,

[NBu₄][U^{VI}(OSi(O^tBu)₃)₄(N)] (**67**), generated by azide photolysis.¹¹⁵ They found complex **67** is stable, but readily reacts with electrophiles such as acid (H⁺) sources and carbon monoxide (CO). They found that the addition of HCl or H₂O/decamethylcobaltocene (Cp₂*Co) to complex **67** yields NH₃ in 100% and 56% yields, respectively. Additionally, reaction of **67** with 1 atm of CO yields the reductive carbonylation product, [NBu₄][U^{IV}(OSi(O^tBu)₃)₄(NCO)] (**83**) (Scheme 16a), which is an analogous reactivity to that previously observed for the terminal U(vi) nitride complex, **65**. Additionally, reaction of 1.0 equiv. of Me₃SiI to complex **83** led to the formation of [U(OSi(O^tBu)₃)₄], as the main uranium-containing species, and Me₃SiNCO. Based on the formation of [U(OSi(O^tBu)₃)₄], the authors were able to develop a synthetic cycle for the formation of Me₃SiNCO from NBu₄N₃ and CO.¹¹⁵ In 2022, Mazzanti, Agapie and co-workers found that preliminary reactivity studies of the heterometallic U(v)-Mo(0)-bridged nitride complex **70** with ¹³CO (1–10 equiv.) resulted in the reductive carbonylation of the nitride, leading to the formation of NaN¹³CO (10–50% yield) and the previously reported Mo(0) carbonyl complexes, [P₂Mo⁰(¹³CO)] or [P₂Mo⁰(¹³CO)₃] (in low yield), as well as multiple unidentified diamagnetic species (Scheme 16b).¹¹⁷ The uranium species formed in the reaction could not be identified, but the formation of NaN¹³CO was unambiguously demonstrated by ¹³C NMR spectroscopy of the reaction mixture in D₂O. The reductive carbonylation of the U(v) nitride most likely proceeds with release of the Mo(0) complex, but reactivity with complex **70** was not ruled out.

In the same year, Xin, Zhu and co-workers reported the reactivity of the transition metal-capped U(v) and U(vi) nitride complexes (**72-M**), and (**71-M**) (M = Rh, Ir), towards acid (H⁺) and H₂.¹²¹ They found that addition of excess PyHCl to the heterometallic uranium nitride complexes, **71-M** and **72-M**, resulted in NH₄Cl in 68–82% yields, respectively (Scheme 16c). Moreover, addition of 1 atm H₂ to complexes, **71-M** and **72-M**, led to a color change in the reaction mixture, however, attempts to isolate single crystals of the products were unsuccessful. The subsequent addition of excess PyHCl to the reaction mixtures



Scheme 16 Reactivity of terminal and transition metal-capped uranium-nitrides supported by various ligands.



bis-nitride complexes was suggested to stem from a decreased nucleophilicity of the second nitride moiety in **11**, due to an increase in oxidation state of one uranium, favoring reductive carbonylation opposed to nucleophilic C–O cleavage in **9**.⁷⁵ Similar to the reactivity of **9**, the U(vi)/U(iv)₃ tetranitride-cluster (**1**) reported by Jori, Mazzanti and co-workers, also performs the cleavage and reductive carbonylation of CO to yield CN[−] and NCO[−], respectively.⁶⁴ From the reaction with stoichiometric quantities of CO, two additional U(iv)/U(v) clusters were obtained, namely, [K₄((OSi(O^tBu)₃)₂U^{IV})₂((OSi(O^tBu)₃)₂U^V)₂(μ₄-N)₂(μ-O)₂(μ₃-O)₂] (**85**), and [K₃((OSi(O^tBu)₃)₂U^{IV})₂((OSi(O^tBu)₃)₂U^V)₂(μ₃-N)(μ-O)(μ₃-O)₄] (**86**), demonstrating that the bridging nitride moieties in **1** could be replaced by oxo-ligands without disrupting the primary structure, and leads only to valence redistribution (bottom, Scheme 17). In the same study, characterization of the putative U(v) oxo bis-nitride, (**1-N**)₂ (Section 2), an intermediate formed in the synthesis of the tetranitride cluster **1**, was carried out by reaction with CO.

Addition of 3.0 equiv. CO to (**1-N**)₂ resulted in an analogous CO cleavage and reductive carbonylation pathway when compared to complex **9**, however, due to the additional oxo-ligand in (**1-N**)₂, this resulted in the release of KCN and KNCO upon formation of the bis-oxo complex, [K₂-([U^{IV}(OSi(O^tBu)₃)₃)₂(μ-O)₂] (**87-K**).⁶⁴ Reactivity and structural confirmation of the putative oxo bis-nitride (**1-N**)₂ was later supported by isolation of the bridging bis-nitride, terminal oxo complex, [Cs₃(U^V(OSi(O^tBu)₃)₃(μ-N)₂(U^V(OSi(O^tBu)₃)₂(κ-O))] [CsOSi(O^tBu)₃] (**3-N**)₂ (Section 2), where reaction of (**3-N**)₂ with 3.0 equiv. CO led to isolation of the bis-oxo U(iv) complex, [Cs₂([U^{IV}(OSi(O^tBu)₃)₃)₂(μ-O)₂] (**87-Cs**), and release of CN[−] and NCO[−], analogous to (**1-N**)₂.⁶⁴

6.2.1.2. CO₂ and CS₂ reactivity. Complex **9** also reacts with CO₂ or CS₂ leading to the redox-neutral, C–O or C–S bond cleavage with concomitant N–C bond formation of one nitride ligand. Addition of 1.0 equiv. CO₂ or CS₂ resulted in isolation of the nitride-oxo-cyanate complex, [K₂([U^V(OSi(O^tBu)₃)₃)₂(μ-N)(μ-O)(μ-NCO))] (**88**), and the nitride-thiocyanate-sulfide complex, [K₂([U^V(OSi(O^tBu)₃)₃)₂(μ-N)(μ-S)(μ-NCS))] (**89**), respectively (top, Scheme 17).⁵² Formation of the oxo-NCO ligands from CO₂, and NCS[−] from CS₂ cleavage, has also been observed for the respective U(v) and U(vi) terminal nitrides, **63-K** and **65** (Section 6.1), as well as the U(iv) bridging mono-nitride, CsU^{IV}=N=U^{IV} (**6-Cs**) (Section 6.2.2). In these previous examples with CS₂, however, formation of a bridging sulfide, similar to **89**, had never been observed. Instead, the terminal U(v) nitride (**63-K**) and the U(iv)/U(iv) bridging mono-nitride (**6-Cs**) complexes form a putative uranium-sulfide which then reacts with CS₂ to yield a trithiocarbonate ligand. The formation of complex **89** was rationalized by the increased sterics in the core of the U(v)/U(v) bis-nitride complex **9**, preventing formation of the trithiocarbonate ligand.

It is important to note that the analogous U(vi)/U(vi) bis-nitride (**13**) also reacted immediately with CO₂, but the reaction products could not be identified.⁷⁵ The formation of thiocyanate (N¹³CS[−]), cyanate (N¹³CO[−]), and cyanide (¹³CN[−]) were

all confirmed by structural and ¹³C NMR spectroscopy analysis of the products after reactions with ¹³CS₂, ¹³CO₂, and ¹³CO.

6.2.1.3. H₂ reactivity. Complex **9** also effects the oxidative cleavage of H₂ to yield the U(iv) bis-imido complex, [K₂-[U^{IV}(OSi(O^tBu)₃)₃(μ-NH)]₂] (**90**).⁵² Similarly, the analogous U(iv)/U(v) complex (**11**) also promotes H₂ cleavage, but instead yields an equimolar amount of the U(iv) bis-imido and bis-amido complexes, **90** and [K₂([U^{IV}(OSi(O^tBu)₃)₃)₂(μ-NH)₂(μ-THF))] (**91**), respectively (top, Scheme 17).⁷⁵ The U(iv)/U(iv) complex (**90**) does not react further with H₂; therefore, it was proposed that the reaction proceeds by first an oxidative cleavage of 1.0 equiv. of H₂, affording transient high-valent and ligand-scrambling bis-μ-NH products, which further react with an additional 1.0 equiv. of H₂, affording a mixture of complexes **90** and **91**. Complex **91** could be independently synthesized by reacting 2.0 equiv. of HNET₃BPh₄ to complex **90**. Alternatively, the U(vi)/U(vi) bis-nitride (**13**) does not effect H₂ cleavage.⁷⁵ Similar oxidative cleavage of H₂ was observed for the monometallic U(v) terminal nitride (**63-K**), whereas the U(vi) derivative (**65**) did not react, similar to **13**.

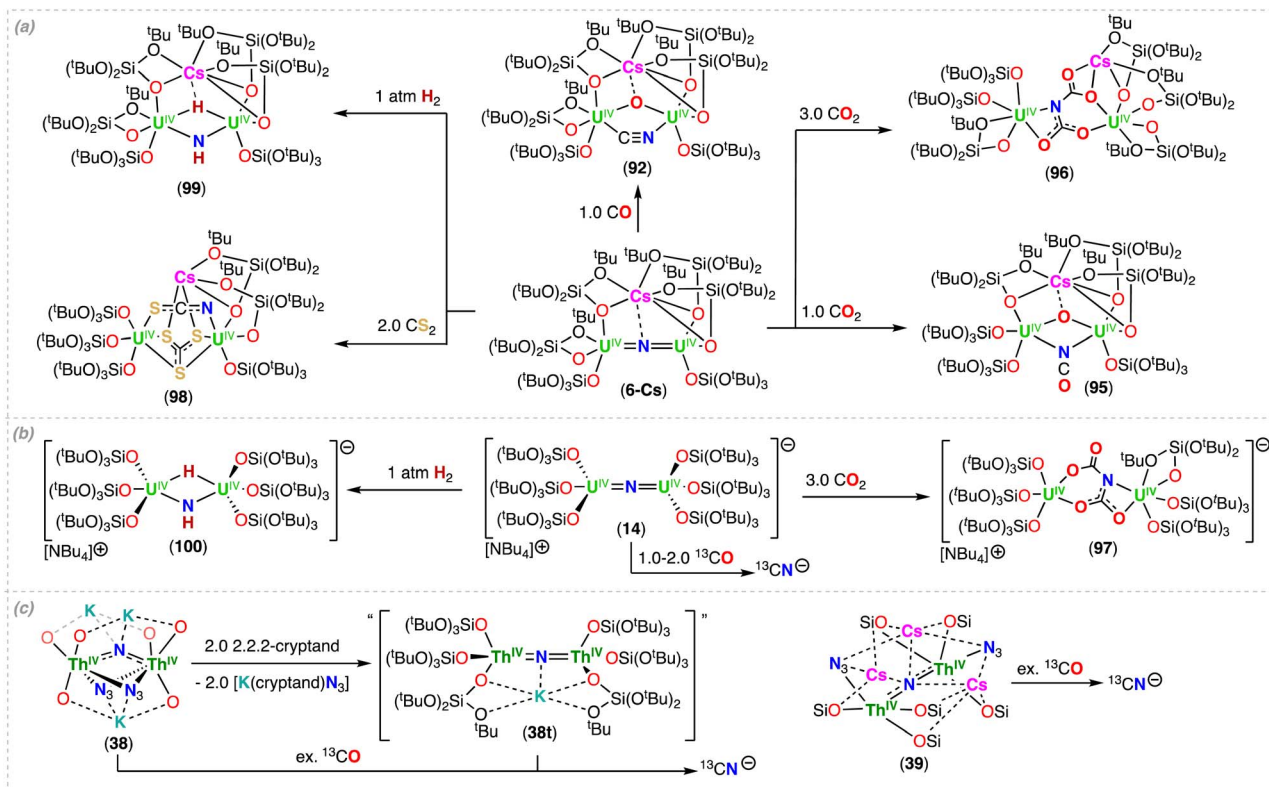
6.2.1.4. Acid (H⁺) reactivity. All nitride complexes described in this section, **9**, **11**, **13**, **1**, (**1-N**)₂, and (**3-N**)₂, were found to react with strong acid (HCl) to afford NH₄Cl typically in high or quantitative yields.

6.2.2. An(iv) systems

6.2.2.1. CO reactivity. The −OSi(O^tBu)₃ complexes, CsU^{IV}=N=U^{IV} (**6-Cs**) and [NBu₄][U^{IV}=N=U^{IV}] (**14**),⁷⁶ show immediate reactivity with CO resulting in C–O cleavage. Complex **6-Cs** cleanly reacts with CO in toluene to afford the bridging oxo/cyanide complex [Cs(U^{IV}(OSi(O^tBu)₃)₃)₂(μ-CN)(μ-O)] (**92**) (Scheme 18a), in which the resultant cyanide ligand can be alkylated by Me₃SiI or MeOTf to afford Me₃SiCN or MeCN, respectively.⁵⁰ Initial computational studies indicated the importance of cooperative binding of the CO by the multimetallic U–N–Cs moiety. However, the reaction of CO with complex **14** in both toluene and THF solutions also led to the formation of CN[−] (Scheme 18b), but in toluene, resulted in more products compared to **6-Cs**, indicating ligand scrambling.⁷⁶ The differences in reactivity of **6-Cs** and **14** with CO in toluene could be explained by an increased stability the inner-sphere Cs cation provides to **92**, by binding four −OSi(O^tBu)₃ ligands and the bridging oxo. For the CO reaction with **14**, crystals suitable for XRD studies could not be isolated. However, when the reaction residue was hydrolyzed with D₂O (pD = 12), CN[−] was observed as the only product, similar to **6-Cs**. Likewise, the Th(iv)/Th(iv) nitride-azide complexes, M₃Th=N=Th (M = K (**38**), Cs (**39**)), containing −OSi(O^tBu)₃ ligands, were also found to cleave CO to CN[−], however, in lower yields (30 and 22% yield, respectively). The reactivity of the nitride moiety in **38** toward CO was increased by removal of two azide ligands and two K cations, in the form of [K(2.2.2-cryptand)][N₃]. Formation of the putative mono-nitride complex, “[K(Th₂(OSi(O^tBu)₃)₆(μ-N))]” (**38t**) and reaction with CO led to an increase in reactivity, forming CN[−] in 70% yield (Scheme 18c).⁸⁷

The analogous U(iv)/U(iv) nitride bridged complex, [NBu₄][U^{IV}=N=U^{IV}] (**15**), supported by −N(SiMe₃)₂ ligands, was reacted with 1.0 atm of CO, resulting in the formation of





Scheme 18 Reactivity of U(IV) and Th(IV)-bridged nitrides supported by siloxide ($-\text{OSi}(\text{O}^t\text{Bu})_3$) ligands.

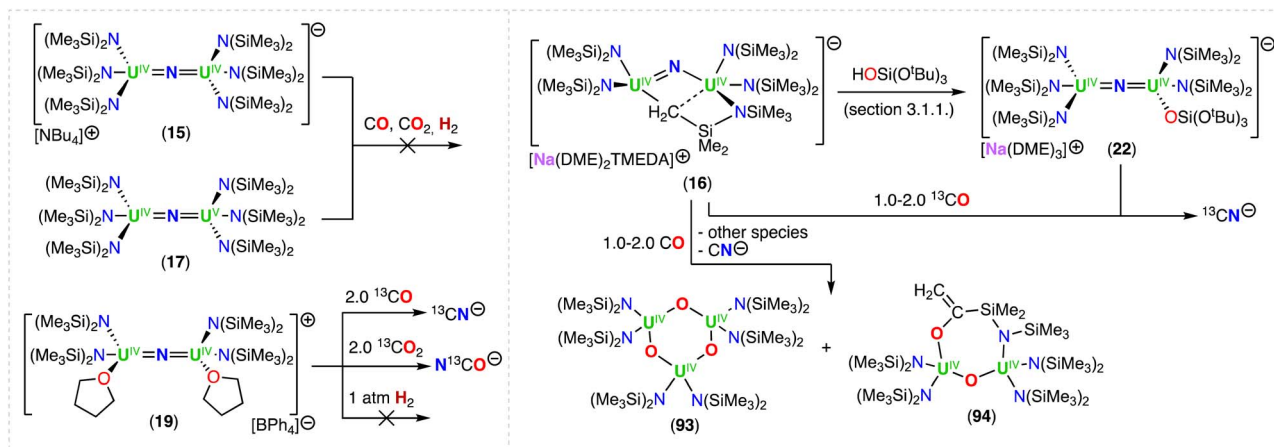
decomposition products not derived from C–O bond cleavage. Additionally, the analogous U(IV)/U(V) all- $\text{N}(\text{SiMe}_3)_2$ complex (17) showed no reactivity upon addition of 1.0 atm of CO .⁷⁶ However, when one $-\text{N}(\text{SiMe}_3)_2$ was replaced with one $-\text{OSi}(\text{O}^t\text{Bu})_3$ ligand to generate the mixed-ligand complex, $[\text{Na}(\text{DME})_3][\text{U}^{\text{IV}}=\text{N}=\text{U}^{\text{IV}}]$ (22), the reactivity with 1.0–2.0 equiv. of CO was observed, but was significantly slower than the all- $-\text{OSi}(\text{O}^t\text{Bu})_3$ complexes, 6-Cs and 14. Single crystals could not be isolated from the reaction mixture, however, CN^- was identified as the only product after hydrolysis and analysis by ^{13}C NMR spectroscopy (Scheme 19).⁷⁶ To further investigate if the U(IV)/U(IV) nitride- $\text{N}(\text{SiMe}_3)_2$ complexes could react with CO , specifically in different oxidation states or in the presence of other ligands, the cyclometallate nitride, first reported by Fortier, Hayton and co-workers, $[\text{Na}(\text{DME})_2(\text{TMEDA})][\text{U}^{\text{IV}}=\text{N}=\text{U}^{\text{IV}}]$ (16),⁴⁰ and the cationic nitride complex, $[\text{U}^{\text{IV}}=\text{N}=\text{U}^{\text{IV}}][\text{BPh}_4]$ (19),⁷⁰ were also reacted with CO .^{76,125} Addition of 1.0–2.0 equiv. of CO to 16 and 19 resulted in their complete consumption, and upon hydrolysis of the reaction residues, similar to 22, resulted in CN^- . From the reaction mixture obtained from reacting 16 with CO , several species were identified and characterized by XRD studies, namely the trimeric bis- $\text{N}(\text{SiMe}_3)_2$ bridging oxo complex, $[\text{U}^{\text{IV}}(\text{N}(\text{SiMe}_3)_2(\mu\text{-O}))_3]$ (93), and a species in which CO inserted into the uranium–methylene bond, $[(\text{N}(\text{SiMe}_3)_2)_2\text{U}^{\text{IV}}(\mu\text{-O})(\text{U}^{\text{IV}}(\mu\text{-}\kappa^2\text{-O},\text{N-OC}(\text{=C})\text{SiMe}_2\text{NSiMe}_3)(\text{N}(\text{SiMe}_3)_2)_2)]$ (94) (Scheme 19).⁷⁶ This type of CO insertion had been observed previously in mononuclear U(IV) metallacycles, but this demonstrated an extension to uranium-nitride complexes.^{126–128}

6.2.2.2. CO_2 and CS_2 reactivity. Addition of 1.0 or 3.0 equiv. of CO_2 to 6-Cs leads to differences in reactivity, with the formation of the bridging oxo/cyanate complex, $[\text{Cs}(\text{U}(\text{OSi}(\text{O}^t\text{Bu})_3)_2)(\mu\text{-NCO})(\mu\text{-O})]$ (95), and the unprecedented electrophilic addition of 2 CO_2 molecules affording the bis-carbamate complex, $[\text{Cs}(\text{U}(\text{OSi}(\text{O}^t\text{Bu})_3)_2)(\mu\text{-NC}_2\text{O}_4)]$ (96), respectively (Scheme 18a).¹²⁹ For complex 14, addition of 3.0 equiv. of CO_2 under similar reaction conditions led to the formation of the analogous bis-carbamate complex, $[\text{NBu}_4][\text{U}^{\text{IV}}(\text{OSi}(\text{O}^t\text{Bu})_3)_2(\mu\text{-NC}_2\text{O}_4)]$ (97) (Scheme 18b).⁷⁶ Complexes 96 and 97 display resonances for the bis-carbamate ($-\text{N}^{13}\text{C}_2\text{O}_4$) moiety at -134.1 and 141.5 ppm in the ^{13}C NMR spectra, respectively. Hydrolysis of the reaction residue was not carried out for 96, instead, addition of D_2O ($\text{pD} = 12$) to 97 and analysis by ^{13}C NMR spectroscopy displayed only $\text{D}^{13}\text{CO}_3^-$.

CS_2 reactivity was also investigated, but only for complex 6-Cs, in which C–S bond cleavage was observed upon 2.0 equiv. of CS_2 , resulting in the formation of the thiocyanate/trithiocarbonate complex, $[\text{Cs}(\text{U}^{\text{IV}}(\text{OSi}(\text{O}^t\text{Bu})_3)_2)(\mu\text{-NCS})(\mu\text{-CS}_3)]$ (98) (Scheme 18a).¹²⁹

The CO_2 reactivity of the all- $\text{N}(\text{SiMe}_3)_2$ complexes (15), and (17) were also investigated, but it was found that exposure to 1 atm of CO_2 led to no changes in the ^1H NMR spectra, indicating no reactivity. In contrast, the mixed-ligand complexes, 22 and 19, and the cyclometallate, 16,^{40,76} all react with CO_2 , but produce complicated mixtures of species. Attempts to obtain single crystals of the products were unsuccessful, however after hydrolysis of the reaction residues with $\text{pD} = 12$ D_2O after





Scheme 19 Reactivity of U(IV)-bridged nitrides supported by amide ($-\text{N}(\text{SiMe}_3)_2$) and heteroleptic analogues.

addition of $^{13}\text{CO}_2$, the formation of N^{13}CO^- as the only product generated by the nitride moiety could be detected by ^{13}C NMR spectroscopy (Scheme 19), where evidence of a dicarbamate was not apparent for any system. The formation of cyanate indicates that the reactions of the $-\text{N}(\text{SiMe}_3)_2$ complexes and excess CO_2 proceed only *via* a N–C bond formation and deoxygenation process. Similar reactivity had been observed in **6-Cs**²⁹ with stoichiometric quantities of CO_2 (Scheme 18a). CS_2 reactivity was not investigated for the $-\text{N}(\text{SiMe}_3)_2$ derivatives.

6.2.2.3. H_2 reactivity. Addition of H_2 to the all $-\text{OSi}(\text{O}^t\text{Bu})_3$ complexes, **6-Cs** and **14**, resulted in the reversible and irreversible formation of the dinuclear U(IV) imide hydride complexes, $[\text{Cs}(\text{U}(\text{OSi}(\text{O}^t\text{Bu})_3)_3)_2(\mu\text{-NH})(\mu\text{-H})]$ (**99**)⁴⁹ and $[\text{NBu}_4][(\text{U}(\text{OSi}(\text{O}^t\text{Bu})_3)_3)_2(\mu\text{-NH})(\mu\text{-H})]$ (**100**),⁵⁹ respectively (Scheme 18a and 18b). Complex **99** was found to transfer the hydride to MeCN and CO_2 to afford the substrate reduction imido–ketimide and formate insertion products, respectively.⁴⁹ Contrary to the reversible binding of H_2 to complex **99**, **100** is stable under dynamic vacuum and shows irreversible binding of H_2 . The differences in the binding of H_2 between the two complexes was rationalized by the solid-state molecular structures. In **99**, the Cs cation lies at the apical position of the hydride ($-\text{H}$) ligand, most likely rendering the U–H interaction more labile and facilitating the elimination of H_2 .

In contrast to the all $-\text{OSi}(\text{O}^t\text{Bu})_3$ complexes, H_2 cleavage was not observed for the all $-\text{N}(\text{SiMe}_3)_2$ (**15**), and (**17**), mixed-ligand, **22** (ref. 76) and **19**,²⁵ or cyclometallate (**16**)⁷⁶ complexes. This was attributed to the reduced nucleophilicity of the nitride moiety when $-\text{N}(\text{SiMe}_3)_2$ ancillary ligands are incorporated in the system. Altogether, these studies show how inner-sphere cations and supporting ligand can affect the reactivity of the uranium-nitride moiety.

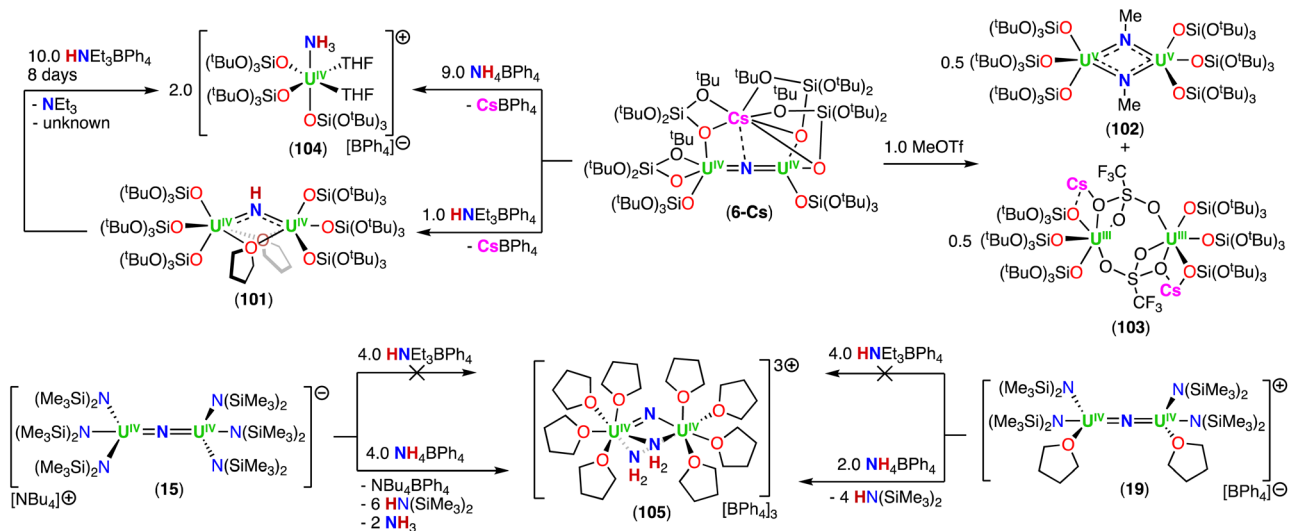
6.2.2.4. Acid (H^+), NH_3 , and alkylation reactivity. Based on the small molecule reactivity described above, complex **6-Cs** was suggested to be more reactive towards electrophiles than in the analogous $-\text{N}(\text{SiMe}_3)_2$ complexes, therefore the reactivity with acids (H^+) and NH_3 , was investigated for diuranium(IV) complexes differing in type and number of supporting ligands.¹²⁵

The nitride in complex **6-Cs**,⁷¹ was found to be easily protonated by addition of 1.0 equiv. of a weak acid, $\text{HNET}_3\text{BPh}_4$, resulting in a mono-imido bridged complex, $[(\text{U}^{\text{IV}}(\text{OSi}(\text{O}^t\text{Bu})_3)_3)_2(\mu\text{-NH})]$ (**101**) (Scheme 20). Formation of the stable mono-imido in complex **101** contrasts the disproportionation observed during the alkylation of **6-Cs** with MeOTf, resulting in isolation of a mixture of species, namely, the U(V) bis-imido, $[(\text{U}^{\text{V}}(\text{OSi}(\text{O}^t\text{Bu})_3)_3)_2(\mu\text{-NMe}_2)]$ (**102**), and the U(III) dimeric Cs-OTf, $[\text{Cs}_2((\text{U}^{\text{III}}(\text{OSi}(\text{O}^t\text{Bu})_3)_3)(\mu\text{-OTf}))_2]$ (**103**), complexes (Scheme 20).⁵⁰ This reactivity with MeOTf was highly unusual as U(IV) complexes tend to be more stable than their U(V) and U(III) counterparts. Only one additional example of disproportionation of a U(IV)-imido complex, $[(\text{U}^{\text{IV}}(\text{Tren}^{\text{TIPS}})(\mu\text{-NH})(\mu\text{-M}))_2]$, has recently been reported (Section 4.2).¹⁰⁴ These examples contrast the formation of the U(IV) mono-imido complex **101**, where protonation does not lead to similar disproportionation reactions.

Further protonation of the imido moiety in **101** to a terminal NH_3 complex, $[\text{U}^{\text{IV}}(\text{OSi}(\text{O}^t\text{Bu})_3)_3(\text{THF})_2(\text{NH}_3)][\text{BPh}_4]$ (**104**), could be achieved by using a large excess of a weak acid, $\text{HNET}_3\text{BPh}_4$, coupled with a longer reaction time, or by means of a stronger acid, NH_4BPh_4 (Scheme 20). The NH_3 binds the U(IV) ion strongly in complex **104**, but can be displaced by addition of strong acid (HCl). Additionally, the U– $\text{OSi}(\text{O}^t\text{Bu})_3$ bonds were found to be stable, even in the presence of stronger acids, such as NH_4BPh_4 , therefore indicating that $-\text{OSi}(\text{O}^t\text{Bu})_3$ supporting ligands are well suited for use when acidic conditions are required, such as in the H^+/e^- mediated catalytic conversion of N_2 to NH_3 .¹²⁵

In contrast to the all $-\text{OSi}(\text{O}^t\text{Bu})_3$ complexes, different reactivity was observed for both the all $-\text{N}(\text{SiMe}_3)_2$ (**15**)⁷⁶ and mixed-ligand (**19**)⁷⁰ nitride-bridged complexes. Opposed to complex **6-Cs**, the nitride in both **15** and **19** are more resistant toward protonation by acids. For example, when a weak acid, such as $\text{HNET}_3\text{BPh}_4$, is employed, the nitride in these complexes is unreactive. This is consistent with the lesser nucleophilic character of the bridging nitride in the $\text{N}(\text{SiMe}_3)_2$ -containing complexes compared to the analogous $-\text{OSi}(\text{O}^t\text{Bu})_3$ systems, which was also supported by their reactivity toward small molecules (CO , CO_2 or H_2). Alternatively, addition of the





Scheme 20 Reactivity of U(IV)-bridged nitrides supported by amide ($-\text{N}(\text{SiMe}_3)_2$) and siloxide ($-\text{OSi}(\text{O}^t\text{Bu})_3$) ligands towards acid and alkylating sources.

stronger acid, NH_4BPh_4 , resulted in the complete loss of $-\text{N}(\text{SiMe}_3)_2$ supporting ligands, while the bridging nitride remains intact. Additionally, when a strong acid is used, such as NH_4BPh_4 , the basic $-\text{N}(\text{SiMe}_3)_2$ ligands promote the N-H heterolytic cleavage of NH_3 . Addition of NH_4BPh_4 (2.0–4.0 equiv.) to complexes **15** and **19**, yielded a stable U(IV)/U(IV) bis- NH_2 , mono-nitride bridged complex, $[(\text{U}^{\text{IV}}(\text{THF})_2)_2(\mu\text{-N})(\mu\text{-NH}_2)]_3[\text{BPh}_4]_3$ (**105**), where only ancillary solvent molecules support the metal center (Scheme 20).¹²⁵

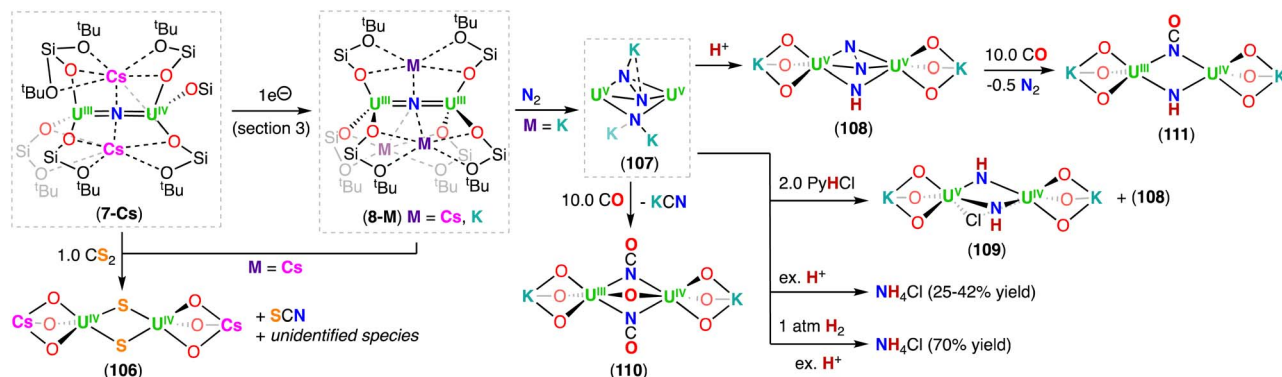
Overall, this demonstrated that basic supporting ligands, such as $-\text{N}(\text{SiMe}_3)_2$, present several disadvantages compared to the $-\text{OSi}(\text{O}^t\text{Bu})_3$ ligands for usage in the development of catalysts for N_2 conversion to NH_3 . Utilizing $\text{OSi}(\text{O}^t\text{Bu})_3$ -containing complexes is not only advantageous for their resistance toward acids, but also for the high reactivity of bound nitrides to yield NH_3 . In contrast, $\text{N}(\text{SiMe}_3)_2$ -supported complexes may be of interest for studies pertaining to the heterolytic bond activation of NH_3 .¹²⁵

6.2.3. U(III) systems

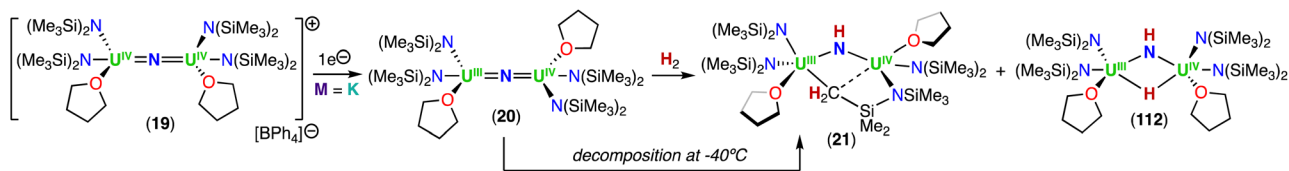
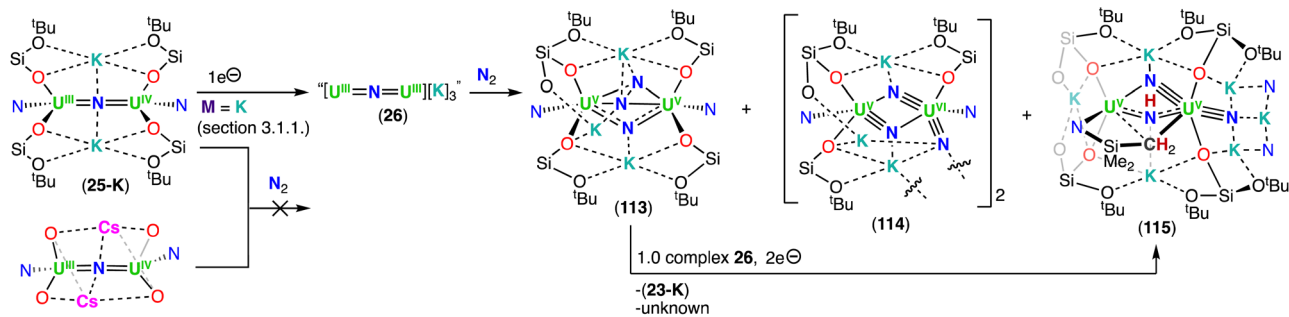
6.2.3.1. $\text{OSi}(\text{O}^t\text{Bu})_3$ complexes. Addition of 1.0 equiv. of CS_2 to the $\text{Cs}_2\text{U}^{\text{III}}=\text{N}=\text{U}^{\text{IV}}$ (**7-Cs**) and $\text{Cs}_3\text{U}^{\text{III}}=\text{N}=\text{U}^{\text{III}}$ (**8-Cs**)

complexes, led to the transfer of the nitride moiety with contaminant C=S bond cleavage, forming the bis-sulfide complex, $[(\text{Cs}(\text{THF}))_2][\text{U}^{\text{IV}}(\text{OSi}(\text{O}^t\text{Bu})_3)_3]_2(\mu\text{-S})_2$ (**106**), and NCS^- . Formation of U(IV) from the U(III) complexes suggests alternative metal-based reactivity in which unidentifiable species were also formed (Scheme 21).⁷²

The reaction of **8-Cs** with N_2 was also investigated, however, the formation of decomposition products led to difficulties in isolation of the newly formed species. Instead, the K-analogue, $\text{K}_3\text{U}^{\text{III}}=\text{N}=\text{U}^{\text{III}}$ (**8-K**) was found to have an increased stability in the solution and solid-state, allowing the study of the reaction with N_2 and characterization of its products. Falcone, Mazzanti and co-workers found that addition of N_2 to complex **8-K** in the solid- or solution-state led to the formation of the U(V)/U(V)- N_2^{4-} complex, $[\text{K}_3[\text{U}^{\text{V}}(\text{OSi}(\text{O}^t\text{Bu})_3)_3]_2(\mu\text{-N})(\mu\text{-}\eta^2\text{-}\eta^2\text{-N}_2)]$ (**107**) (Scheme 21).⁴⁸ The dinitrogen molecule undergoes a $4e^-$ reduction to the side-on hydrazido moiety (N_2^{4-}) with subsequent oxidation of the U(III) centers to U(V). The isolation of the hydrazido complex **107** provided the first example of a $4e^-$ reduction of N_2 by a molecular complex of uranium, and led to the first example of uranium promoted N_2 functionalization. The observed reactivity is the



Scheme 21 Reactivity of U(III)-bridged nitrides supported by siloxide ($-\text{OSi}(\text{O}^t\text{Bu})_3$) ligands. The $-\text{Si}(\text{O}^t\text{Bu})_3$ moieties of the ligand for most complexes have been omitted for clarity.

Scheme 22 Reactivity of U(III)-bridged nitrides supported by amide ($-\text{N}(\text{SiMe}_3)_2$) ligands.Scheme 23 Reactivity of U(III)-bridged nitrides supported by amide ($-\text{N}(\text{SiMe}_3)_2$) and siloxide ($-\text{OSi}(\text{O}^t\text{Bu})_3$) ligands. Most of the $-\text{O}^t\text{Bu}$ moieties of the ligand have been omitted for clarity.

result of the high flexibility of macrocyclic K-siloxide framework that allows bending of the $\text{U}=\text{N}=\text{U}$ fragment to bind and reduce the N_2 moiety. Isolation of the N_2^{4-} complex allowed further study of the parameters controlling N_2 binding and reduction. In particular, the effect of alkali ions and type of ancillary ligands on the reactivity of the U(III)/U(III) nitride was explored (see below).⁴⁸ Additionally, complex **107** could be further functionalized by addition of acids (H^+), CO, and H_2 , differently from what was previously observed for N_2 complexes of the f-elements where addition of these molecules had led only to N_2 release. First, addition of 1.0 equiv. of 2,4,6-tri-tertbutylphenol led to nitride protonation forming the mono-imido-hydrazido U(V) complex, $[\text{K}_2[\text{U}^{\text{V}}(\text{OSi}(\text{O}^t\text{Bu})_3)_3]_2(\mu\text{-NH})(\mu\text{-}\eta^2\text{-}\eta^2\text{-N}_2)]$ (**108**). In contrast, when a strong acid (PyHCl or HCl) was employed, protonation of the nitride and $-\text{N}_2^{4-}$ ligand occurred, resulting in a mixture of **108** and the U(V)/U(IV) bis-imido complex, $[\text{K}_2((\text{U}^{\text{V/IV}}(\text{OSi}(\text{O}^t\text{Bu})_3)_3)_2(\mu\text{-NH})_2(\mu\text{-Cl}))]$ (**109**) (Scheme 21). Addition of excess (20.0 equiv.) PyHCl to **107** resulted in the formation of $^{14}\text{NH}_4\text{Cl}$, as confirmed by ^1H NMR spectroscopy, where a mixture of $^{15/14}\text{NH}_4\text{Cl}$ was observed when the reaction is carried out with the isotopically enriched analog, $[\text{K}_2([\text{U}^{\text{V}}(\text{OSi}(\text{O}^t\text{Bu})_3)_3]_2(\mu\text{-NH})(\mu\text{-}\eta^2\text{-}\eta^2\text{-}^{15}\text{N}_2)]$ (^{15}N -**107**). The yields of NH_4Cl ranged between 25–42% depending on the acid used, and could be increased by first carrying out a reduction with H_2 followed by addition of HCl (77% yield). Although isolable species from H_2 reactivity with complex **107** could not be identified, the increase in NH_4Cl suggested that H_2 cleaved the N–N bond of the $-\text{N}_2^{4-}$ ligand, providing an extremely rare case of N_2 reduction by H_2 in molecular complexes, and the first in uranium chemistry.⁴⁸

The reactivity of complexes **107** and **108** were also investigated with CO. Addition of excess CO to **107** afforded the bridging oxo bis-cyanate complex, $[\text{K}_2([\text{U}^{\text{IV}}(\text{OSi}(\text{O}^t\text{Bu})_3)_3]_2(\mu\text{-O})(\mu\text{-NCO})_2)]$ (**110**), with concomitant formation of KCN, resulting from the reductive

carbonylation of the N_2^{4-} moiety and CO cleavage by the bridging nitride ligand. The imido- N_2^{4-} complex, **108**, displayed a decreased reactivity in comparison to the nitrido- N_2^{4-} complex **107**, resulting a mixed valent U(III)/U(IV) complex, $[\text{K}_2((\text{U}^{\text{III/IV}}(\text{OSi}(\text{O}^t\text{Bu})_3)_3)_2(\mu\text{-NH})(\mu\text{-NCO}))]$ (**111**), and displacement of N_2 . Here, the addition of CO results in disproportionation of the $-\text{N}_2^{4-}$ ligand (Scheme 21).⁴⁸

6.2.3.2. $\text{N}(\text{SiMe}_3)_2$ and $\text{OSi}(\text{O}^t\text{Bu})_3$ heteroleptic complexes. To effect the overall $6e^-$ reduction of N_2 to nitrides, it was postulated that replacing the ancillary $-\text{OSi}(\text{O}^t\text{Bu})_3$ ligands with the more electron-donating $-\text{N}(\text{SiMe}_3)_2$, could possibly increase the reducing potential of the uranium and promote six electron transfer followed by N_2 cleavage. Reduction of the previously reported anionic U(IV) complexes, **15** and **16**, failed to produce the desired U(III) species. The inability to reduce the uranium center in these complexes was correlated to the more electron-rich character of the $-\text{N}(\text{SiMe}_3)_2$ ligands compared to $-\text{OSi}(\text{O}^t\text{Bu})_3$.⁷⁰ Therefore, reduction of the mixed-ligand U(IV) nitride system, **19**, containing four $-\text{N}(\text{SiMe}_3)_2$ ligands and two THF molecules, was pursued, resulting in the $1e^-$ reduction to yield the $\text{U}^{\text{III}}=\text{N}=\text{U}^{\text{IV}}$ complex (**20**) (Section 3.1.1).⁷⁶ This complex was found to be unreactive toward N_2 . However, it was highly reactive towards C–H bonds, resulting in (1) the 1,2-addition of the C–H bond from the $-\text{N}(\text{SiMe}_3)_2$ ligand across the uranium–nitride bond resulting in complex **21** (Scheme 22); (2) the C–H activation of toluene; and (3) the heterolytic C–H cleavage of phenylacetylene by the nucleophilic nitride. Additionally, complex **20** effects the heterolytic cleavage of H_2 yielding a mixture of the U(III)/U(IV) hydride–imide complex, $[(\text{U}^{\text{IV/III}}(\text{N}(\text{SiMe}_3)_2)_2(\text{THF})(\mu\text{-NH})(\mu\text{-H}))]$ (**112**) and complex **21**,⁷⁶ whereas the analogous U(IV)/U(IV) complex was found to be unreactive toward H_2 (Scheme 22).¹²⁵ Similar reactivity was observed for the U(IV)/U(IV) all- $\text{OSi}(\text{O}^t\text{Bu})_3$ complex, **6-Cs**,⁴⁹



demonstrating the importance of the oxidation state and ancillary ligands in promoting the reactivity of the nitride.

In a recent study, Keener, Mazzanti and co-workers reported the U(III) mixed-ligand systems containing a varying combination of $-\text{OSi}(\text{O}^t\text{Bu})_3$ and $-\text{N}(\text{SiMe}_3)_2$ ligands in order to promote the multielectron transformation of N_2 . The differences in the electronic and steric properties of these ligands allowed for the tuning of the redox properties and reactivity of the nitride complexes.⁷⁹ Addition of N_2 to the mixed-ligand $\text{M}_2\text{U}^{\text{III}}=\text{N}=\text{U}^{\text{IV}}$ ($\text{M} = \text{K}$ or Cs) complexes, **25-K** and **25-Cs**, resulted in unreacted starting materials. However, addition of N_2 to the putative “[$\text{K}_3\text{U}^{\text{III}}=\text{N}=\text{U}^{\text{III}}$]” complex, **26**, resulted in the analogous reactivity observed for **8-K**,⁴⁸ in which **26** promotes the $4e^-$ reduction to yield the mixed-ligand $\text{U}(\text{v})/\text{U}(\text{v})-\text{N}_2^{4-}$ complex, $[\text{K}_3(\text{U}^{\text{V}}(\text{OSi}(\text{O}^t\text{Bu})_3)_2(\text{N}(\text{SiMe}_3)_2)(\mu-\text{N})(\mu-\eta^2:\eta^2-\text{N}_2)]$ (**113**) (Scheme 23).⁷⁹ Converse to the reaction with **8-K**, additional N_2 cleavage products were isolated from the reaction mixture, namely, $[\text{K}_3(\text{U}^{\text{VI}}(\text{OSi}(\text{O}^t\text{Bu})_3)_2(\text{N}(\text{SiMe}_3)_2)(\text{N})(\mu-\text{N})_2(\text{U}^{\text{V}}(\text{OSi}(\text{O}^t\text{Bu})_3)_2(\text{N}(\text{SiMe}_3)_2))]_2$ (**114**), and $[\text{K}_4((\text{OSi}(\text{O}^t\text{Bu})_3)_2\text{U}^{\text{V}}(\text{N}))(\mu-\text{NH})(\mu-\kappa^2:\text{C},\text{N}-\text{CH}_2\text{SiMe}_2\text{NSiMe}_3)(\text{U}^{\text{V}}(\text{OSi}(\text{O}^t\text{Bu})_3)_2[\text{K}(\text{N}(\text{SiMe}_3)_2]_2)]_2$ (**115**) (Scheme 23).

The tris-nitride complex, **114**, was proposed to form from the overall $6e^-$ cleavage of the N_2 moiety. It was proposed that $5e^-$ are transferred by the two U(III) centers to yield a $\text{U}(\text{v})/\text{U}(\text{vi})$ intermediate, where an additional $1e^-$ arises from an external reducing source, most likely the “[$\text{K}_3\text{U}^{\text{III}}=\text{N}=\text{U}^{\text{III}}$]” (**26**) precursor. In complex **115**, N_2 cleavage also occurred, but with $2e^-$ arising from an external source, and undergoing a 1,2-addition of a C–H bond of $-\text{N}(\text{SiMe}_3)_2$ across the nitride moiety. Complex **115** could be independently synthesized by addition of 1.0 equiv. of complex **26** ($2e^-$) to the $\text{U}(\text{v})/\text{U}(\text{v})-\text{N}_2^{4-}$ complex (**113**), resulting in concomitant formation of the K-analog of the $\text{CsU}^{\text{IV}}=\text{N}=\text{U}^{\text{IV}}$ precursor, $\text{KU}^{\text{IV}}=\text{N}=\text{U}^{\text{IV}}$, overall demonstrating that the U(III)/U(III) complex **26** provides 1 or $2e^-$ to further reduce the bound N_2^{4-} moiety suggesting that the formation of complexes **114** and **115** involves two dinuclear U(III) complexes.⁷⁹

7. Conclusions

In summary, the past ten years have witnessed an amazing expansion of actinide-nitride chemistry with, most notably, the isolation of several examples of molecular uranium terminal- and bridging-nitrides in a broad range of oxidation states. Although this chemistry remains currently limited to a handful of supporting ligands, several routes have been identified for the synthesis of uranium nitrides. The nature of the supporting ligand is key, in both conferring stability for the targeted nitride complexes, but also in determining the reactivity and electronic structure of the nitride moiety. Notably, bridging nitrides provide an attractive route to promote magnetic coupling between uranium centers, where the bonding interaction with the supporting ligand appears to be critical for the communication to occur. Strong antiferromagnetic coupling between uranium centers in various oxidation states was observed for supporting $-\text{OSi}(\text{O}^t\text{Bu})_3$ ligands, but not for $-\text{N}(\text{SiMe}_3)_2$. It could be anticipated that a suitable choice of the supporting ligand may be used in

order to implement the electronic and geometric parameters leading to ferromagnetic interactions. Moreover, the short $\text{U}\cdots\text{U}$ distances measured in some bis-nitride complexes suggests that these are well poised to implement $\text{U}-\text{U}$ bonding interactions, if further reduction of the complex is within reach.

Uranium-nitrides formed from dinitrogen cleavage present a great interest for studying the mechanism and key parameters of dinitrogen reduction and functionalization. Moreover, the recent progress in uranium nitride chemistry has shown that uranium nitrides can effect a broad range of reactivity, and that supporting ligands are key in tuning the reactivity towards the desired products.

The first examples of thorium bridged-nitride complexes have also been recently isolated, in which thorium terminal nitrides should be within reach. These preliminary results anticipate that thorium nitride chemistry should also undergo an important development in the near future. By carefully tuning the choice of supporting ligand and reaction conditions, it may also be possible to access homo- and heterometallic nitride bridged complexes containing Th, or Th and U, in low oxidation states, which may result in very interesting bonding interactions.

While no examples of molecular nitride complexes of heavier actinides such as neptunium and plutonium remain unknown, the recent isolation of a terminal $\text{Np}(\text{v})$ oxo complex¹³⁰ suggests that a Np nitride may be in reach.

Nitride bridged $\text{An}(\text{III})$ complexes, analogous to **8-M** ($\text{M} = \text{K}$, Cs), were also computationally identified for Np and Pu by Panthi, Odoh and co-workers,¹³¹ suggesting that the possibility of expanding the molecular nitride chemistry beyond uranium exists, and despite the experimental difficulties, is certainly an attractive perspective in transuranic chemistry.

Author contributions

Dr Maria and Dr Keener contributed equally to writing the original draft and to reviewing and editing the manuscript. Prof. Mazzanti conceived the outline, supervised the writing and contributed to reviewing and editing the manuscript.

Conflicts of interest

There are no conflicts to declare.

Acknowledgements

Leonor Maria acknowledges support from Fundação para a Ciência e a Tecnologia (FCT) through projects UIDB/00100/2020 (CQE) and LA/P/0056/2020 (IMS) and contract IST-ID/091/2018. Marinella Mazzanti acknowledges support from Swiss National Science Foundation grant number 200020, 212723 and the Ecole Polytechnique Fédérale de Lausanne (EPFL).

References

- S. J. K. Forrest, B. Schluschaß, E. Y. Yuzik-Klimova and S. Schneider, *Chem. Rev.*, 2021, **121**, 6522–6587.



- 2 S. Kim, F. Loose and P. J. Chirik, *Chem. Rev.*, 2020, **120**, 5637–5681.
- 3 M. J. Chalkley, M. W. Drover and J. C. Peters, *Chem. Rev.*, 2020, **120**, 5582–5636.
- 4 A. I. O. Suarez, V. Lyaskovskyy, J. N. H. Reek, J. I. van der Vlugt and B. de Bruin, *Angew. Chem., Int. Ed.*, 2013, **52**, 12510–12529.
- 5 J. J. Scepaniak, R. P. Bontchev, D. L. Johnson and J. M. Smith, *Angew. Chem., Int. Ed. Engl.*, 2011, **50**, 6630–6633.
- 6 C. R. Clough, J. B. Greco, J. S. Figueroa, P. L. Diaconescu, W. M. Davis and C. C. Cummins, *J. Am. Chem. Soc.*, 2004, **126**, 7742–7743.
- 7 J. M. Smith, *Prog. Inorg. Chem.*, 2014, **58**, 417–470.
- 8 M. Streit and F. Ingold, *J. Eur. Ceram. Soc.*, 2005, **25**, 2687–2692.
- 9 A. V. Lizunov, A. A. Semenov, A. S. Anikin, A. V. Moiseev, A. P. Zhirnov and E. O. Soldatov, *At. Energ.*, 2022, **132**, 1–7.
- 10 G. W. C. Silva, C. B. Yeaman, L. Z. Ma, G. S. Cerefice, K. R. Czerwinski and A. P. Sattelberger, *Chem. Mater.*, 2008, **20**, 3076–3084.
- 11 G. W. C. Silva, C. B. Yeaman, A. P. Sattelberger, T. Hartmann, G. S. Cerefice and K. R. Czerwinski, *Inorg. Chem.*, 2009, **48**, 10635–10642.
- 12 G. W. C. Silva, C. B. Yeaman, P. F. Weck, J. D. Hunn, G. S. Cerefice, A. P. Sattelberger and K. R. Czerwinski, *Inorg. Chem.*, 2012, **51**, 3332–3340.
- 13 B. J. Jaques, B. M. Marx, A. S. Hamdy and D. P. Butt, *J. Nucl. Mater.*, 2008, **381**, 309–311.
- 14 Y. Arai and K. Minato, *J. Nucl. Mater.*, 2005, **344**, 180–185.
- 15 F. Haber, *Angew. Chem.*, 1914, **27**, 473.
- 16 F. Haber, *Ammonia German Patent, DE Pat.*, 229126, 1909.
- 17 S. S. Parker, J. T. White, P. Hosemann and A. T. Nelson, *J. Nucl. Mater.*, 2019, **526**, 151760.
- 18 S. S. Parker, S. Newman, A. J. Fallgren and J. T. White, *JOM*, 2021, **73**, 3564–3575.
- 19 A. J. Parkison, S. S. Parker and A. T. Nelson, *J. Am. Ceram. Soc.*, 2016, **99**, 3909–3914.
- 20 M. Takano, A. Itoh, M. Akabori, T. Ogawa, M. Numata and H. Okamoto, *J. Nucl. Mater.*, 2001, **294**, 24–27.
- 21 Y. Suzuki, Y. Arai, Y. Okamoto and T. Ohmichi, *J. Nucl. Sci. Technol.*, 1994, **31**, 677–680.
- 22 K. M. Peruski, *Front. Nucl. Eng.*, 2022, **1**, 1044657.
- 23 X. Wang, L. Andrews, B. Vlasisavljevich and L. Gagliardi, *Inorg. Chem.*, 2011, **50**, 3826–3831.
- 24 L. Andrews, X. F. Wang, Y. Gong and G. P. Kushto, *J. Phys. Chem. A*, 2014, **118**, 5289–5303.
- 25 L. Andrews, X. F. Wang, Y. Gong, B. Vlasisavljevich and L. Gagliardi, *Inorg. Chem.*, 2013, **52**, 9989–9993.
- 26 L. Andrews, X. Wang, R. Lindh, B. O. Roos and C. J. Marsden, *Angew. Chem., Int. Ed.*, 2008, **47**, 5366–5370.
- 27 R. D. Hunt, J. T. Yustein and L. Andrews, *J. Chem. Phys.*, 1993, **98**, 6070–6074.
- 28 K. Sankaran, K. Sundararajan and K. S. Viswanathan, *J. Phys. Chem. A*, 2001, **105**, 3995–4001.
- 29 D. W. Green and G. T. Reedy, *J. Chem. Phys.*, 1978, **69**, 552–555.
- 30 B. Vlasisavljevich, L. Andrews, X. Wang, Y. Gong, G. P. Kushto and B. E. Bursten, *J. Am. Chem. Soc.*, 2016, **138**, 893–905.
- 31 G. P. Kushto, P. F. Souter and L. Andrews, *J. Chem. Phys.*, 1998, **108**, 7121–7130.
- 32 D. W. Green and G. T. Reedy, *J. Mol. Spectrosc.*, 1979, **74**, 423–434.
- 33 T. W. Hayton, *Chem. Commun.*, 2013, **49**, 2956–2973.
- 34 P. L. Diaconescu, *Nat. Chem.*, 2010, **2**, 705–706.
- 35 A. L. Odom, P. L. Arnold and C. C. Cummins, *J. Am. Chem. Soc.*, 1998, **120**, 5836–5837.
- 36 K. Meyer, D. J. Mindiola, T. A. Baker, W. M. Davis and C. C. Cummins, *Angew. Chem., Int. Ed. Engl.*, 2000, **39**, 3063–3066.
- 37 I. Korobkov, S. Gambarotta and G. P. A. Yap, *Angew. Chem., Int. Ed.*, 2002, **41**, 3433–3436.
- 38 W. J. Evans, S. A. Kozimor and J. W. Ziller, *Science*, 2005, **309**, 1835–1838.
- 39 G. Nocton, J. Pécaut and M. Mazzanti, *Angew. Chem., Int. Ed.*, 2008, **47**, 3040–3042.
- 40 S. Fortier, G. Wu and T. W. Hayton, *J. Am. Chem. Soc.*, 2010, **132**, 6888–6889.
- 41 A. R. Fox, P. L. Arnold and C. C. Cummins, *J. Am. Chem. Soc.*, 2010, **132**, 3250–3251.
- 42 D. M. King and S. T. Liddle, *Coord. Chem. Rev.*, 2014, **266–267**, 2–15.
- 43 D. M. King, F. Tuna, E. J. L. McInnes, J. McMaster, W. Lewis, A. J. Blake and S. T. Liddle, *Science*, 2012, **337**, 717–720.
- 44 D. M. King, F. Tuna, E. J. L. McInnes, J. McMaster, W. Lewis, A. J. Blake and S. T. Liddle, *Nat. Chem.*, 2013, **5**, 482–488.
- 45 R. K. Thomson, T. Cantat, B. L. Scott, D. E. Morris, E. R. Batista and J. L. Kiplinger, *Nat. Chem.*, 2010, **2**, 723–729.
- 46 P. A. Cleaves, D. M. King, C. E. Kefalidis, L. Maron, F. Tuna, E. J. L. McInnes, J. McMaster, W. Lewis, A. J. Blake and S. T. Liddle, *Angew. Chem., Int. Ed.*, 2014, **53**, 10412–10415.
- 47 M. Yadav, A. Metta-Magaña and S. Fortier, *Chem. Sci.*, 2020, **11**, 2381–2387.
- 48 M. Falcone, L. Chatelain, R. Scopelliti, I. Živković and M. Mazzanti, *Nature*, 2017, **547**, 332–335.
- 49 M. Falcone, L. N. Poon, F. Fadaei Tirani and M. Mazzanti, *Angew. Chem., Int. Ed.*, 2018, **57**, 3697–3700.
- 50 M. Falcone, C. E. Kefalidis, R. Scopelliti, L. Maron and M. Mazzanti, *Angew. Chem., Int. Ed.*, 2016, **55**, 12290–12294.
- 51 M. Falcone, L. Chatelain, R. Scopelliti and M. Mazzanti, *Chimia*, 2017, **71**, 209–212.
- 52 L. Barluzzi, L. Chatelain, F. Fadaei-Tirani, I. Zivkovic and M. Mazzanti, *Chem. Sci.*, 2019, **10**, 3543–3555.
- 53 L. Chatelain, E. Louyriac, I. Douair, E. Lu, F. Tuna, A. J. Wooles, B. M. Gardner, L. Maron and S. T. Liddle, *Nat. Commun.*, 2020, **11**, 337.
- 54 P. Roussel and P. Scott, *J. Am. Chem. Soc.*, 1998, **120**, 1070–1071.
- 55 F. G. N. Cloke and P. B. Hitchcock, *J. Am. Chem. Soc.*, 2002, **124**, 9352–9353.
- 56 W. J. Evans, S. A. Kozimor and J. W. Ziller, *J. Am. Chem. Soc.*, 2003, **125**, 14264–14265.



- 57 S. M. Mansell, N. Kaltsoyannis and P. L. Arnold, *J. Am. Chem. Soc.*, 2011, **133**, 9036–9051.
- 58 E. Lu, B. E. Atkinson, A. J. Wooles, J. T. Boronski, L. R. Doyle, F. Tuna, J. D. Cryer, P. J. Cobb, I. J. Vitorica-Yrezabal, G. F. S. Whitehead, N. Kaltsoyannis and S. T. Liddle, *Nat. Chem.*, 2019, **11**, 806–811.
- 59 M. Falcone, L. Barluzzi, J. Andrez, F. Fadaei Tirani, I. Zivkovic, A. Fabrizio, C. Corminboeuf, K. Severin and M. Mazzanti, *Nat. Chem.*, 2019, **11**, 154–160.
- 60 P. L. Arnold, T. Ochiai, F. Y. T. Lam, R. P. Kelly, M. L. Seymour and L. Maron, *Nat. Chem.*, 2020, **12**, 654–659.
- 61 N. Jori, T. Rajeshkumar, R. Scopelliti, I. Ivković, A. Sienkiewicz, L. Maron and M. Mazzanti, *Chem. Sci.*, 2022, **13**, 9232–9242.
- 62 M. M. Rodriguez, E. Bill, W. W. Brennessel and P. L. Holland, *Science*, 2011, **334**, 780–783.
- 63 K. Grubel, W. W. Brennessel, B. Q. Mercado and P. L. Holland, *J. Am. Chem. Soc.*, 2014, **136**, 16807–16816.
- 64 N. Jori, L. Barluzzi, I. Douair, L. Maron, F. Fadaei-Tirani, I. Zivković and M. Mazzanti, *J. Am. Chem. Soc.*, 2021, **143**, 11225–11234.
- 65 S. S. Rudel, H. L. Deubner, M. Müller, A. J. Karttunen and F. Kraus, *Nat. Chem.*, 2020, **12**, 962–967.
- 66 L. Maria and J. Marçalo, *Inorganics*, 2022, **10**, 121.
- 67 W. J. Evans, K. A. Miller, J. W. Ziller and J. Greaves, *Inorg. Chem.*, 2007, **46**, 8008–8018.
- 68 X. Xin, I. Douair, Y. Zhao, S. Wang, L. Maron and C. Zhu, *J. Am. Chem. Soc.*, 2020, **142**, 15004–15011.
- 69 X. Xin, I. Douair, Y. Zhao, S. Wang, L. Maron and C. Zhu, *Natl. Sci. Rev.*, 2022, nwac144, DOI: [10.1093/nsr/nwac144](https://doi.org/10.1093/nsr/nwac144).
- 70 C. T. Palumbo, R. Scopelliti, I. Zivkovic and M. Mazzanti, *J. Am. Chem. Soc.*, 2020, **142**, 3149–3157.
- 71 C. Camp, J. Pécaut and M. Mazzanti, *J. Am. Chem. Soc.*, 2013, **135**, 12101–12111.
- 72 L. Chatelain, R. Scopelliti and M. Mazzanti, *J. Am. Chem. Soc.*, 2016, **138**, 1784–1787.
- 73 R. K. Rosen, R. A. Andersen and N. M. Edelstein, *J. Am. Chem. Soc.*, 1990, **112**, 4588–4590.
- 74 A.-C. Schmidt, F. W. Heinemann, W. W. Lukens Jr. and K. Meyer, *J. Am. Chem. Soc.*, 2014, **136**, 11980–11993.
- 75 L. Barluzzi, F.-C. Hsueh, R. Scopelliti, B. E. Atkinson, N. Kaltsoyannis and M. Mazzanti, *Chem. Sci.*, 2021, **12**, 8096–8104.
- 76 C. T. Palumbo, L. Barluzzi, R. Scopelliti, I. Zivkovic, A. Fabrizio, C. Corminboeuf and M. Mazzanti, *Chem. Sci.*, 2019, **10**, 8840–8849.
- 77 B. Vlasisavljevich, P. L. Diaconescu, W. L. Lukens Jr, L. Gagliardi and C. C. Cummins, *Organometallics*, 2013, **32**, 1341–1352.
- 78 J. Du, D. M. King, L. Chatelain, E. Lu, F. Tuna, E. J. L. McInnes, A. J. Wooles, L. Maron and S. T. Liddle, *Chem. Sci.*, 2019, **10**, 3738–3745.
- 79 M. Keener, F. Fadaei-Tirani, R. Scopelliti, I. Zivkovic and M. Mazzanti, *Chem. Sci.*, 2022, **13**, 8025–8035.
- 80 P. Scott and P. B. Hitchcock, *Polyhedron*, 1994, **13**, 1651–1653.
- 81 S. Fortier, G. Wu and T. W. Hayton, *Dalton Trans.*, 2010, **39**, 352–354.
- 82 D. M. King, B. E. Atkinson, L. Chatelain, M. Gregson, J. A. Seed, A. J. Wooles, N. Kaltsoyannis and S. T. Liddle, *Dalton Trans.*, 2022, **51**, 8855–8864.
- 83 Q. Zhu, W. Fang, L. Maron and C. Zhu, *Acc. Chem. Res.*, 2022, **55**, 1718–1730.
- 84 P. Wang, Y. Zhao and C. Zhu, *Organometallics*, 2022, **41**, 2448–2454.
- 85 J. Du, C. Alvarez-Lamsfus, E. P. Wildman, A. J. Wooles, L. Maron and S. T. Liddle, *Nat. Commun.*, 2019, **10**, 4203.
- 86 S. L. Staun, D.-C. Sergentu, G. Wu, J. Autschbach and T. W. Hayton, *Chem. Sci.*, 2019, **10**, 6431–6436.
- 87 F.-C. Hsueh, L. Barluzzi, M. Keener, T. Rajeshkumar, L. Maron, R. Scopelliti and M. Mazzanti, *J. Am. Chem. Soc.*, 2022, **144**, 3222–3232.
- 88 N. Kaltsoyannis, *Inorg. Chem.*, 2000, **39**, 6009–6017.
- 89 N. Kaltsoyannis, *Chem. Soc. Rev.*, 2003, **32**, 9–16.
- 90 L. Maria, I. C. Santos, V. R. Sousa and J. Marçalo, *Inorg. Chem.*, 2015, **54**, 9115–9126.
- 91 N. Tsoureas, A. F. R. Kilpatrick, C. J. Inman and F. G. N. Cloke, *Chem. Sci.*, 2016, **7**, 4624–4632.
- 92 M. D. Straub, L. M. Moreau, Y. S. Qiao, E. T. Ouellette, M. A. Boreen, T. D. Lohrey, N. S. Settineri, S. Hohloch, C. H. Booth, S. G. Minasian and J. Arnold, *Inorg. Chem.*, 2021, **60**, 6672–6679.
- 93 T. Cantat, B. L. Scott and J. L. Kiplinger, *Chem. Commun.*, 2010, **46**, 919–921.
- 94 N. L. Bell, L. Maron and P. L. Arnold, *J. Am. Chem. Soc.*, 2015, **137**, 10492–10495.
- 95 D. E. Smiles, G. Wu, N. Kaltsoyannis and T. W. Hayton, *Chem. Sci.*, 2015, **6**, 3891–3899.
- 96 D.-C. Sergentu, G. T. Kent, S. L. Staun, X. Yu, H. Cho, J. Autschbach and T. W. Hayton, *Inorg. Chem.*, 2020, **59**, 10138–10145.
- 97 S. L. Staun, G. Wu, W. W. Lukens and T. W. Hayton, *Chem. Sci.*, 2021, **12**, 15519–15527.
- 98 D. M. King, P. A. Cleaves, A. J. Wooles, B. M. Gardner, N. F. Chilton, F. Tuna, W. Lewis, E. J. L. McInnes and S. T. Liddle, *Nat. Commun.*, 2016, **7**, 13773.
- 99 X. Li, Y. Roselló, Y.-R. Yao, J. Zhuang, X. Zhang, A. Rodríguez-Forteza, C. de Graaf, L. Echegoyen, J. M. Poblet and N. Chen, *Chem. Sci.*, 2021, **12**, 282–292.
- 100 W. Krätschmer, L. D. Lamb, K. Fostiropoulos and D. R. Huffman, *Nature*, 1990, **347**, 354–358.
- 101 A. R. Fox and C. C. Cummins, *J. Am. Chem. Soc.*, 2009, **131**, 5716–5717.
- 102 M. A. Boreen, G. Rao, D. G. Villarreal, F. A. Watt, R. D. Britt, S. Hohloch and J. Arnold, *Chem. Commun.*, 2020, **56**, 4535–4538.
- 103 K. C. Mullane, H. Ryu, T. Cheisson, L. N. Grant, J. Y. Park, B. C. Manor, P. J. Carroll, M.-H. Baik, D. J. Mindiola and E. J. Schelter, *J. Am. Chem. Soc.*, 2018, **140**, 11335–11340.
- 104 J. Du, I. Douair, E. Lu, J. A. Seed, F. Tuna, A. J. Wooles, L. Maron and S. T. Liddle, *Nat. Commun.*, 2021, **12**, 4832.
- 105 J. D. Rinehart and J. R. Long, *J. Am. Chem. Soc.*, 2009, **131**, 12558–12559.



- 106 V. Mougél, L. Chatelain, J. Pécaut, R. Caciuffo, E. Colineau, J.-C. Griveau and M. Mazzanti, *Nat. Chem.*, 2012, **4**, 1011–1017.
- 107 M. Pepper and B. E. Bursten, *Chem. Rev.*, 1991, **91**, 719–741.
- 108 J. Du, J. A. Seed, V. E. J. Berryman, N. Kaltsoyannis, R. W. Adams, D. Lee and S. T. Liddle, *Nat. Commun.*, 2021, **12**, 5649.
- 109 L. Maria, N. A. G. Bandeira, J. Marçalo, I. C. Santos, A. S. D. Ferreira and J. R. Ascenso, *Inorg. Chem.*, 2022, **61**, 346–356.
- 110 J. F. Berry, E. Bill, E. Bothe, S. D. George, B. Mienert, F. Neese and K. Wieghardt, *Science*, 2006, **312**, 1937–1941.
- 111 C. Vogel, F. W. Heinemann, J. Sutter, C. Anthon and K. Meyer, *Angew. Chem., Int. Ed.*, 2008, **47**, 2681–2684.
- 112 M. G. Scheibel, B. Askevold, F. W. Heinemann, E. J. Reijerse, B. de Bruin and S. Schneider, *Nat. Chem.*, 2012, **4**, 552–558.
- 113 E. M. Zolnhofer, M. Käß, M. M. Khusniyarov, F. W. Heinemann, L. Maron, M. van Gastel, E. Bill and K. Meyer, *J. Am. Chem. Soc.*, 2014, **136**, 15072–15078.
- 114 J. Sun, J. Abbenseth, H. Verplancke, M. Diefenbach, B. de Bruin, D. Hunger, C. Würtele, J. van Slageren, M. C. Holthausen and S. Schneider, *Nat. Chem.*, 2020, **12**, 1054–1059.
- 115 L. Barluzzi, R. Scopelliti and M. Mazzanti, *J. Am. Chem. Soc.*, 2020, **142**, 19047–19051.
- 116 Q. Meng, L. Abella, Y.-R. Yao, D.-C. Sergentu, W. Yang, X. Liu, J. Zhuang, L. Echegoyen, J. Autschbach and N. Chen, *Nat. Commun.*, 2022, **13**, 7192.
- 117 L. Barluzzi, N. Jori, T. He, T. Rajeshkumar, R. Scopelliti, L. Maron, P. Oyala, T. Agapie and M. Mazzanti, *Chem. Commun.*, 2022, **58**, 4655–4658.
- 118 A. J. Ayres, M. Zegke, J. P. A. Ostrowski, F. Tuna, E. J. L. McInnes, A. J. Wooles and S. T. Liddle, *Chem. Commun.*, 2018, **54**, 13515–13518.
- 119 K. T. Horak, A. Velian, M. W. Day and T. Agapie, *Chem. Commun.*, 2014, **50**, 4427–4429.
- 120 S. Lin, D. E. Herbert, A. Velian, M. W. Day and T. Agapie, *J. Am. Chem. Soc.*, 2013, **135**, 15830–15840.
- 121 X. Xin, I. Douair, T. Rajeshkumar, Y. Zhao, S. Wang, L. Maron and C. Zhu, *Nat. Commun.*, 2022, **13**, 3809.
- 122 T. W. Hayton, J. M. Boncella, B. L. Scott, P. D. Palmer, E. R. Batista and P. J. Hay, *Science*, 2005, **310**, 1941.
- 123 P. A. Cleaves, C. E. Kefalidis, B. M. Gardner, F. Tuna, E. J. L. McInnes, W. Lewis, L. Maron and S. T. Liddle, *Chem. - Eur. J.*, 2017, **23**, 2950–2959.
- 124 D. M. King, F. Tuna, J. McMaster, W. Lewis, A. J. Blake, E. J. L. McInnes and S. T. Liddle, *Angew. Chem., Int. Ed.*, 2013, **52**, 4921–4924.
- 125 M. Keener, R. Scopelliti and M. Mazzanti, *Chem. Sci.*, 2021, **12**, 12610–12618.
- 126 O. Bénard, J.-C. Berthet, P. Thuéry and M. Ephritikhine, *Inorg. Chem.*, 2010, **49**, 8117–8130.
- 127 S. J. Simpson and R. A. Andersen, *J. Am. Chem. Soc.*, 1981, **103**, 4063–4066.
- 128 P. L. Arnold, Z. R. Turner, A. I. Germeroth, I. J. Casely, G. S. Nichol, R. Bellabarba and R. P. Tooze, *Dalton Trans.*, 2013, **42**, 1333–1337.
- 129 M. Falcone, L. Chatelain and M. Mazzanti, *Angew. Chem., Int. Ed.*, 2016, **55**, 4074–4078.
- 130 M. S. Dutkiewicz, C. A. P. Goodwin, M. Perfetti, A. J. Gaunt, J.-C. Griveau, E. Colineau, A. Kovács, A. J. Wooles, R. Caciuffo, O. Walter and S. T. Liddle, *Nat. Chem.*, 2022, **14**, 342–349.
- 131 D. Panthi, O. Adeyiga, N. K. Dandu and S. O. Odoh, *Inorg. Chem.*, 2019, **58**, 6731–6741.

